3. Scientific Methods

by Dieter Vieweger/Jutta Häser/ Patrick Leiverkus/Götz Bongartz/Gilles Bülow/Johannes Große Frericks/Dietmar Biedermann/Armin Rauen/Knut Rassmann/Samantha Reiter/Katja Soennecken/Linda Olsvig-Whittaker/David Adan-Bajewitz

3.1. Animated 3D-Models of Archaeological Excavation Contexts from Tall Zirāʿa (*Pls. 3.1* and *3.2*; *Apps. 3.5–3.11*)

by Dieter Vieweger/Jutta Häser

Fig. 3.1 3D-reconstruction of the Late Bronze Age city on Tall Zirāʿa. Film: *App. 3.9* (Source: archimetrix.de/BAI/GPIA).

Within the scope of the 'Gadara Region Project', the Biblical Archaological Institut Wuppertal (BAI) engaged C. Panneck and H. Siegel from the company 'Archimetrix visuelle Kommunikation' to work on a reconstruction project. Two archaeological contexts from the Late Bronze Age and the Iron Age were selected, and 3D-models were created. The primary object was to provide accessibility for a wide range of people.

In the first instance, an impression of a idealised Four Room House from the Iron Age I/II was created, which could be entered interactively, and explored by a virtual visitor (*Figs. 3.2* and *3.3*; *Apps. 3.6–3.9*). The second project produced an animated film, presenting the Late Bronze Age city on Tall Zirāʿa. As if viewed from above the city, the animation presents an aerial view of the city and leads the observer through the streets and into the interior of a sanctuary (*Figs. 3.1* and *3.9* and *3.10; Apps. 3.6* and *3.7*). The reconstructions are based not only on results from the current excavations at Tall Zirāʿa, but also on comparative contexts at other archaeological sites, such as the excavations at Tall al-Fāriʿa (Tirza) and Tall Qasīla (Yarkon), as well as on architectural information from the written sources[1].

3D-reconstructions provide a dual function; on the one hand, they force the archaeologist to reproduce all aspects of archaeological contexts faithfully, through all periods of their use or occupation, and therefore to reconstruct them completely in architecture or shape. On the other hand, they also help to understand the function(s) of the various installations; such as those for cooking and baking, or those for ceramic productions. Finally, they provide better understanding of the physical reality for constructions such as walls and roofs; thus, virtual reality plays an important role in answering questions concerning materials and construction methods (*Chap. 3.4.*).

The 3D-reconstructions were also very useful for the excavation process, as they cause the archaeologist to scrutinise contexts more precisely in order to discern further information; for example, about the masonry, the production method(s) for handicrafts, or even about the construction methods themselves. Such critical analyses which took place during the creation of the 3D-models

1 See e.g.: Chambon 1984, 24 Fig. 3.31–3.47 (Tall al- Fāriʿa [Tirza]);http://sara.theellisschool.org/ironage/places/tellqasile.html (12.7.2016) (Tall Qasīla [Yarkon]); Mazar 1999, 103–108 (Tall Qasīla [Yarkon]); Mazar 2008, 319–336 (Tall Qasīla [Yarkon]).

led to complex debates about the limits and opportunities of interpretation possibilities, and the methodological verifiability of general assumptions. In order to provide a correct illustration of the building structures, an 'articulation' of opinions was required during ongoing critical discussions regarding the virtual reconstructions.

3D-reconstructions should lead to increased archaeological discourse among archaeologists and other experts working in the field. Furthermore, 3D-animations should be used in the presentation of archaeological contexts on sites and in museums, in order to provide the general public with a visual impression of the historic appearance and the former functions of the reconstructed contexts, thus imparting a better understanding of ancient life.

The special benefits of virtual 3D-reconstructions become evident when compared to physical building replicas; for example, the houses of Tall Qasīla (Yarkon) in the Eretz Israel Museum in Tel Aviv. Such reconstructions not only replicate a fixed stage of research and state of preservation, which does not always reflect current theory or condition, but also require ongoing repairs and maintenance. The Tall Qasīla houses were strongly in need of repair and were given up due to their high maintenance costs.

In contrast, virtual 3D-reconstructions can be changed easily, and adapted to ongoing excavation and interpretation. Moreover, it is always possible to add more information and comparative examples, thus ensuring that reconstructions of the contexts are up-to-date with current research. Finally, 3D-reconstructions bridge the gap between the experience of living in the modern world and imagining the way of life in earlier historical periods. Within the scope of a museum presentation, they enable the results of the Tall Zirā'a excavations to be accessible to, and understood by, a wider audience.

3.1.1. Reconstruction of an Iron Age I Four Room House (*Pl. 3.1; Apps. 3.6–3.8*)

The Four Room House was chosen for virtual 3D-construction for two reasons.

Firstly, the settlement on Tall Zirā'a was rebuilt immediately after its destruction around 1200 BC, either by an earthquake or by an incident. The new settlement was superimposed over the existing walls from the Late Bronze Age city, but without a city wall. Although the Iron Age I settlement continued the tradition of the Late Bronze Age courtyard-houses (especially in the southern part of Area I) Four Room Houses, which are a typical variant of residential architecture for the Iron Ages I and II (1200–520 BC; Strata 13–10), were built in the northern part of Area I. Such houses, with rooms entered from an exterior courtyard, were perfectly adapted to the dry climate of Palestine during the Iron Age. Such houses were first found in Israel. However, they had a wider distribution both east and west of the Jordan River, and are closely connected to the Late Bronze Age period.

Secondly, the Palestinian mountain environment was marginal in terms of agriculture at that time; rainfall was insufficient for many crops, compelling the inhabitants to follow mixed agriculture (tillage, olive trees, vineyards, horticulture) combined with hunting and (if possible) fishing, as well as livestock breeding, principally sheep and goats. The Four Room House was an optimal adaption for these requirements, as it provided lodging for humans as well as animals as well as space for storage, drying and preparation of a variety of food.

The Four Room House in the 3D-model was constructed as closely as possible with the same procedures as those used in the Iron Age. At first a low wall base of fieldstones was built, in order to create a foundation and ensure stability (*Fig. 3.2; Pl. 3.1*); it also acted as a barrier to keep the house dry from underneath, to enable moisture sensitive goods such as cereals to be stored. The base was then coated with straw and local clay. The straw prevents the clay from crumbling, and provides thermal

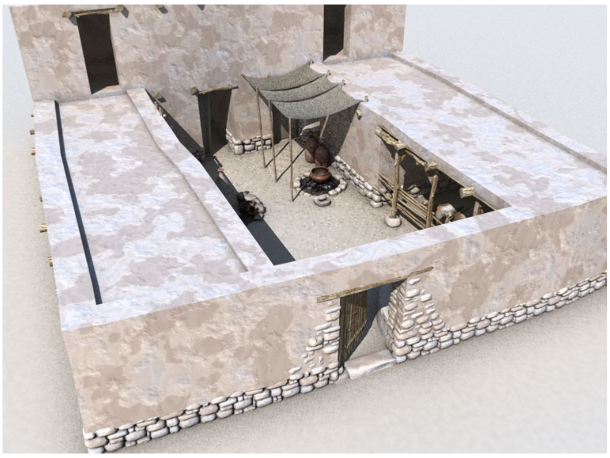

Fig. 3.2 3D-reconstruction of an Iron Age I Four Room House. Film: *App. 3.7* (Souce: archimetrix.de/BAI/GPIA).

Fig. 3.3 3D-reconstruction of the courtyard of an Iron Age I Four Room House. Film: *App. 3.6* and *3.7* (Souce: archimetrix.de/BAI/GPIA).

insulation. In most cases, the clay walls were plastered with a calcareous clay layer, which kept away moisture and vermin (for the construction see *App. 3.6*).

The roofs were supported by short timbers sourced from the local area; long beams were probably too valuable for house construction, and reserved for prestigious buildings. The width of the room therefore was limited by the length of the root beams. Several layers of thin branches, brushwood, straw and reeds were applied over the beams. Then, in order to make the roof impermeable, they were covered with clay, which had to be maintained regularly. Depending on the space available, and the financial status of the owner, a second floor could be built to provide more living space. The flat roof was used to dry the harvest and as a living area in the summer months.

The 3D-reconstruction also reveals what the internal areas may have looked like when in use, for such activities as milling, baking and food storage. A ceramic kiln was included, to represent the highly developed craftmanship which enriched everyday life (*Fig. 3.3*).

A virtual, independent, self-determined tour is possible through all the rooms, using Microsoft software; additionally animated scenes of the house construction, as well as daily activities, are available for Microsoft and MAC OS X software systems (*Apps. 3.7* and *3.8*).

3.1.2. Reconstruction of the Late Bronze Age City (*Pl. 3.2; Apps. 3.9–3.11*)

A second project between the Biblical Archaeological Institute Wuppertal (BAI) and the company 'Archimetrix visuelle Kommunikation' attempted to reconstruct the Late Bronze Age city on Tall Zirā'a (*Fig. 3.1*). Not only the massive architecture, but also the valuable findings and high percentage of imported ceramics from Cyprus, Syria and the rest of the Eastern Mediterranean prefigure the importance of the city as a trade and craft centre. Here ceramics, metal, glass, faience and quartz frits were produced or processed. It is therefore quite conceivable that the Late Bronze Age city on Tall Zirā'a was the centre of a citystate located at the important trade route leading from the Mediterranean to Dimašq (Damascus).

The 3D-reconstruction of this city is based on excavation results from 2003 until spring 2008. The most recent Bronze Age stratum in Area I was completely excavated over a surface area of 1,750 m^2 (Stratum 14); the most prominent structure was a massive casemate wall, which protected the settlements north-western flank. In the southern part of Area I, the wall ended in a large tower protruding inwards towards the city (*Fig. 3.6; Figs. 1.52* and *1.53*); it included a partitioned long-room temple, possibly a small sanctuary (*Fig. 3.4; App. 3.10*). Originally the researchers interpreted the architectual remains south of the tower as a gate. But now, it is certain that the city had only one gate, located in the east.

Also in the southern part of Area I, a large courtyard house with several rooms was detected. Noteworthy are the carefully designed fire pit, storage facilities in the form of several stonelined, pear-shaped silos, and a double mud brick wall, preserved to a hight of approx. 1 m and 1.2 m thick. The interior wall was plastered with a 5 cm thick lime layer on both sides, while the western, 2 m thick outer wall of the building was also the southern extension of the city wall.

Next to the tower on the city side were three houses, each with a central courtyard (*Figs. 1.52* and *1.53*). North of these was a prominent building with a large room, whose roof was supported by a pillar; another room adjoins it further to the north. Because of its two long, narrow spaces, this may have been a staircase. To the east of the room was a very carefully paved courtyard, with several rooms on its eastern side. This building complex was a *temple in antis*; i.e. a rectangular *cella* with a porch formed by the protruding side walls (*antae*).

A city plan detailing what the city probably looked like was produced; based on the contexts discovered during the excavations as well as photogrammetric and

Fig. 3.4 3D-reconstruction of the sanctuary in the tower. Film: *App. 3.10* (Source: archimetrix.de/BAI).

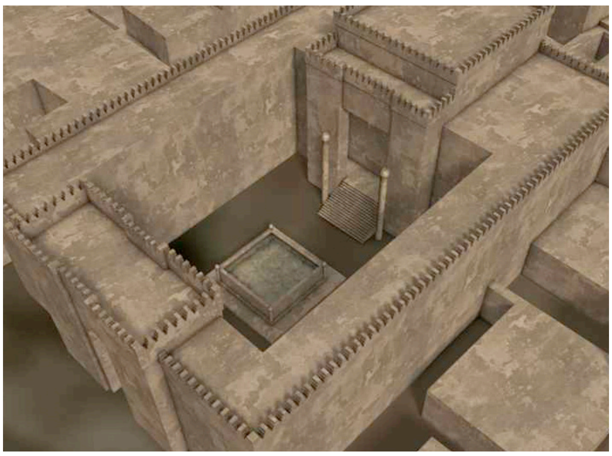

Fig. 3.5 3D-reconstruction of a temple type used in the Southern Levant. Film: *App. 3.9* (Source: archimetrix.de/BAI).

Figs. 3.6–3.7 3D-reconstruction of the Late Bronze Age city on Tall Zirā'a. Left: The western side of the city (Area I); right: the south side (with Area III). Film: *App. 3.9* (Source: archimetrix.de/GPIA/BAI).

geophysical surveys of the total area. It permits an idea of the settlement on Tall Zirā'a. The designs of the city wall, residential buildings and monumental structures, such as temples and a palace for example, are based on typological conclusions from verified references for the Southern Levant during the Late Bronze Age. Due to the massive extant remains in the excavated section of the casemate wall and the adjacent tower, the vertical dimensions of these building structures can be estimated realistically. The form of the battlements, ornamentation and other formal aspects were modeled by the company 'Archimetrix visuelle Kommunikation' based on comparable buildings in the Levant.

An important factor which had to be taken into account when dealing with the challenges posed by the reconstruction was to consider the constrution conditions and building restraints, as well as the economic and cultural aspects, of urban development of that period.

As explained above, the appearance of the Late Bronze Age city on Tall Zirā'a (*Apps. 3.9* and *3.10*; *Fig. 3.1*; *Pl. 3.2*) can be established according to archaeological research and the reconstruction of the city plan. The settlement was surrounded by a massive city wall with several towers, which followed the crest of the hill. Originally the researchers thought that there were two gates, as shown in the 3D-model. But the close examination of the excavation contexts proved that this assumption was wrong. There was only one gate on the east side of the hill. Its location is corroborated topographically by a pronounced access path to the settlement. Typologically, it could have been a Zigzag-Gate ('Knickachs-Tor') as they were typically used in Late Bronze Age cities in that region. However, its design and dimensions shown in the 3D-reconstruction are fictious.

The eastern gate was used mainly for transport and trade. It is logical to place the storage facilities near the gates (*Fig. 3.8*).

Because water was vital and perhaps scarce during the summer, the abundant water flow from the artesian spring in the centre of the tall within the settlement must have been considered a wonderful, divine phenomenon, and a temple was almost certainly located near it (*Fig. 3.5*). The size and orientation of the temple in the reconstruction, however, is based on academic assumptions rather than archaeological evidence. The urban area was developed by analogy with the excavated houses from other parts of the tall. The streetscapes are designed in the same way; for example, there is no archaeological proof for the location of a palace at the highest point in the north of the tall, but there is a strong probability that such a building could have been constructed there.

The animation of the Late Bronze Age city ends with the windowless small sanctuary in Area I. Its interior and exterior appearance can be accurately reconstructed due to the archaeological contexts found until spring campaign 2008 (*Fig. 3.4; App. 3.10*). Later excavations revealed a forecourt with a *temenos* wall lying to the east of the temple. Inside the forecourt was an unusual altar; the top layer was made from ceramic sherds, which had been accurately placed to create a pattern. These architecture features are not integrated in the 3D-reconstructions due its later discovery.

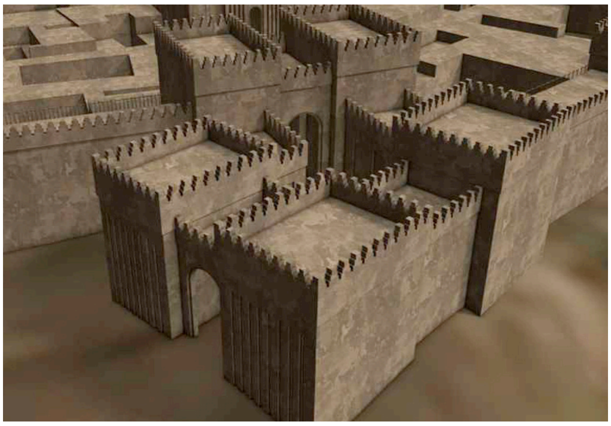

Fig. 3.8 3D-reconstruction of the main gate. Film: *App. 3.9* (Source: archimetrix.de/BAI).

Plate 3.1: Reconstruction stages of an Iron Age I Four Room House (Film: *App. 3.6*)

1. Construction of the foundation wall

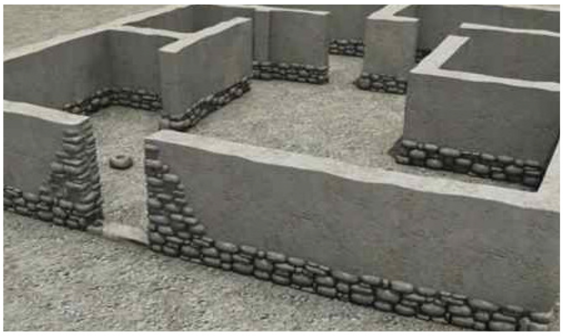

2. Construction of the rising mud brick walls

3. Construction of the roof step 1

4. Construction of the roof step 2

5. Construction of a second storey step 1

6. Construction of a second storey step 2

7. Overview of the Four Room House

8. Reconstruction of the courtyard

Plate 3.2: Reconstruction stages of the Late Bronze Age city on Tall Zirāʻa (Film: *App. 3.11*)

1. View on the excavation area (Area I)

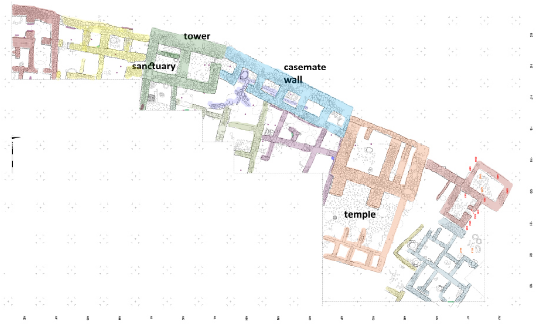

2. Architectural scetch of the foundations walls in Area I

3. and 4. Graphical supplement to the excavated structures in Area I: houses, temples, streets, gate, city wall etc.

5. Area I. Insertion of people in order to get an impression of size ratio

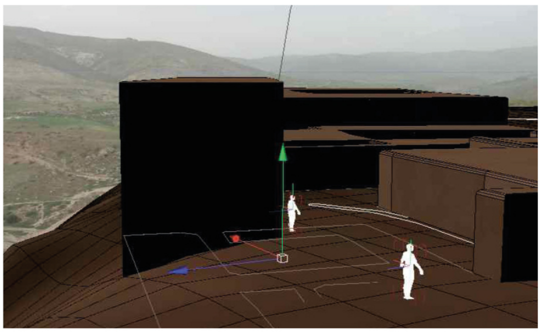

6. Area I. Drawing up of quadratic building structures

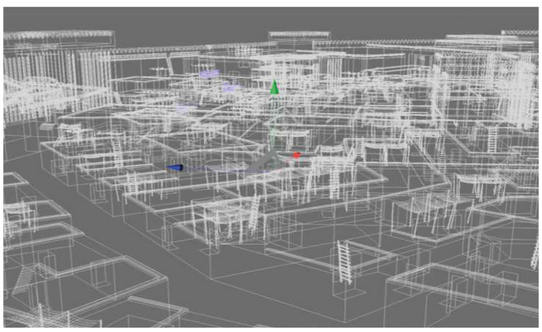

7. The computer calculates the height and extent of the buildings

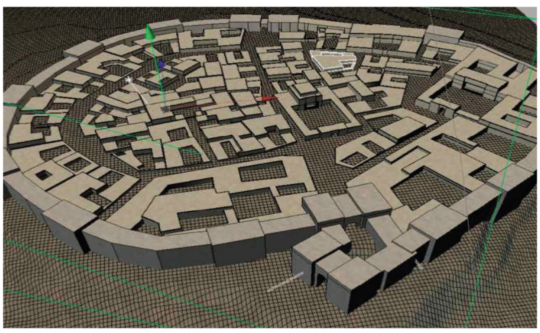

8. 3D-reconstruction of the Late Bronze Age city

3.2. Aerial Survey and Photogrammetry (*Apps. 3.1–3.4*)

by Patrick Leiverkus/Götz Bongartz

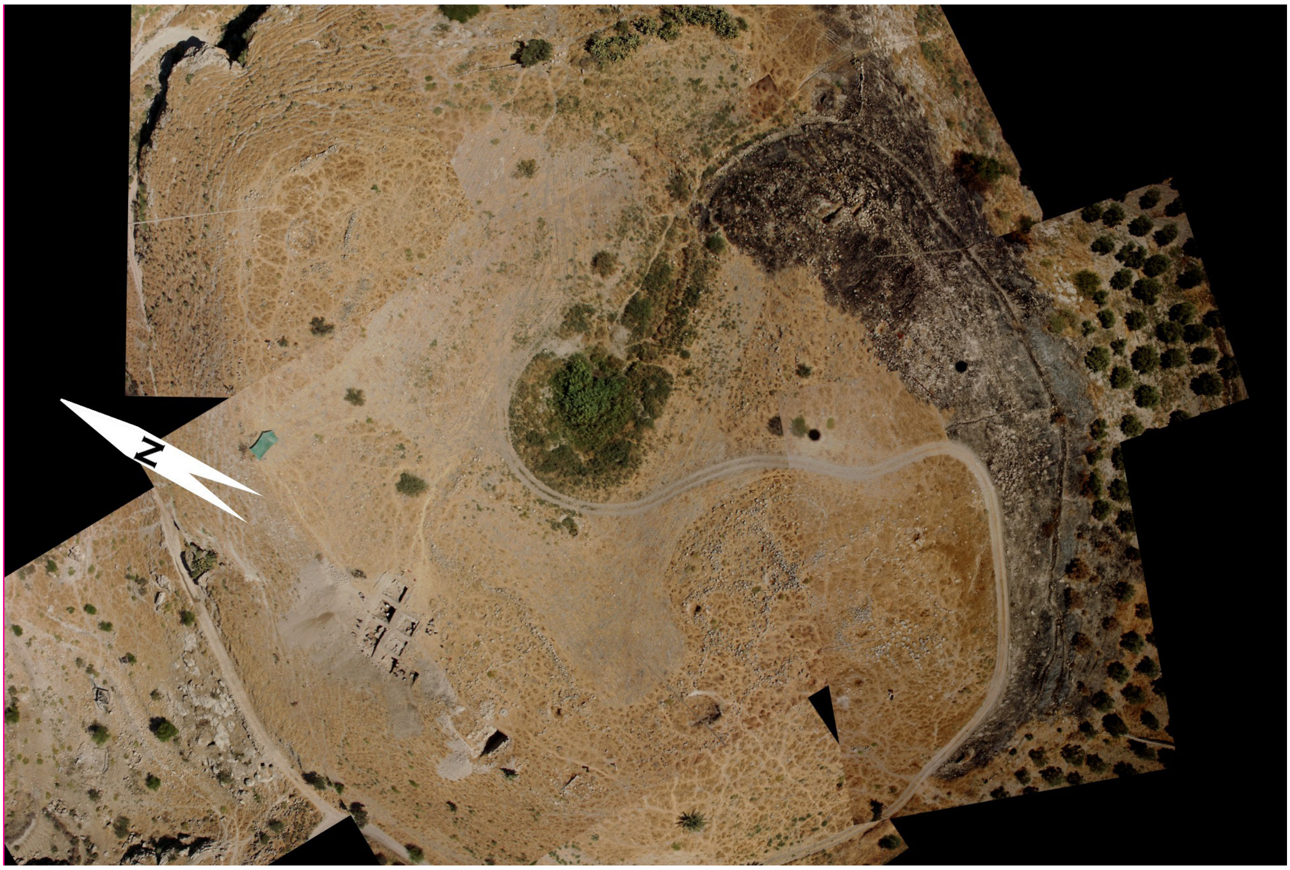

Fig. 3.9 Aerial view of Tall Zirāʿa. Mosaic of rectified photographs taken from a helium filled balloon in 2003 (Source: J. Kleb).

Excavations destroy—this fact is common knowledge and often deplored. Still, nothing can be done about it. Destruction is an integral part of excavating. If all goes well, what remains after the campaign has been completed, is a detailed excavation report for the world's archaeological libraries, a comprehensive work documentation, and an accessible, well-ordered store containing the artefacts. On the site, however, the actual evidences of the past—especially those from Pre-Classical periods—can only seldom be preserved and thus, after a few years, are hardly presentable.

Therefore every modern excavation campaign should strive for exhaustive documentation of the daily progress to ensure that as little information as possible gets lost between the actual event of excavating and its final report of the excavation. This should ideally also allow researchers to reconstruct correlations that may have been overlooked at the time of the excavation at a later date and thus arrive at new conclusions. Following this concept, experiments were undertaken that went as far as installing video cameras at the excavation squares, conducting daily interviews with the excavators, and also recording group discussions nonstop. But even this unreserved conservation of each and every piece of information provides no satisfactory solution to the problem of sensible documentation. Given the flood of material, nobody will ever be able to correctly assess the objective excavation progress and reconstruct it for publication without sorting the vital data from the less important ones. The concept of comprehensive data recording only postpones the necessary, inevitable task of selection, analysis, and interpretation. Apart from this, vast quantities of data would accumulate over time that could currently be neither processed nor safely stored.

For this reason, a methodically sound documentation of the excavation works as well as the careful storage of the finds are the real 'treasure' to be retrieved and preserved. This includes diaries, drawings, photographs, and databases—but also the stone-by-stone architectural plans of the excavated relics. Traditionally, they are drawn to scale on graph paper during the excavation campaigns by means of metre sticks and coloured pencils. These efforts are supported by modern surveying instruments, usually a tachymeter that measures single points with centimetre precision. These calibrated control points make it possible to connect any newly drawn plan with the master plan. Plans like these that contain control points can be digitalised in CAD systems.

However, drawing in the field poses several problems. First, every drawing or sketch lacking photographic documentation raises the suspicion of subjectivity. After all, people only draw what they (recognise and) see, and in their drawings they emphasise objects according to their own interpretation of the excavation while it is taking place. In all likelihood they will miss some elements or cannot consider certain connections in their interpretations because the future excavation progress is yet unknown. In addition, manual documentation is very timeconsuming and requires a lot of precious manpower. Both time and manpower are very valuable resources, especially during excavation campaigns abroad that usually have to be confined to only a few weeks per year.

This is why the necessity arose on Tall Zirā‘a during the past eleven years to objectify the documentation of the excavated, i.e. later destroyed, strata and to optimise it temporally. The aim was to reduce the necessary manpower while significantly improving, i.e. objectifying, the quality of documentation. This was realised by the implementation of innovative methods that were tested during excavation campaigns and proved themselves in practice. They will be described below.

3.2.1. Photogrammetry and Documentation of Archaeological Features

by Patrick Leiverkus

3.2.1.1. Digital Photogrammetry

In the campaign of 2003, digital photogrammetry of excavation squares was introduced on Tall Zirā‘a. It has proven to be both easy to perform with little technological effort and precision, and efficient and fast, compared to conventional drawings.

In order to document the excavation progress, the worked squares that are 5 m x 5 m in size, are photographed daily from a vertical perspective with the aid of a portable rod, at an altitude of at least 4 m (*Fig. 3.10*). Afterwards the distortion by the camera's perspective is rectified. Finally the digital images are adjusted to each other by way of ground control points (i.e. the corner points of the squares) (*Figs. 3.11* and *3.12*).

At the beginning, the daily photographs complemented the excavators' hand drawings but they eventually often replaced them completely. It was easy for the documenting square leader to mark the finds on the photo prints and add them to the documentation. Moreover, this procedure compels the excavator to adjust the sketches he or she made during the dig to the aerial view photograph that is less prone to manipulation, to check the finds' correct locations, and to review his or her personal interpretation from a different perspective. Since the photographs are taken at regular daily intervals, it is possible at a later time to reconstruct the excavation progress to the day. Furthermore, the photographs are very accurate in every detail; in that respect they are vastly superior even to very good drawings. It is important, however, that the rectified photos are taken by a surveyor in cooperation with an archaeologist who has constantly been supervising the excavation at the respective square. This ensures that the recordings of the excavation progress take place regularly at convenient moments.

For many years these images have also been used for making architectural plans of the excavated relicts that are fully correct in terms of position and masonry detail. Rectified images are a reliable foundation for digitization in a CAD system. The advantages are obvious: the production of these square images is much faster and easier than that of hand-drawn plans. However, there are also disadvantages: the twodimensional rectification only encompasses the level on which the ground control points are located. If walls jut out from this level, they remain distorted due to the perspective. The more the walls protrudes upwards and the farther it is located at the image's margins, the stronger the distortion becomes. This is particularly obvious when the overlapping fringe zones of two pictures have to be connected.

Additional photographs and ground control points as well as working with several rectification planes can help avoid these problems. This, however, will significantly increase the necessary labour input. And still, more often than not the final result will remain unsatisfactory because, in spite of manual finishing, an exact correspondence of the overlapping zones can only be approximated.

Fig. 3.10 Photographing with a telescope pole (Source: GPIA/BAI).

Fig. 3.11 Unrectified image of Square AL 117 (Source: GPIA/BAI).

Fig. 3.12 Rectified image of Square AL 117 (Source: GPIA/BAI).

3.2.1.2. Representation of a Spatial Structure by Means of Image-Based 3D-Reconstruction (*Apps. 3.1–3.3*)

In the spring and summer of 2011, a technology was implemented in the excavation routine on Tall Zirāʿa that incorporates an innovation from computer sciences, 'structure from motion'. This technology was developed in the 1980s in the field of computer vision with the purpose of reconstructing three-dimensional structures from (camera-recorded) motion sequences; more specifically, from a set of static images[2]. It always aims at evaluating the camera's positions from the set of images in order to grasp the geometries depicted. For this purpose, conspicuous spots or characteristics are identified in the individual images (usually automatically) that can easily be relocated in the entire set. Since every picture has been taken from a slightly different perspective, the exact position of these spots varies from one image to the next. With the aid of these shifts the camera's individual positions and thus ultimately a 3D-model can be reconstructed. The 3D-reconstruction by means of close-range photogrammetry constitutes a very robust method of producing exact models of a static scene that is only inferior to laser scanning with respect to accuracy. Although, due to the camera's limited resolution, the quality of the images diminishes with increasing distance, this technique can still deliver satisfactory reconstructions even at longer ranges.

The great advantage of the 'structure from motion' technique is its simplicity. While laser scanners are very expensive devices, photogrammetrical surveying can be performed with ordinary photo cameras. This is particularly advantageous during an excavation in the field where it is nearly impossible to get spare parts or new equipment should any damage occur. Another advantage is the speed of shooting. Our test scene was documented in less than a minute while a laser scanner would have needed significantly more time. Only photographing reflective surfaces is still tricky and thus in need of improvement: these objects cannot be detected unless they are sprayed with talcum powder.

The technique of 'structure from motion' allows archaeologists to digitally reconstruct the three-dimensional structure of a specific object or excavation area from a set of photographs taken from different perspectives. During an excavation, walls, installations, or entire areas are photographed in this manner from different perspectives. These images are fed into 3D-modelling software which uses the data to generate 3D- models that allow the visualization of the individual finds and their correlating positions from random points of view. The models' accuracy makes it possible to present an exact, undistorted perspective of the excavation area that can easily serve as the foundation of a digital (architectural) drawing. Therefore, the results of this method constitute a quantum leap with regard to stone-by-stone representations of the planum.

However, it should be noted in this context that skilful and comprehensive photograph is only one aspect of the evaluation process. Calculating and generating the models by means of a high-capacity computer is a very tedious task and should not be underestimated even though it is largely automated.

The technique is useful in even more respects: it allows the researcher to 'peep behind walls' even in retrospect. Other than two-dimensional images, the 3D-models enable him to change his point of view and investigate random details in various contexts that have not been considered before. Accordingly, the interpretation of excavation finds can be reevaluated with hindsight and thus also be improved. Examples of digital images such as described are appended (*Apps. 3.1–3.3*).

2 For the technology of 'structure from motion', see Bongartz 2011.

3.2.2. Aerial Photogrammetry for the Creation of Maps (*App. 1.3*)

by Patrick Leiverkus

In order to get image data suitable for 3D-reconstruction it is necessary to take aerial photographs. There are basically two options: land-based pictures, taken for instance by means of a telescopic pole, or airborne images, photographed from a helicopter or a similar aircraft.

At first the shots of the excavation squares were taken with the aid of a pole of 5 m in height on which a digital single lens reflex camera linked to a remote release was mounted (*Fig. 3.10*). Via video glasses the photographer could take more or less precise pictures of the squares. However, handling the pole was very tedious and exhausting. So, in 2003, the idea was born to mount the camera on a weather balloon filled with helium and to draw this device across Tall Zirāʻa with a line. The camera position was controlled by means of either a TFT monitor or a head display, the latter of which proved especially efficient in bright sunlight. A relatively small carrier balloon turned out to be the best choice (*Figs. 3.13* and *3.14*).

The images procured by a remote-controllable camera platform mounted to a helium balloon, taken from a maximum altitude of 135 m and covering an area of up to 15,000 m^2 per image were very satisfactory (*Figs. 3.15* and *3.14*). They are intended to serve as survey photographs for site plan data on the one hand and as informative documentation on the excavation site and its surroundings on the other. The single rectified images are connected to form a map via ground control points.

Despite the method's overall success, however, the balloon proved to be very wind-sensitive, even implicating the risk of total loss since it was only attached to a slim line. Moreover, the necessary helium was often difficult to procure and, besides, the balloon itself was very fragile.

For these reasons, it was resolved in the campaign of 2011 to introduce an independent aircraft as a novel, airborne photogrammetrical device. The possible options were those of a helicopter or of suspended platforms. Since helicopters are difficult to handle and also susceptible to faults, due to their complicated mechanical system, a suspended platform was decided on. Because of its higher level of flight safety and also for financial reasons an octocopter assembly kit has been chosen. The octocopter can fly up to an altitude of 250 m and has a range of 2 km. It is remote-controlled and transmits the potential photographic shooting area to the pilot via video glasses (*Figs. 3.15* and *3.16; App. 1.3*).

A series of images taken from elevated altitudes—i.e. from an aircraft such as a balloon, an octocopter, a helicopter, or a small airplane—can serve to generate 3D-models that document entire excavation sites or survey areas precisely to centimetres and thus make them accessible for future examination and processing.

A final remark: A three-dimensional documentation such as described above only requires the tools that are necessary in any case during an excavation campaign: camera, tachymeter or differential GPS, CAD system, mobile telescopic pole, and aircraft. The high-capacity computers only have to be equipped with a 3D-modelling software that, after an initial instruction has taken place, can essentially be operated without in-depth technical knowledge.

Fig. 3.13 Application of a helium filled balloon (Source: GPIA/BAI).

Fig. 3.14 Aerial photograph of Area I, taken from a helium filled balloon. Photograph taken in 2005 (Source: GPIA/BAI).

Fig. 3.15 Airborne octocopter. Film: *App. 3.1* (Source: GPIA/BAI).

Fig. 3.16 Aerial photograph of Area II. Photograph taken from the octocopter in 2011 (Source: GPIA/BAI).

3.2.3. Three Application Examples (*Apps. 1.3* and *3.1–3.4*)

by Götz Bongartz

3.2.3.1. Large Scale: The Tall Zirā'a (*Apps. 1.3* and *3.1*)

The technology described above was applied in order to generate a digital image of Tall Zirā'a as a whole. To this end an octocopter equipped with a high-resolution camera flew over and circled the excavation site multiple times at an selected altitude (*App. 1.3*). In the process, pictures were taken at altitudes from 20 m to 80 m, which served to reconstruct the entire region as a 3D-model (*Fig. 3.17*). This digital model can now be observed from any angle on the computer screen. Since it can be randomly turned and zoomed it offers interesting views of the excavation site as a whole and, if desired, even detailed insights into selected sectors (*App. 3.1*). Apart from that, the model has been printed out by a 3D-printer and thus be used as tangible illustrative material.

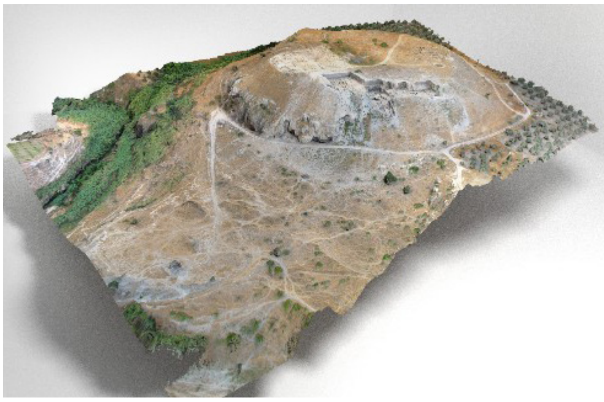

Fig. 3.17 3D-model of Tall Zirā'a: *App. 3.1* (Source: BAI/GPIA).

3.2.3.2. Medium Scale: Areas and Squares (*Apps. 3.2* and *3.3*)

The daily archaeological documentation was aided by 3D-reconstructions of complete excavation squares (or even entire areas) that could be used to create exact rectified images (e.g. Square AL 117, *Fig. 3.12*). Since the three-dimensional perspective can be adjusted with regard to the viewing angle it is also useful for a retrospective inspection of findings that may not have been properly appreciated at the time of the excavation. Since the octopoter was already deployed on the tall, it was available and expedited the process. However, pictures taken manually on the ground would also have been adequate (*Fig. 3.18; Apps. 3.2* and *3.3*).

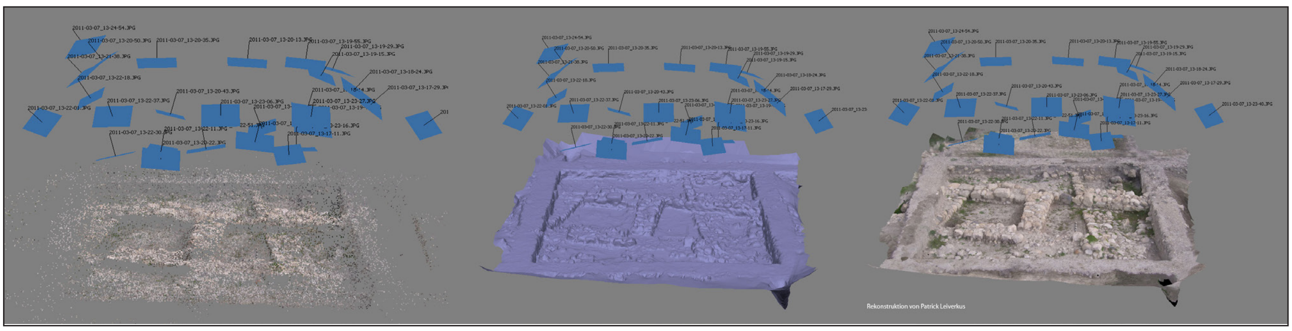

Fig. 3.18 Workflow for image-based 3D-reconstruction in an archaeological context (Source: BAI/GPIA).

3.2.3.3. Small Scale: Objects (*App. 3.4 a–c*)

3D-documentation of single finds has been especially valuable for the Biblical Archaeological Institute Wuppertal (BAI). In the course of the excavations, hundreds of objects were transported from Tall Zirāʻa to Wuppertal where they were cleaned and restored in a time-consuming process. In order to a) sufficiently document these objects—that meanwhile have all been shipped back to Jordan—and b) also have them 'available' for future screening for conspicuous features/characteristics that have as yet been undetected or disregarded, three-dimensional scans of each and every object of pottery or metal were made (*Fig. 3.19*; see examples of movable 3D-images in *App. 3.4 a–c*). Moreover, these data enable us to fabricate exact replicas.

3D-technology has been successfully applied for many years in the field of construction research, among others.

In order to guarantee a high level of quality down to the minutest detail as well as colour fastness, the Biblical Archaeological Institute Wuppertal (BAI) has developed an individual scanning system that employs a 3D-scanner exclusively constructed for this purpose and a special software by means of which BAI staff members can edit the pictures and data in a few steps and reconstruct a 3D-image of the find.

In contrast to the laborious and time-consuming method of documenting archaeological finds by means of manual drawings three-dimenional scans provide a less arduous way of documentation. They eliminate the element of interpretive subjectivity while at the same time permitting the capture of an object's surface (including processing traces and stress marks etc.) with millimetre precision. In addition to printed publications, 3D-models are also fit for beamer-based presentations and publications on the Internet. A 3D-model is much more detailed than any drawing and thus a reliable copy of the artefact.

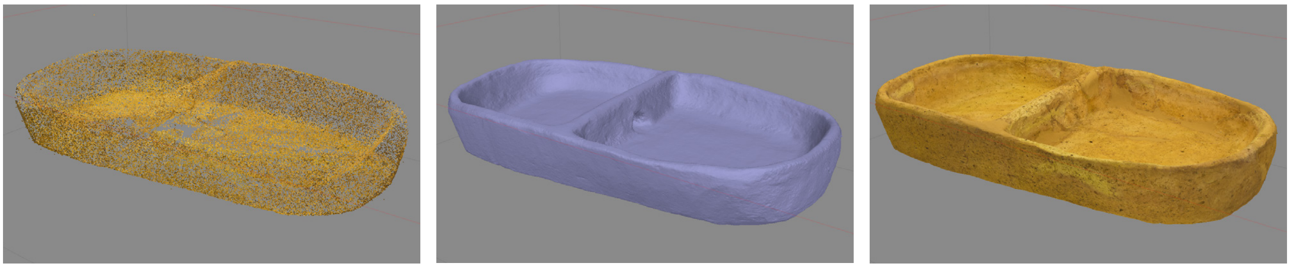

Fig. 3.19 Workflow for 3D-image of an object, TZ 006835-016: 1. Point cloud 2. Model without texture 3. Model with texture (Source: BAI/GPIA).

3.3. Colorimetric Examination of Ceramic

by Gilles Bülow/Johannes Große Frericks

Most ceramics are classified into ware groups primarily based on their colour, firing quality, tempering, sherd quality, and surface treatment[3]. The colour's key figure is usually determined by matching it visually with a colour table such as the Munsell table (Munsell Soil Color Charts, Baltimore 1954). However, this method involves several disadvantages: First, visual perception is very subjective and dependent on the prevailing lighting conditions (that often vary to a large extent); moreover, the colours listed in the colour tables often do not really match those of the pottery fragments. For this reason, the Biblical Archaeological Institute Wuppertal (BAI), respectively W. Auge, and the 'Department of Printing and Media Technology' of the Bergische University of Wuppertal have jointly introduced an objective physical method of measurement.

For the purposes of this project, a CIELAB-based colour-classifying program for archaeological finds (ceramics) was developed by optimising a typographical technique for its application in the field of archaeology[4]. It eliminates the element of uncertainty (caused by the subjective visual colour matching by a human being) by turning it into an objective procedure that can be carried out at the excavation site with only little technical equipment. The colorimetry is performed by means of a spectrophotometer and a specially developed computer program ('BAI Computer') that determines the ware groups as well as the closest chromaticity on the Munsell soil color chart. Colorimetric metering works with an internal source of light, based on the CIE-L*a*b* colour system. Thus, the ceramics can be classified unambiguously via objective measurements, clearly defined measurement conditions, and a likewise defined colour space to determine ware groups.

3 Kerner – Maxwell 1990, 240.

4 On the development of a CIELAB-based color classifying program for archaeological finds (pottery) see project work by G. Bülow and J. Große Frericks: Bülow – Große Frericks 2009.

3.3.1. The L*a*b* Colour System (*Fig. 3.20*)

Spectrophotogrammetrical classification of pottery takes place within the CIE colour space (*Fig. 3.20*). The CIE-L*a*b colour system is based on the theory of complimentary colours and was developed in 1976 by the CIE (Commission Internationale de l'Éclairage, International Lighting Commission).

In a three-dimensional space, all colours visible to the human eye can be illustrated and described by the three coordinates L*, a*, and b*. The L* axis serves as lightness coordinate while a* and b* describe the colour shade. Spectral distributions, such as the remissions of finds, can be converted into L*a*b* coordinates with the help of a reference illuminant.

The CIE-L*a*b* colour space was applied for the colour classification of the pottery for the following reasons:

- The CIE-L*a*b* colour system allows characterizing each specific colour (on a measured piece of pottery) by a triplet of numbers (L*, a*, b*).
- The characterisation of colours by triplets of numbers facilitates data processing with Excel (more specifically: with VBA). Thus, colour values can be archived or used for further calculations.
- The CIE-L*a*b* colour system allows calculating the (colour) difference of two colour points by application of the Delta-E or the CIEDE2000 formula. The high quality of such colour difference calculations has been established, e.g. by test series conducted by the Fogra Research Association Print'[5].
- The rendition of the colours by means of L*-, a*-, and b*-axes is comparatively easy to conceive and comprehend even for nonspecialists.

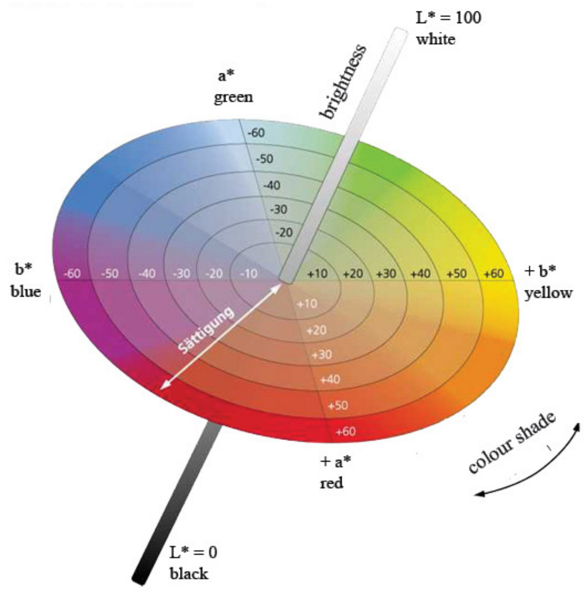

Fig. 3.20 The CIE-L*a*b* colour system (Source: G. Bülow/J. Große Frericks).

3.3.2. The Program ('BAI Computer')

The program collecting the L*a*b* values (obtained by converting the spectral distribution with the aid of the standard illuminant D65, that is equivalent to natural daylight and thus more or less reflects the visual colour matching conditions on the excavation site), classing them with ware groups, and defining the nearest 'Munsell soil colour' sample was developed on the bases of Microsoft Excel and its integrated scripting language Visual Basic Applications (VBA). It was called 'BAI computer' in reference to the Biblical Archaeological Institute Wuppertal (BAI).

3.3.2.1. Method of Classification of Pottery Ware Groups by Means of the 'BAI Computer' *(Fig. 3.21)*

The 'BAI computer' collects the L*a*b* data, processes them, and, among other things, finally establishes the pottery sherd's ware group.

The measured find's identification number and its subgroup are recorded in the 'BAI computer's' entry mask. As soon as the data are complete, the calculations are carried out. The results appear in a pop-up window and are moreover added to a spreadsheet.

Once the data pool of measured ceramics is large enough to safely assume that it reflects the characteristic chromaticity of a particular ware group, tolerances and target values are defined by means of the L*a*b* values.

From now on, when a piece of pottery is measured, it can be classed with a certain ware group as long as the values are located within previously defined tolerances. If not, the distance from the closest target value is used for classification.

5 Kraushaar et al. 2008, 42.

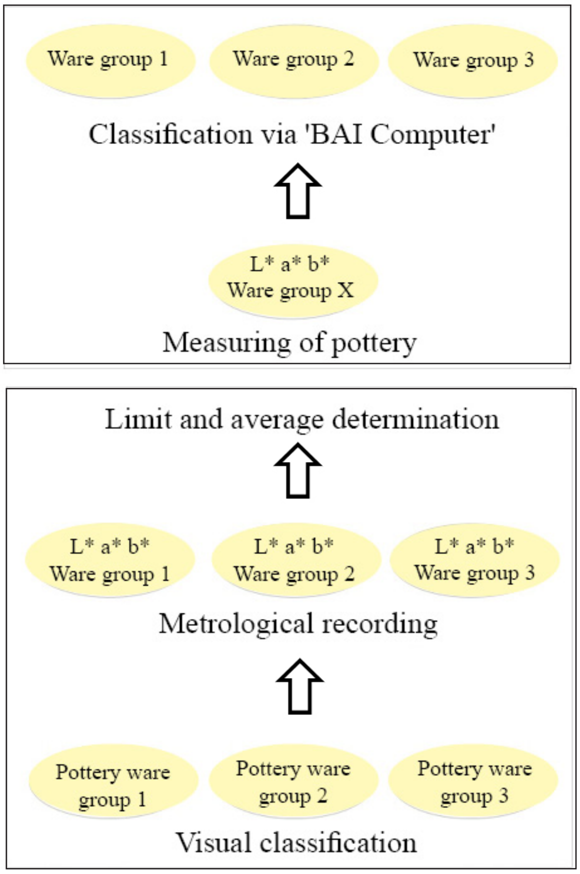

Fig. 3.21 Method of classification of pottery ware groups by means of the 'BAI Computer' (Source: G. Bülow/J. Große Frericks).

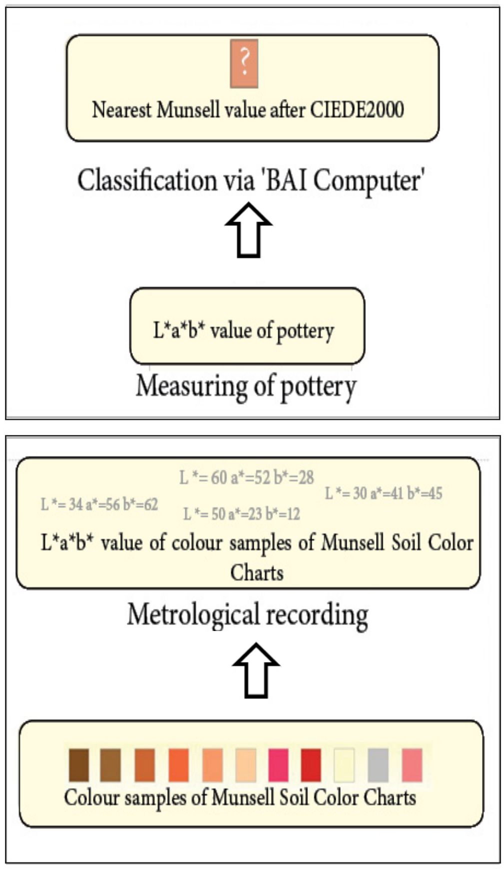

Fig. 3.22 Method of allocation of Munsell value by means of the 'BAI Computer' (Source: G. Bülow/J. Große Frericks).

3.3.2.2. Method of Allocation of Munsell Value by Means of the 'BAI Computer' *(Fig. 3.22)*

At first all colour samples of the 'Munsell soil colour charts' were recorded by spectrophotometry. The measured L*a*b* values along with their respective Munsell colour codes were then entered on an Excel spread sheet.

Now, when a sherd's L*a*b* data are registered, the nearest L*a*b* value will be matched to a colour sample from the 'Munsell Book of Soil Color' by means of colour difference calculation. CIEDE2000 is applied for calculating the colour difference because it takes into account the sensitivity of the human eye to colour differences[6].

3.3.3. Methods of Measurements and Definition of L*a*b* Tolerances

Whether the 'BAI Computer' is fit for practical application largely depends on its ability to evaluate the measurement data. To find out, about 8000 measurements of ceramics were carried out.

At first, pottery specialists of the Biblical Archaeological Institute (BAI) classed the finds visually with particular ware groups according to the 'Munsell soil color charts'. Afterwards, the finds were recorded by a spectrophotometer (X-Rite Eye-One Pro Spectrophotometer and its appendant software X-Rite Key Wizard Software Win by the company X-Rite Europe, Ltd.). In the process, four measurements were carried out at different points—both on the interior and on the exterior—of the pottery sherd. The average value of these four measurements marks the sherd's L*a*b* value. The reliability of the measuring method is guaranteed by observing standard deviations. Thus, it is ensured that the four individual measurements do not differ too widely, and falsification of the results by outliers is prevented.

A ceramic find's L*a*b* values are entered on an Excel spreadsheet along with its Tall Zirāʻa inventory number, the ware group it was originally classed with,

6 Cf. Schläpfer 2002, 76.

and its Munsell value. Thus, it can be assigned the correct L*a*b* value of a specific ‘Munsell soil color’ sample by means of colour difference calculation.

The measured data were then used to create diagrams that represent the coordinates on the a*/b*-, L*/a*-, and L*/b*-planes as a point within the L*a*b* colour space (*Graph 3.1*). The aim of visually depicting the L*a*b* triplet of numbers is to show the approximate colour spaces of the individual ware groups.

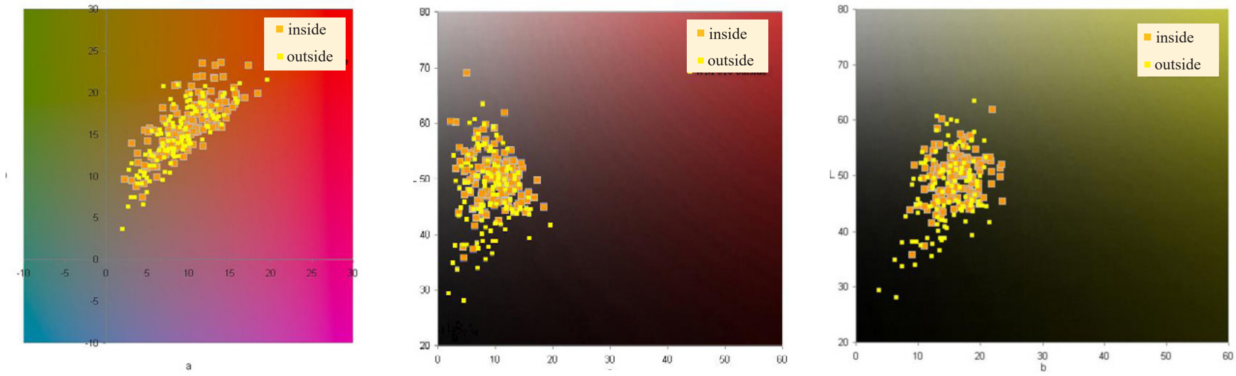

Graph. 3.1 Depiction of measured data as scatterplots on three layers, exemplified by ware group WM 610 (Source: G. Bülow/J. Große Frericks).

3.3.3.1. Determination of L*a*b* Tolerances

The scattering range of the results is wide and cannot be confined arbitrarily. Moreover, depicting the results as scatterplots may be visually appealing and allow colour interpretation; however, it does not reflect the frequency of occurrences of measured data within a certain domain. Thus, further diagrams were created that also represent the frequency distribution of the L*-, a*-, and b*-values (*Graph 3.3*).

These diagrams illustrate the frequency in which certain L*-, a*-, and b*-values occur among the ceramics of a particular ware group.

After analysing the frequency distributions of individual ware groups, experienced archaeologists and experts in the field of ceramics established the ware groups’ respective L*-, a*-, and b*-tolerances.

The L*a*b* tolerances define a minimum and a maximum value for each of the three coordinates. Any piece of pottery belongs to a certain ware group if its L*a*b* values lie within this range. Should the L*a*b* values of a ceramic find lie outside the range of one ware group or be in a range where the L*a*b* tolerances of two ware groups overlap, the spatial distance (delta E value) to the closest L*a*b* target value is the decisive factor (*Graph 3.2*).

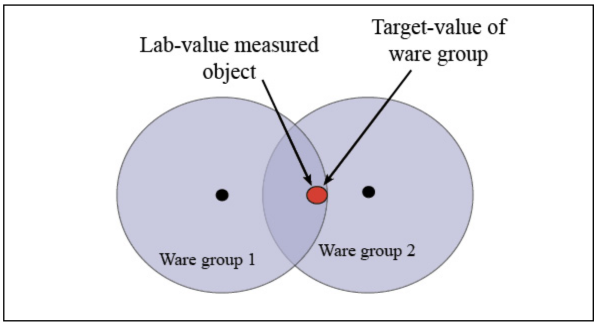

Graph 3.2 Example of a measuring object in an overlapping zone (Source: G. Bülow/J. Große Frericks).

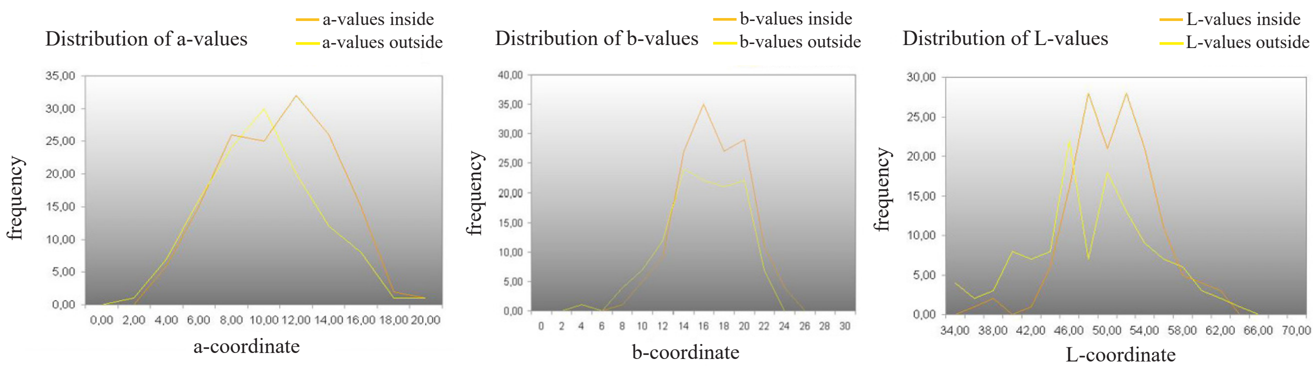

Graph 3.3 Frequency distribution of the L*-, a*-, and b*-values, exemplified by ware group WM 610 (Source: G. Bülow/J. Große Frericks).

3.3.3.2. Calculation of Target Value

Finally, all measured values of a ware group that lie within the established tolerances are registered on a new spreadsheet, and a new mean value is calculated. These mean values form the L*a*b* value that is characteristic of a specific ware group.

3.3.3.3. Comparison of Pottery Ware Groups

When categorising the pieces of pottery visually, the different ware groups overlap to a certain extent. The degree of overlapping allows an assessment of the 'BAI Computer's' classification quality:

- If it is low, there is a distinct colour distinction between two ware groups; classification is mostly unambiguous and recognizable to the human eye.
- If it is high, many ceramic finds may lie in a threshold range where only the spatial distance to the nearest target value can class them with one ware group or another. A visual classification is difficult. This is where the 'BAI Computer' is helpful: it classes the pieces of pottery unambiguously with a specific ware group.

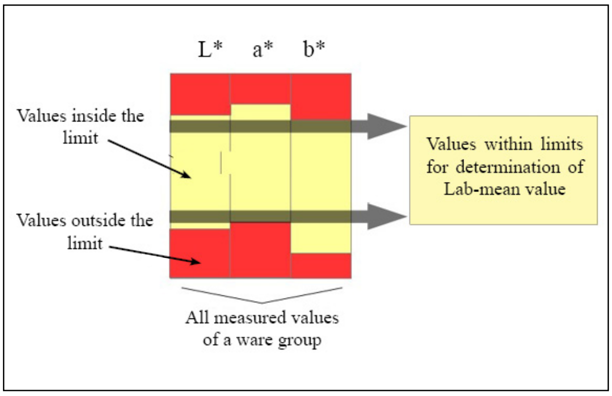

Graph. 3.4 Measured values lying within the defined tolerances (Source: G. Bülow/J. Große Frericks).

3.3.4. Conclusion

3.3.4.1. Measuring Methodology

Colorimetric examination by means of a spectrophotometer and the program/'BAI computer' allows an objective classification of ware groups. However, the process of measuring is sensitive and requires a certain qualification. For instance, it is of the utmost importance that the measuring device rests solidly on the measured object. Even the slightest shaft of light intruding from the side can influence the result and thus render the measurement useless.

Unfortunately, even strict adherence to the measuring guidelines cannot completely eliminate the element of subjectivity—for instance when choosing the measuring points deemed representative of the find's characteristic colour value. Eventually it is always the measuring archaeologist who decides which of the often multiple colour shades on a piece of ceramic reflects its original colour. This example also shows that comprehensive knowledge of the chromophoric components on ceramics as well as good communication among the archaeologists are indispensable.

3.3.4.2. Classification into Pottery Ware Groups

After a few initial trials in the field, the BAI's pottery specialists perceived the 'BAI computer's' classifications of ware groups as comprehensible and correct. To assess the program's reliability, they were given finds with L*a*b* values that were located in the overlapping ranges of two ware groups and had been assigned to either of them by the 'BAI computer'. Here, too, the computer's classifications were approved by the archaeologists.

Due to every individual observer's subjective perception, it is not possible to judge a ware group classification as downright correct or incorrect. On the whole, however, we can summarise that by implementing objective measurements and clear definition of the ranges of ware groups decision-making has been made easier and more reliable.

3.3.4.3. Statistical Evaluation

One of the advantages of applying statistical evaluation is its flexibility. No matter what the colour ranges of the individual ware groups are and how much they overlap—their ranges and mean values can always be calculated. This means that even at other excavation sites with completely different subgroups and ware groups these could be classed by entering and evaluating data by means of this method.

Visualising the results with the aid of diagrams has proved to be a very helpful method because it facilitates understanding the results for the observer. This is an advantage since staff members who are not familiar with the L*a*b* colour space may be involved in defining the ranges.

However, there is also a disadvantage to the method of statistical evaluation: in order to achieve a representative result and allow recognizing outliers for what they are, a relatively large number of measuring objects (finds) is necessary. And even if the 'BAI computer' can classify ware groups based on statistically evaluated data, independent of human interference—these data are still acquired on the basis of a set of finds that had primarily been divided into ware groups by visual classification.

This demonstrates once again that absolute objectivity is not possible. The visual classification of finds by qualified staff is indispensable and forms the basis for the spectrophotometrical definition of ware groups by means of the 'BAI computer'.

3.3.4.4. Classification of Munsell Values

The Programm/'BAI computer' classes each find with the closest Munsell chromaticity.

It is a positive aspect that the calculation of the nearest Munsell value is based on the CIEDE2000 colour difference formula and thus takes into consideration the colour difference perception of the human eye.

The method of classifying an object's Munsell value by measuring the distance of its chromaticity from the nearest chromaticity of a Munsell colour sample is without doubt pragmatic and self-evident. Still it is difficult to appreciate the value of classification by means of the Munsell value. In the course of the huge number of measurements that were performed, the Munsell value classifications were visually compared to the colour samples of the Munsell book of soil color on a regular basis. Some of the results were comprehensible or even identical, sometimes completely different colour samples had been chosen. However, this is not simply a phenomenon of the 'BAI computer': when discussing the matter with archaeologists from the BAI, there were also widely differing views on the colour shades of some pieces. What can be done to preclude these discrepancies?

To begin with, it has to be stated that a Munsell value classification that satisfies each and every onlooker does not exist. However, the problem might be solved by optimizing the function that calculates the Munsell value by factoring in the results of visual classifications. To this end, a set of characteristic pieces of pottery covering all ware groups could first be assessed by spectrophotometry and then be assigned a Munsell value by a group of archaeologists after visual screening under standard lighting. The results could be added to the database and compared to the BAI computer's classifications. If a trend could be detected, such as "The BAI computer tends to match saturated red finds with unsaturated Munsell colour samples", corrective parametres could be drawn up to counteract this discrepancy. However, it is dubious whether the possible benefit would be worth the time and effort necessary for writing such a complex operation and for the additional visual classifying procedures.

Still, this example, as well as the research in other task fields, shows that working on the subject matter from a technical point of view has added several novel ideas to the previous approach.

3.4. Experimental Archaeology (*Pls. 3.3–3.9*; *App. 3.5*)

edited by Dieter Vieweger/Jutta Häser[7]

In addition to the excavations and surveys carried out in the context of the 'Gadara Region Project', experimental studies on the technological advancement of skilled crafts and trades in ancient times were performed in cooperation with the Biblical Archaeological Institute Wuppertal (BAI; resp. W. Auge), the 'German Mining Museum Bochum', and the University of Hannover's archaeometric research group. These studies focussed on both the material clay and the production of ceramics and glass (W. Auge, partly in cooperation with M. Schulze and H. Brückelmann). Special attention was given to the production of ceramics in the Bronze and Iron Ages. Moreover, a tabun was reconstructed, and in the process the technique of baking bread was analyzed (*Chap. 3.4.1.*).

7 This article is written by D. Vieweger and J. Häser; it is based on the research results of W. Auge (BAI Wuppertal); detailed informations will be published in Volume 9 (W. Auge, Archaeometry, in: D. Vieweger – J. Häser (eds.), Tall Zirā'a 9, forthcoming).

In their provenience analyses, archaeometric examinations provided information on the local pottery production and on imports from different regions of the Levant or the Eastern Mediterranean area (*Chap. 3.8.1.*). The archaeological experiments were conducted to make these theoretical conclusions about the different classes of ceramics and their different modes of production practically comprehensible and thus test their logical rigour. In doing this, the technological skills and knowledge of potters as well as the technology of kiln construction in their respective historical eras could be assessed and appreciated.

Based on the results of chemical and mineralogical analyses and on the state of knowledge of traditional pottery in northern Jordan or other regions of the Southern Levant and the Eastern Mediterranean area[8], the production of a few selected pottery classes and their forms was re-enacted. In the process, attention was paid to all production steps, from the clay mining in the surroundings of Gadara to the fabrication of the respective final product. The following issues were paramount:

- Search for places of clay mining
- Mining and methods of processing the clay (including tempering/alloys)
- Technical and artistic forming of the pottery according to the respective era, with or without a potter's wheel
- Surface processing (including slip or engobe)
- Painting and ornament
- Firing and different baking procedures
- Kiln construction

In the years from 2001 to 2012, several kilns were reconstructed in Germany and in the Gadara region. They were used for experiments on the production of ceramics (*Chap. 3.4.2.*) as well as for producing raw glass experimentally and for melting glass (*Chap. 3.4.3.*).

Apart from the excavation finds, ethnological studies among the descendants of traditional potters and kiln builders as well as written sources served as models in these endeavours (see e.g. *Chap. 3.4.2.2.*).

3.4.1. Reconstruction of a Tabun (*Pls. 3.3–3.4*)

Quite a few tabuns for baking bread (*Fig. 3.24*) as well as kilns which might have been used for the processing of glass objects were found on the Tall Zirāʿa. Tabuns were used in almost every epoch.

Samples of several tabun walls were taken for chemical and mineralogical analyses. The results of these analyses served as references for identifying locally produced ceramics and for localising clay deposits in the Tall Zirāʿa's surroundings.

In order to allow the researchers to study the construction method of tabuns along with their manner of functioning, M. Saleh—a farmer living on the grounds of Gadara who had learned the tradition of kiln building from his mother, an experienced tabuniye, who still assisted him in his works—was ordered to build a tabun in the year of 2003 (*Fig. 3.23; Pls. 3.3* and *3.4*). In the process, only traditional building techniques were applied.

The tabun built by M. Saleh was fully functional and was used for baking pita bread and meat alike during many excavation campaigns.

One focus of the experiment was the tempering and the grogs employed. The clay came from a deposit near Umm Qēs that W. Auge and D. Vieweger had explored during the summer campaign of 2003. The most important temper added were organic matter such as reed shreds, rush, and goat hair, and also calcite. Their function was to guarantee the kiln's heat resilience (expansion during firing and contraction during cooling-off) without being damaged (cracks etc.).

The reconstruction of a tabun moreover allowed the researchers to understand in detail the construction and building process of the kilns found on the Tall Zirāʿa. The kiln wall was constructed according to the tongue and groove principle (*Pls. 3.3* and *3.4*).

Other interesting insights were gained about the manufacturing and firing of the kiln itself, the details of the tabun's manner of functioning (how to handle the embers and the ashes; how to fan the fire; how to prepare the food) and especially about the way the operator was able in ancient times to manage and recognise the different degrees of heat without being equipped with the technical tools available today. The people in antiquity will have achieved the latter by observing both the flames/embers and the warming of the kiln's surface.

Figs. 3.23–3.24 Left: Reconstructed tabun; right: Iron Age I tabun. Stratum 13, Area I, Square AE 115, Context 3258 (Source: GPIA/BAI).

8 Cf. e.g. London 1990 and Ohnefalsch-Richter 1913.

3.4.2. Construction of Pottery Kilns (*Pls. 3.5–3.9; App. 3.5*)

Although there is sufficient analytical and archaeological evidence pointing to the fact that the vast majority of Pre-Classical ceramics—especially the large ware groups WM C Buff, WM C R2B as well as all cooking pot (CP) groups—were produced locally there is still no positive archaeological proof of the presence of a pottery workshop on the Tall Zirāʻa. It can be assumed that these would have been located on the edge of the permanently water-bearing stream in the Wādī al-ʻArab or on the wide slopes of the lower cities. Unfortunately, though, all archaeological relics on these sites were destroyed by bulldozers in the course of the construction works for the dam project and when planting olive groves. Still, various potter's wheels made of basalt were found during the excavations on the tall.

In order to clarify the possibility of an earlier local pottery production, three differently constructed kilns were built during the campaigns of 2001, 2006, and 2012, and subsequently used for firing ceramics (*Chaps. 3.4.2.1., 3.4.2.4.* and *3.4.3.3.*).

3.4.2.1. Construction of an Updraft Kiln in 2001

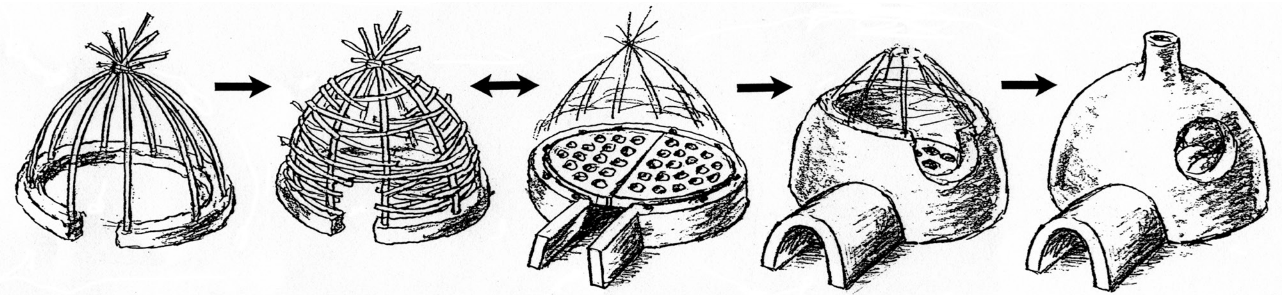

Fig. 3.25 Construction of an updraft kiln (Source: BAI/GPIA; drawings made by E. Brückelmann).

Fig. 3.26 The replica of an updraft kiln (Source: BAI/GPIA).

In 2001, an updraft kiln was recreated which had been in use in the Near East in Pre-Classical times, such as found in Iran (e.g. in Tepe Sialk; for the construction of such a kiln see *Fig. 3.25*)[9].

The kiln was formed from a clay-straw composite covering a framework of twigs. In front of the stoking hole, a poking channel was built; at the top, a hole was left as a smoke funnel to which an extension could be affixed. There was also a side hole for inserting the vessels (*Fig. 3.26*).

During the kiln's construction and while firing the ceramics first insights were gained which in turn were helpful during the later experiments.

3.4.2.2. Ethno-Archaeology as an Approach to Better Understanding Technical Procedures

When preparing for building another kiln in the summer of 2006, the researchers not only drew on the models but also on the methods of ethno-archaeology, a cultural anthropological discipline. This branch of research observes and examines traditional ways of living and working of present-day tribes or inhabitants of certain regions and, by way of analogy, tries to infer the corresponding circumstances in earlier, primarily nonliterate, eras[10].

The following fields of application are especially auspicious[11]:

- Comparison of forms
- Functional identification of objects and finds
- Comparison of technological procedures
- Comparison of social, political, and economic structures

9 Cf. Majidzadeh 1975/1976, 207–221.

10 Basics on the matter and on application of the method cf. London 1990. For an outline of the systematics of ethno-archaeological analogies, see Näser 2005.

11 On this, see Näser 2005; Watson 1999, 49 f.

An approach like this can disclose new possible ways of interpreting specific archaeological issues and, if applicable, widen their range. Thus it may be possible to find explanations that support the assumptions arrived at by investigating the finds.

In the summer of 2006, the excavation team from the Tall Zirāʻa visited a pottery workshop near Zarqa, an industrial centre of Jordan. They studied traditional technological procedures that have survived into the present, such as: origin of the different sorts of clay, their conditioning, the manufacturing process, the forms of the various vessels as well as construction, capacity, and operating mode of the kilns. The insights gained during this excursion were very helpful for the reconstruction and utilisation of the new kiln on the Tall Zirāʻa. However, while the present-day search for clay and its preparation can definitely be compared to the same activities in Pre-Classical times, kiln construction, firing, the amount of material needed, and the necessary degrees of heat are only comparable with classical (Hellenistic/Roman/Byzantine) kilns.

3.4.2.3. Construction of an Updraft Kiln in 2006 *(Pls. 3.5* and *3.6; App. 3.5)*

After successfully building a tabun in the summer of 2003, the preparations for constructing a pottery kiln modelled after the Late Bronze Age kiln of the Tell Brak (Syria) were taken up[12].

In order to find out the operating requirements it was necessary to analyse the (original) firing temperatures of the pieces of pottery found on the Tall Zirāʻa. To do so, cut ends of ceramic sherds underwent laboratory tests to find out their chemical and mineralogical compositions. The temperatures at which the ceramics had been formerly fired or, alternatively, temperatures necessary for firing the local clays could be found out by means of firing experiments. The chemical analyses revealed that the local clays contain large amounts of CaO and their compositions strongly resemble those of the ceramics of the ware groups WM C R2B, WM C Buff or Cl Bu2Br found on the Tall Zirāʻa. As the firing experiments with ceramic samples of these ware groups showed, the temperatures were between 550–600 °C and 750–800 °C.

In a pottery workshop in Brüggen-Born (Germany), the potter H. Brückelmann tested the clays available in the surroundings of Gadara for their suitability to be fired into ceramics (plasticability and firing experiments in an electric kiln). At the end of these preliminary tests in June 2006 a prototype of the envisaged kiln was built and loaded with 30 vessels formed from clays from the Tall Zirāʻa and from the surroundings of Umm Qēs. They emulated the Bronze Age and Iron Age ceramic vessels found on the Tall Zirāʻa. The kiln was heated to 700 °C and 750 °C, respectively. The ceramic firings themselves could be carried out appropriately and the yield was satisfying with only 10 % breakage. However, the vessels' quality did not reach the models' functional characteristics. Moreover, the kiln was not very heat-resistant and broke down after the second operating test. This was due to the major temperature fluctuations between day and night in Brüggen-Born and also to the fact that the time allotted for the construction of the kiln had been much too short to allow it to dry out sufficiently before being taken into operation.

Fig. 3.27 Reconstruction of a pottery kiln on the Tall Zirāʻa in 2006. Film: *App. 3.5* (Source: BAI/GPIA).

The insights gained from this experiment were incorporated into the construction and into the drying and heating process of the pottery kiln later built near the Tall Zirāʻa. This kiln was built in Umm Qēs by M. Saleh, using the clays from Gadara/Umm Qēs that had evolved from the weathering of basalt. The clay was tempered with goat hair and straw chaff (*Pls. 3.5* and *3.6; App. 3.5*).

The kiln was constructed layer upon layer over the course of several days and then dried in the open air for a long time. Following that, when it had reached a 'leather-hard' condition, it was 'baked out', i.e. completely dried, for three days at a constant heat level.

The reconstructed kiln was 0.75 m in height with a wall thickness of 0.05 m and a diametre of 0.50 m; the firing chamber's capacity was approx. 100 litre. The wall was erected over a bottom plate and a second, vent-holed floor and connected to them by means of tongue and groove joints. The upper part of the kiln had a smoke outlet and could be removed for filling the chamber. Finally, there was also an opening for adding fuel (*Fig. 3.27*).

12 For the kiln in Tall Brak, see Eiland 1998/1999, 69–84.

H. Brückelmann formed about 50 vessels from local clay (*Fig. 3.28*). They conformed to the ware groups WM C R2B and WM C Buff and were copies of vessels from the Middle Bronze/Late Bronze/Iron Ages. They were fired in the reconstructed kiln, using first wood (during the heating-up phase) and then dung as fuel. Temperatures of 700–750 °C were easy to attain and also to maintain over longer stretches of time. The firing yield of undamaged ware was 90 %. However, some vessels that had been located on the vent-holed floor and had been exposed to the fire more or less directly developed blistering/bursting after a little while (overheating!). It turned out, though, that this type of kiln cannot permanently maintain temperatures above 700 °C that are required for fring highly SiO_2-containing ceramics (i.a. Cl Red, Roman – Byzantine period). For attaining these firing temperatures, the necessary energy consumption renders any kind of economical working impossible. However, even after the efforts to reach temperatures of over 700 °C the kiln was still in a good condition. This will be ultimately due to the addition of special tempering materials during its construction as well as the specific method of drying and heating the kiln before putting it to use.

Fig. 3.28 Hanna Brückelmann forming ceramic vessels (Source: BAI/GPIA).

For comparison, after two firing procedures in the kiln, a batch of ceramics was fired in an open fire. However, the yield of undamaged, well-fired vessels was lower (50 % breakage) in the open fire and significantly more fuel was needed than in the closed kiln. The non-efficiency of this procedure was thus evident.

The experiments could demonstrate the following:

(1) A single-duct pottery kiln made from clay is absolutely capable of firing ceramics from local (calcite-rich) clays with a satisfying yield of undamaged ware.

(2) Temperatures of 700–750 °C are easy to attain and maintain over a longer stretch of time in an oriental environment. Baking temperatures of over 900 °C, however, that were customary in Roman times, e.g. for the ware groups Cl Red and Cl Red BS, could not be reached with this type of kiln.

(3) The calcite-rich clays used for manufacturing the ceramics are not suited for firing temperatures more than 750 °C.

(4) Firing pottery in an open fire can also achieve respectable results. However, the disadvantages are obvious: non-uniform and uncontrollable temperature distribution and energy loss because of strong radiation of heat.

(5) The following work stages could be analysed and documented (*Pls. 3.5* and *3.6*):

- Search for clay, and clay mining
- Composition of the ingredients for tempering
- Grinding, sifting, and compounding of clays
- Production of tempering (blending, pounding, and churning)
- Production of the bottom plate (pounding, measuring and excision)
- Production of the vent-holed floor
- Connecting the vent-holed floor and the bottom plate
- Building the kiln wall (tongue and groove system)
- Manufacturing a kiln lid with a controllable smoke outlet
- Firing the kiln: filling the kiln with dung, firing the dung thoroughly from the inside and from the outside
- Firing the ceramics: filling of the kiln, raising the temperature by means of a temperature ramp, opening of the kiln and removal of the ceramics

A short film documenting the different work stages of material procurement and the building and operation of the pottery kiln can be found in the appendix to this volume (*App. 3.5*).

3.4.2.4. Construction of a Quadruple-Shelled Kiln in 2012 *(Pls. 3.8* and *3.9)*

In Area I two multilayered, carefully insulated kilns dating from the Iron Age II were found standing side by side in 2009 (Stratum 10, Area I, Square AT 121, Context 4100; *Fig. 3.29*). Their outstanding features are their characteristic shape (oval), their good isulation and a quadruple-shelled wall: two layers of clay, one filling layer (soil or air) and one layer of ceramic sherds. The latter also served as additional heat reservoirs and insulators (on the construction of kilns of this type, see also *Pl. 3.8*). The advantage of this type of construction is its extraordinary energy efficiency: even at an inside temperature of significantly more than 900 °C the outer shell was surprisingly cool.

Since comparable specimens could also be verified in the Late Bronze Age (Stratum 14) the question arises whether they were used for firing ceramics and/or processing glass (for melting and cooling-off) and which temperatures could be attained and maintained in the process. The kiln modelled after these exemplars was therefore tested with respect both to firing ceramics and to melting glass (*Chap. 3.4.3.*).

When the experiment was conducted it became obvious that kilns of this type were very well suited for firing ceramics (*Chap. 3.4.2.3.*). Contrary to the Late Bronze Age, cylindrical and only single-leaf kiln reconstructed in 2006, this one could easily reach and maintain a firing temperature of more than 900 °C.

The cooking pots fabricated in this process were subsequently tested for their serviceability (leak tightness, abrasion resistance, thermal and mechanical stability, etc.). Finally they were used for preparing soup and millet gruel over an open flame[13].

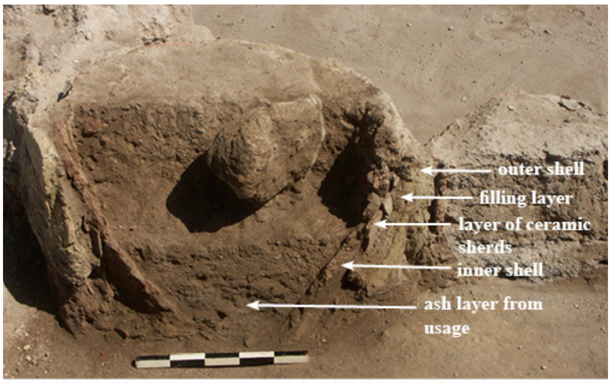

Fig. 3.29 Quadruple-shelled kiln. Stratum 10, Area I, Square AT 121, Context 4100 (Source: GPIA/BAI).

3.4.3. Experiments on Melting Glass and the Processing of Raw Materials

In the course of the summer campaign of 2010, experiments were started on melting glass and on fabricating raw glass out of the raw materials naturally occurring on the Tall Zirā'a and in its surroundings. A possible melting and cooling procedure had been previously tested in the laboratory of the company Schott GmbH (Schott, Ltd.) in Mainz, Germany, and was applied for the on-site experiments.

3.4.3.1. Production of Raw Glass

Several test arrangements, some of them inside at the kitchen stove and some of them outside in a hollow in the earth, were reconstructed. The raw materials used were silex and quartz gravel, and different reaction mixtures were applied (*Fig. 3.30*). Some of these were heated in a tin box, the others in a porcelain crucible. For kindling the coal, additional air was supplied by means of a blow-dryer instead of a pair of bellows.

The successes in producing glass were only rudimentary: during the experiments, the reaction mixtures melted only partially or only to a little extent on the surface; some tests even yielded no results at all, neither a chemical reaction nor melt flow. However, one experiment was conducted successfully with a reaction mixture consisting of 13 g SiO_2 (silex) und 1.7 g Na_2CO_3 (sodium carbonate) that was kept in a plastic bag. To begin with, the silex powder was treated with hydrochloric acid in order to eliminate any possible trace of carbonates before adding the sodium carbonate. This was done to guarantee the development of CO_2. Afterwards the mixture was decanted and washed with water several times. First the mixture of SiO_2 and hydrochloric acid was decanted and then, during the cleaning process, that of SiO_2 and water. In both instances decanting meant that the solid matter was given time to precipitate on the crucible floor and

Fig. 3.30 Above: Quartz gravel as raw material; below: silex as raw material (Source: BAI/GPIA).

13 Schwermer 2014, 61.

then the superfluous dissolution (hydrochloric acid/water) was poured off so that the silex was left. The matter was weighed while it was still slightly humid and then ground in a mortar with sodium carbonate. The reaction mixture was heated in a tin can standing in an earth hollow. The coal in this hollow had been heated in advance. The test duration was 60 minutes. It resulted in a strong melt flow; moreover, small glass pellets and a glint could be discerned (*Fig. 3.31*).

An experiment for the production of glass using quartz gravel can also be considered partially successful. The reaction mixture consisted of 1.5 g SiO_2 (silex) and 0.3 g Na_2CO_3 (sodium carbonate) along with 10 % Na_2O (sodium oxide) and was suspended with water. It was heated in a porcelain crucible that was placed in the earth for better insulation. The porcelain crucible was coated with a humid mass of $CaCO_3$ (calcium carbonate) on the inside bottom. The coals were additionally fanned by means of a blow-dryer. The test duration was 30 minutes (*Fig. 3.32*). As a result, the mixture was semi-vitrified and there was a slight melt flow; moreover, a few small glass pellets could be discerned.

The fact that the efforts at fabricating glass were only partially successful can be mainly ascribed to the kiln's failure to produce the necessary temperatures. Quartz sand/gravel requires very high temperatures since its melting point is relatively high (more than 1500 °C).

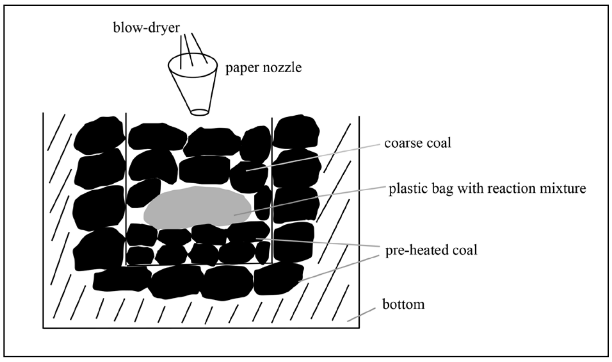

Fig. 3.31 Raw glass made from mixture of 13 g SiO_2 (silex) and 1.7 g Na_2CO_3 (Na_2O 10 %) (Source: BAI/GPIA).

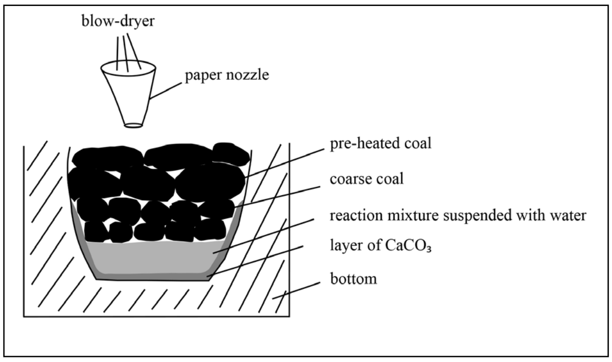

Fig. 3.32 Raw glass made from mixture of 1.5 g SiO_2 (silex) and 0.3 g Na_2CO_3 suspended with water (Source: BAI/GPIA).

3.4.3.2. Melting Raw Glass

Experiments to melt glass were carried out both in open air and inside on a stove with different reaction mixtures and vessels. These experiments were only rudimentally successful since some of the reaction mixtures did not melt at all, others melted only partially and were sometimes sintered together.

An experiment with a reaction mixture consisting of 10 g glass, 1.7 g Na_2CO_3 (sodium carbonate), and 10 % Na_2O (sodium oxide), which was kept in a plastic bag, was more successful. The mixture was heated in a tin can standing in an earth depression. Prior to that, the coal had been preheated. The coal was fanned with a blow-dryer for approx. 45 minutes; then the tin can was left sitting in its cavity with a closed lid for another approx. 30 minutes (*Fig. 3.33*). There was a strong melt flow, especially where the coal had direct contact with the can. A few small glass pellets were also discernible.

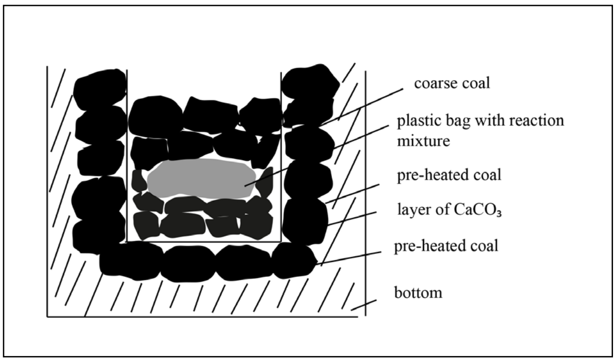

Fig. 3.33 Glass made from the reaction mixture of 10 g glass and 1.7 g Na_2CO_3 and 10 % Na_2O in a plastic bag (Source: BAI/GPIA).

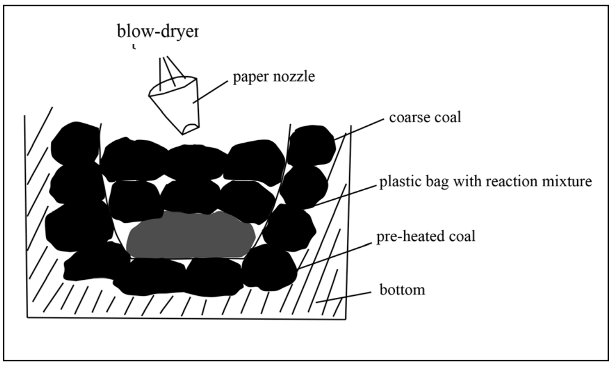

Fig. 3.34 Glass made from 4.2 g glass, 0.3 g Na_2Co_3 and 5 % Na_2O in a plastic bag (Source: BAI/GPIA).

Another experiment was conducted with a reaction mixture consisting of 4.2 g glass, 0.3 g Na_2CO_3 (sodium carbonate) and 5 % Na_2O (in a plastic bag) in a porcelain crucible. The test duration was 20 minutes. The porcelain crucible containing the reaction mixture was placed in an earth depression which had been preheated with coal. The coal was additionally fanned with a blow-dryer. To begin with, the glass obtained during a previous experiment described above was pestled and subsequently ground together with the soda in a mortar (*Fig. 3.34*). The mixture melted together, and a gas evolution took place.

The glass melting experiments were only partially successful because the necessary high temperatures of more than 900 °C could either not be reached or not be maintained long enough.

3.4.3.3. Glass Production in the Quadruple-Shelled Kiln

Apart from the glass melting experiments described above one more was conducted in the quadruple-shelled kiln in 2012 (*Figs. 3.35* and *3.36*). There, different sorts of glass were fused at more than 1000 °C in ceramic or plaster moulds formed like a spacer bead (e.g. TZ 010337-001; *Fig. 3.45*) or like the female figurine (TZ 015318-001; *Fig. 3.88*). The quadruple-shelled kiln could easily reach temperatures of more than 1000 °C (*Chap. 3.4.2.4.*).

Fig. 3.35 Filling the kiln with glass samples (Source: BAI/GPIA).

Fig. 3.36 Glass production in the kiln (Source: BAI/GPIA).

3.4.3.4. The Glass Production on Tall Zirā'a

The results of the glass melting experiments demonstrate that fusing glass on the Tall Zirā'a was possible. There are other finds which let assume that glass production and/or processing was not only possible but really executed. These finds are raw glass (TZ 012474-001; *Fig. 3.37*), amorphous and spherical glass granulate (TZ 016622-001; *Fig. 3.38*), a spherical bead without piercing (TZ 007546-001; *Fig. 3.40*) and a wound bead with its clay core of still intact (TZ 016663-001; *Fig. 3.39*).

In the northern part of Area I (Stratum 13, Square AP 119, Context 1317) a working area was found with a *mazzebe*, a working stone and hammer stones (e.g. TZ 015991-001, TZ 015994-001; *Fig. 3.41*) and several 'industrial vessels' were found (*Fig. 3.44*). It has been suggested that this kind of vessels were used in a production process without defining the kind of material processed. Maybe it was used in the processing of glass but this has still

Figs. 3.37–3.38 Left: Raw glass found on Tall Zirā'a, TZ 012474-001. Area I, AQ 120, Context 3421; right: glass granulate, TZ 016622-001 (Source: GPIA/BAI).

Figs. 3.39– 3.40 Semi-finished products. Left: bead with its clay core still intact, TZ 016663-001. Dimensions: H 0.8, D (max.) 1.4; right: bead, TZ 007546-001. Dimensions: H 1, D (max.) 3 (Source: GPIA/BAI).

Fig. 3.41 Working area with *mazzebe* and basket-shaped vessel. Stratum 13, Area I, Square AP 120, Context 4852 (Source: BAI/GPIA).

Fig. 3.42 Basket-shaped ceramic vessel, TZ 006835-016. Dimensions: L 51, W 30, H 6.3 (Source: BAI/GPIA).

to be proven. In the same context, there was also a remarkable two-chambered, basket-shaped ceramic vessel (TZ 006835-016; *Fig. 3.42*) discovered. Its specific function is as yet uncertain; maybe it was made for coating objects with suspensions for faience fabrication or it had a cultic function like a similar two-chambered, basket-shaped basalt trough found in Tall Ḥālaf.

Large numbers of glass objects from the Classical era were habitually found on the tall. The large number of glass finds from Pre-Classical times, however, are uncommon in the context of further finds in the Southern Levant since glass was usually recycled. This is an additional argument for the processing or even production of glass on the tall.

Among the valuable Pre-Classical finds are many, mostly spherical beads, a female figurine (TZ 015318-001; *Fig. 3.82*), a zoomorphic pendant (TZ 015314-001; *Fig. 3.88*), beads (e.g. TZ 014558-001; *Fig. 3.44*), two pendants (e.g. TZ 010337-001), and several rod-shaped beads (e.g. TZ 013881-001; *Fig. 3.45*).

Fig. 3.43 Left: industrial vessel, TZ 004291-001. Dimensions: D (max.) c. 9, D (opening) 3.6; right: industrial vessel, TZ 002843-001. Dimensions: H c. 19; D (foot) 12 (Source: GPIA/BAI).

Figs. 3.44–3.45 Left: spacer bead, TZ 014558-001. Dimensions: L 3.3, W 3.5, H 1.5; right: rod-shaped bead, TZ 013881-001. Dimensions: H 2.2, D (max.) 0.6 (Source: BAI/GPIA).

Plate 3.3: Stages of a tabun's construction, Part I (campaign 2003)

1.–3. Search of the clay and its dismantling

4.–6. Compilation of the ingredients for the tempering: rushes, straw, and goat hair

7.–9. Grinding, sieving and mixing of clays

10.–12. Producing of the temper

13.–15. Construction of the bottom

Plate 3.4: Stages of a tabun's construction, Part II (campaign 2003)

16.–18. Construction of the vent-holed bottom

19.–24. Construction of the kilnwall with the cleanout

25.–27. Firing the tabun

28.–30. Preparing the food and baking of the bread

Plate 3.5: Stages of a kiln's construction, Part I (campaign 2006) (Film: *App. 3.5*)

1.–2. Exploiting the clay

3.–5. Compilation of the ingredients for the temper: rushes, straw and goat hair

6–8. Grinding and sieving

9.–11. Producing the temper: mixing, pitching, milling

12.–14. Construction of the bottom: pitching, measuring and cutting

Plate 3.6: Stages of a kiln's construction, Part II (campaign 2006) (Film: *App. 3.5*)

15.–17. Construction of the vent-holed bottom

18.–20. Construction of the kilnwall

21.–23. Construction of the lid

24.–26. Producing of vessels and engobe

27.–29. Firing of the kiln: lower part is placed on the glow

Plate 3.7: Stages of a kiln's construction, Part III (campaign 2006) (Film: *App. 3.5*)

30.–32. Firing of the kiln: joining the different parts of the kiln and its firing

33.–35. Burn out of the dung from outside and inside

36.–37. Firing of the ceramic: filling of the kiln

38.–40. Firing of the ceramic: inreasing the heat and measuring the temperature

41.–43. Firing of the ceramic: opening of the kiln and taking off the ceramic

Plate 3.8: Construction of a quadruple-shelled kiln

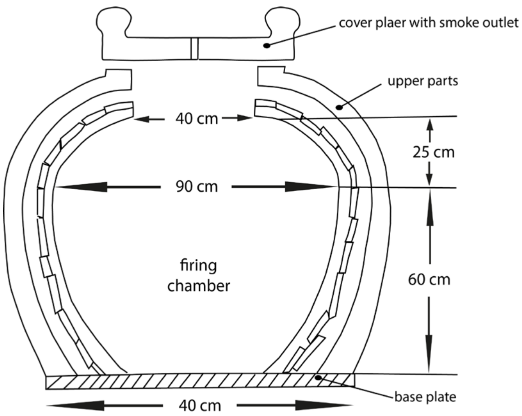

Sketch of the quadruple-shelled kiln

Construction of the quadruple-shelled kiln

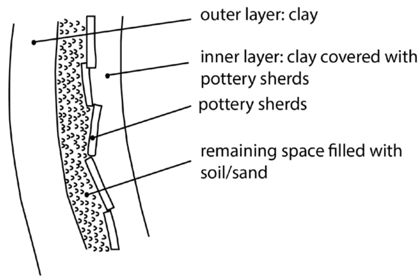

Cross section of the kiln wall

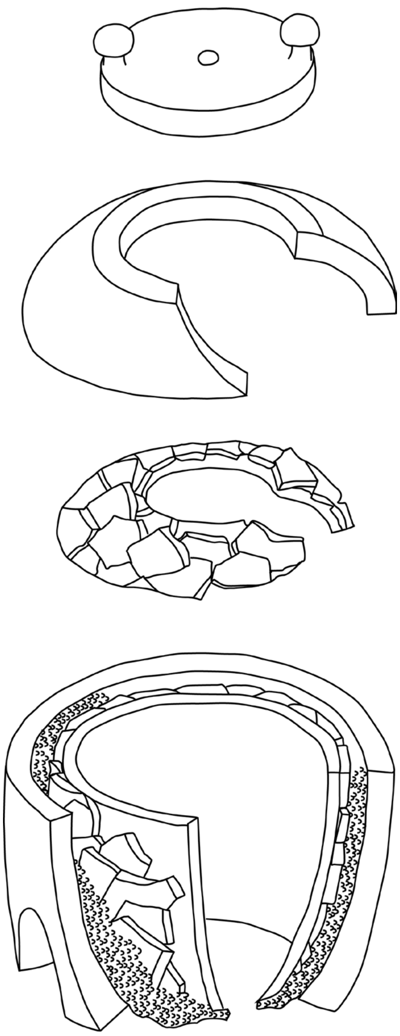

Different parts of the quadruple-shelled kiln

Construction of the quadruple-shelled kiln

Plate 3.9: Firing of ceramics in the quadruple-shelled kiln

1. Producing the ceramics 2. and 3. Filling the kiln with ceramics

4.–6. Closing the kiln, sealing the lid, and firing the kiln

7.–9. Measuring the heat

10.–12. The product

3.5. Geophysics

by Patrick Leiverkus/Armin Rauen/Dieter Vieweger/Dietmar Biedermann/Knut Rassmann/Samantha Reiter

Fig. 3.46 Tomography (Source: BAI/GPIA).

Fig. 3.47 Geoelectrics (Source: BAI/GPIA).

In the campaigns of 2001, 2007, and 2014 geophysical explorations were undertaken on the Tall Zirā'a, employing different measuring methods (*Chaps. 3.5.1.* and *3.5.3.*). Besides the classic archaeological survey methods deep drillings were also carried out in 2007 (*Chap. 3.5.2.*).

3.5.1. Geophysical Survey in 2001

by Patrick Leiverkus/Armin Rauen/Dieter Vieweger

Within the scope of the geophysical exploration on Tall Zirā'a, geoelectric mapping and twodimensional as well as three-dimensional tomographic techniques were brought into action in September/October, 2001 (*Figs. 3.46* and *3.47*). The measurements took place on the plateau and on the western slope.

The aim of the geophysical survey was:

- To be able to plan archaeological excavations in advance and to develop exact strategies for the planned excavations
- To acquire knowledge of non-excavated areas
- To leave undisturbed larger excavation areas for coming generations

For the purpose of the geophysical exploration a LGM 4-Point Light µC and a Geolog 2000 GeoTom were used[14]. On Tall Zirā'a more than 50 profiles in various configurations could be measured. Two important results can be presented:

(1) The first profile shows a measurement (in dipol-dipol configuration) which runs across the tall in an east-west direction and yields essential geological insights (*Graph 3.5*). For this, 63 electrodes were positioned at a distance of 2 m from each other. In the profile shown below a cultural layer of 5–6 m thickness can be recognised, showing a low-ohmic value (up to 100 Wm to the max.) below the dried-up surface which, as expected, appears as a high-ohmic anomaly (more than 160 Wm).

14 For the geophysical surveys undertaken see e.g.: Vieweger – Häser 2005, 8–10; Vieweger et al. 2003, 205 f.

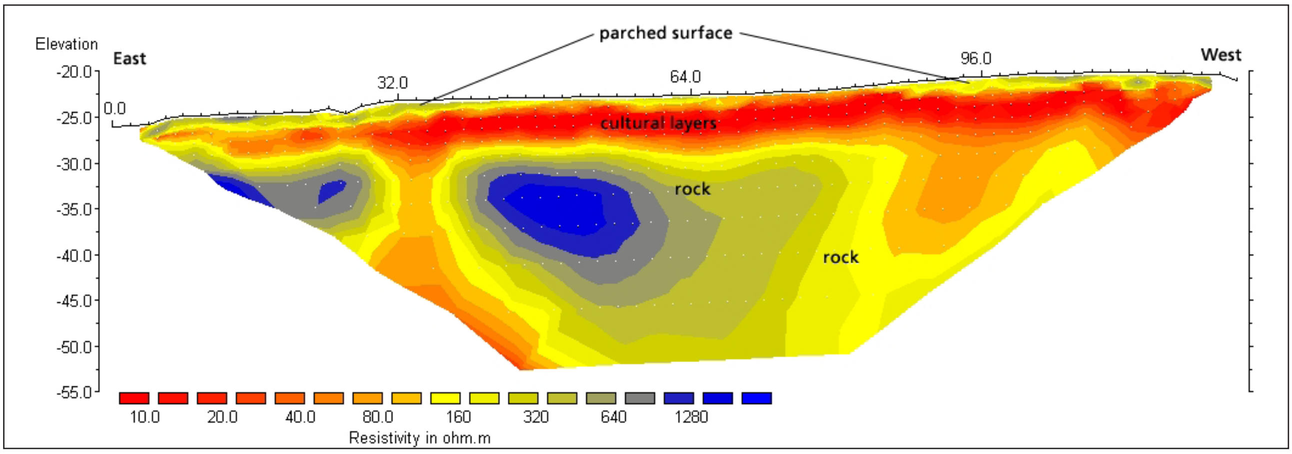

Graph 3.5 East-west profile of the tall plateau (measurement: dipol-dipol configuration, 2 m electrode gap, 63 electrodes; Iteration 4, RMS-fault = 24.5) (Source: BAI/GPIA).

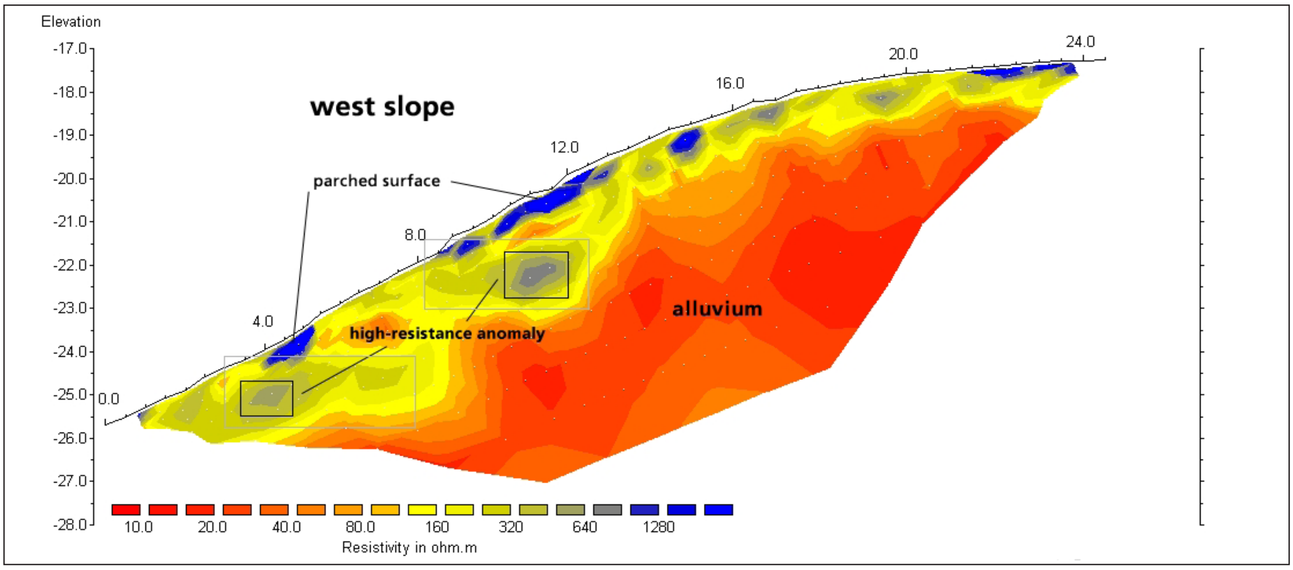

Graph 3.6 West slope profile (measurement: dipol-dipol configuration, 0.5 m electrode gap, 50 electrodes; Iteration 4, RMS-fault 12.9) (Source: BAI/GPIA).

An important observation of the measurements confirms the enormous thickness of the cultural layer of the Tall Zirāʻa.

In the east of the tall, the bedrock almost reaches up to the surface. Since the whole tall slopes slightly towards the east, the water from the artesian spring drained off in that direction. Probably the striking down-going double-conic (low-ohmic) area at 32.0 m is to be seen in connection with the artesian spring.

The deep 'basin' in the area of 94.0 m could be one of the many sinter caves in the tall.

(2) On the west slope about 20 parallel placed profiles were plotted and measured with 50 electrodes at 0.5 m distance (*Graph 3.6*). Here the dipol-dipol configuration was also used in order to ensure a better resolution of the screen process prints. This way, a location of the walls on the tall's slopes was hoped for, which was not possible on the surface. In the illustrated model, two high-ohmic anomalies can be traced at 4.0 m and 11.0 m, lying up to 2 m below the surface. Since these anomalies occur in all 20 parallel profiles, it can be assumed that they are related to the remains of city wall structures.

3.5.2. Crosshole Investigations in 2007

by Dietmar Biedermann

Fig. 3.48 Geological depth profile (Source: BAI/GPIA).

Fig. 3.49 Insertion of the borehole equipment (Source: BAI/GPIA).

The informative capacity of geophysical examinations is usually limited to a few metres below the surface of the terrain to be explored. The resolution accuracy declines with increasing depth, independent of the method used. This applies to both wave-based methods such as ground radar and seismology and potential drop methods such as geoelectricity (*Fig. 3.52*) and geomagnetism. This circumstance is particularly disadvantageous when it comes to very large excavation sites like the Tall Zirā'a. Where excavation depths of 18 m and more are necessary these methods cannot provide any information on structures buried in the deeper layers, especially if there are several archaeological strata.

This problem can be solved by the method of crosshole examinations. For this, two boreholes are drilled at a distance of several metres (*Fig. 3.48*). Depending on the method applied, either ground radar antennae or geoelectric probe heads are lowered into these boreholes (*Fig. 3.49*). Afterwards the terrain between them is explored geophysically, thus achieving a much better resolution in the deeper strata than would have been possible with measurements from the surface. In order to find out whether crosshole examinations can be conducted on the Tall Zirā'a with its partially very complex layering, the engineering office 'Hani Karasneh' from Irbid was consigned in 2007 to drill six boreholes 7 m deep and then conduct geoelectric measurements. The holes were drilled by means of the dry drilling method with air flushing. They were driven in the north-western area of the tall. The location and orientation of the drillings is represented in *Figs. 3.50* and *3.51*.

In order to meet archaeological requirements in terms of precision the electrodes were placed at a distance of 0.3 m from each other, allowing an object resolution of approx. 0.5 m. The measurements were conducted by means of a combination of surface and depth soundings.

The boreholes were regularly spaced in a grid of two parallel rows, each with three drillings set at a distance of 2.5 m from each other. The measurements were carried out by means of multielectrode equipment developed by the company 'Erich Lippmann Geophysical Instruments' that allows simultaneous activation of 50 electrodes.

In the course of the works on the Tall Zirā"a multiple measurements from borehole to borehole were conducted to assemble a database for future processing.

The data obtained could later be processed by a mathematical inversion programme and then be converted into depth cuts. The following figure presents two selected depth cuts. The first figure shows an image along the 2 m x 6 m grid, the second one a profile running at right angles to it. Areas with low conductivity are represented red, those with better conductivity are blue. *Graph 3.8*, showing the first profile between borehole 1 and borehole 3, reveals a filling zone (yellow) approx. 1 m beneath the parched surface (blue), that clearly contains structures at 2 m, 6.5 m, and 10.5 m. During the excavations in the years 2008 to 2011, they could be identified as large edificial structures.

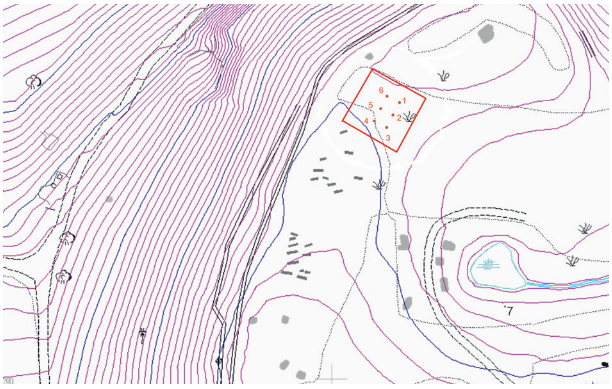

Figs. 3.50–3.51 Location and orientation of the drillings carried out in 2007 (Source: BAI/GPIA).

Fig. 3.52 Geoelectric depth profile at the north-eastern side of the tall (Source: BAI/GPIA).

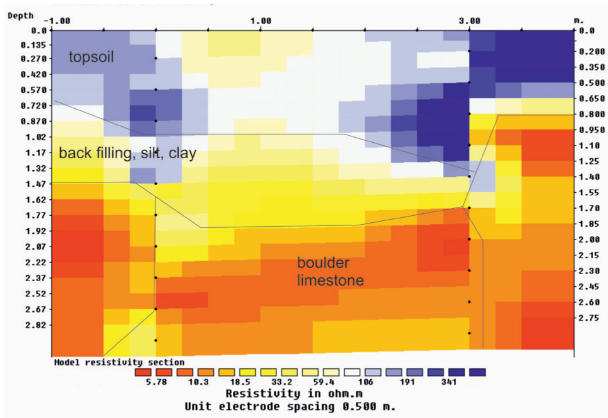

Graph 3.7 Profile of borehole 2 and 3. Iteration 2 Abs. error = 28.4 % (Source: BAI/GPIA).

Graph 3.7 shows the same depth sounding. A surface layer of approx. 0.6 m is followed by a filling layer, which in turn is followed by a zone filled with rocks (red). In this case, however any further distinction cannot be made due to the limited resolution of the geoelectrical equipment.

When combining the depth cuts of all measurements conducted, structures consisting of single limestone rocks are discernible. Naturally, no conclusions pertaining to the form and function of possible buildings can be drawn from the single measurements.

To summarise, this method definitely appears to be very promising for future survey tasks since it yields a higher resolution of images taken in greater depths or regardless of the depth required than measurements conducted only from the surface.

However, even the method of crosshole examinations has its limits in that it cannot provide further insights when the excavation circumstances are complex since then the method-inherent resolution of the geoelectrical equipment is only approx. 0.2–0.3 m and thus cannot depict more delicate structures.

Another disadvantage of crosshole investigation is that in the process of drilling the boreholes parts of the archaeological strata are destroyed. However, this destruction is actually only very marginal.

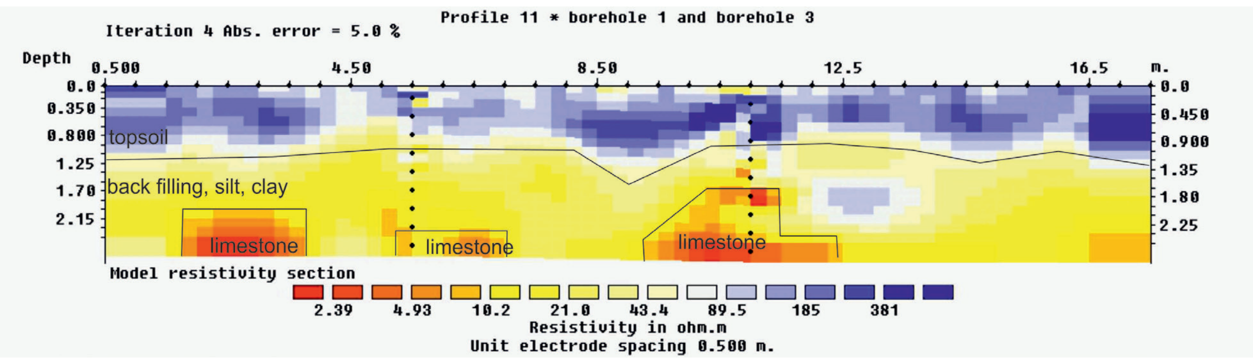

Graph 3.8 Profile of borehole 1 and 3. Iteration 4 Abs. error = 5.0 % (Source: BAI/GPIA).

3.5.3. Seeing Beneath the Ground—Geomagnetic Prospection in 2014

by Knut Rassmann/Samantha Reiter

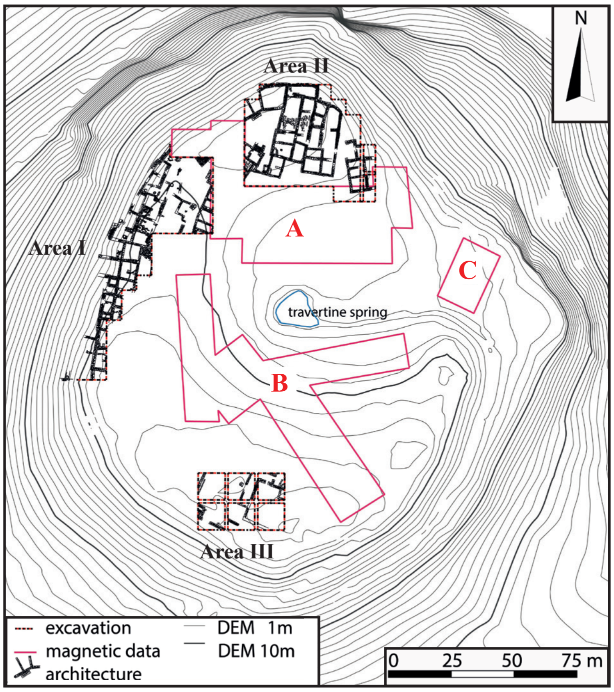

Fig. 3.53 Tall Zirā'a. Overview of the location of the magnetic prospection. Archaeological remains of Stratum 3 (Source: K. Rassmann/S. Reiter).

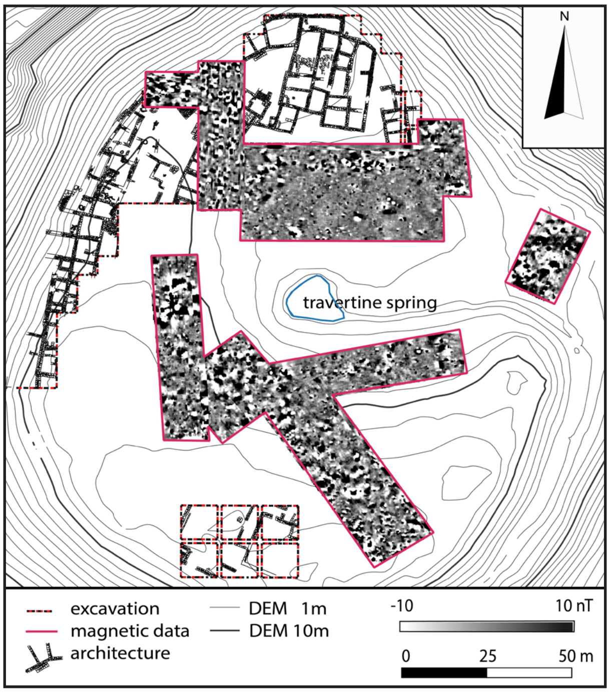

Fig. 3.54 Tall Zirā'a. Overview of the magnetic prospection (Source: K. Rassmann/S. Reiter).

The 'Technical Department of the 'Romano-Germanic Commission of the German Archaeological Institute' in Frankfurt conducted a magnetic prospection campaign on Tall Zirā'a in 2014. This campaign was intended as a means of revealing architectural remains outside the excavation area so that they might be interpolated into walls and building structures along the periphery of the excavation.

To this end, the team surveyed three disparate parts of the tall (Area A–C; see *Fig. 3.53*) by means of a high-resolution SENSYS MAGNETO ARCH five sensor array. Tall Zirā'a's magnetic prospection potential is limited by its many layers and the low magnetic contrast of the limestone which was the principle building material used on site. Despite these limitations, the magnetic prospection revealed some indications of higher concentrations of building remains and a smaller number of walls within an area of 0.5 ha.

3.5.3.1. Technical Equipment and Data Processing

The prospection was conducted by a 5-channel magnetometer (SENSYS MAGNETO ARCH) mounted on a hand-propelled fibreglass carriage. The gradiometers were set at 0.25 m or 0.5 m intervals. A walking pace of c. 4–5 km/h yielded a mesh of 0.25 m/0.50 m by approx. 0.06 m–0.08 m. The magnetometer systems used 5 FGM-650B tension band fluxgate vertical gradiometers with 650 mm sensor separation, a ±3000 nT measurement range and 0.1 nT sensitivity. The prospection was organised in small rectangular fields as close to the excavation areas as possible. Although the corner points of the prospection areas were measured by DGPS, the carriage was also combined with an odometer in order to provide the most precise location information possible for the measurment lines.

3.5.3.2. Data Processing

The SENSYS MonMX, DLMGPS and MAGNETO®-ARCH software package was used for data acquisition, primary data processing, interpolation and export. Because each track contained the measurements of the 5 or 16-channels and the DGPS data, it was saved separately. Postprocessing, however, was completed with Oasis montage 8. To effectuate the changeover, the results were exported as surfer 7 file (which can be easily imported into GIS). The maps presented here were produced with Quantum GIS 2.8. The use of surfer 7 files enables the modification of threshold and colour scale. Based on the surfer 7 files, contour maps in two different resolutions were calculated by the GRASS too r.contour.step. The first of these was completed with a range from -100 to +100 nT in classes of 10 nT which should visualise the locations of basalt stones and iron contamination. A second map showing a range -10 to +10 nT in classes of 1 nT objects visualises objects which have less magnetic contrast. The latter can be used to analyse data with lower contrasts, such as limestone architecture.

3.5.3.3. Methodological Remarks

Magnetic prospections on multi-layer settlements (especially talls) are both complicated and challenging. The long-term use of sites leads to numerous overlapping archaeological features from different occupation periods. Magnetic prospection normally detects structures up to a depth of 1.2 m–1.5 m. Naturally, in those instances in which the structures overlap, one is faced with the problem of bringing the structures thereby revealed into the appropriate chronological order. The contrast of an anomaly depends upon the strength of its magnetic field as well as its depth (distance to the device). This means that an object with a strong magnetic field, like a burnt brick would produce a clearer signal at -0.8 m than an unburnt clay brick at a depth of 0.4 m.

A further disadvantage to the Tall Zirā'a prospection was the necessarily small size of prospection areas. The analysis and interpretation of magnetic data gets easier with larger prospection areas. The reading of magnetic data has a great deal to to do with pattern recognition. For example, it is easier to understand a Copper Age settlement with numerous burnt houses within a large prospection area stretching over dozens of ha than it is to come to grips with a small area on a multi-layer settlement. This problematic constellation often becomes even more complicated with recent contamination or destruction events. Despite these limitations, prospections on talls are often successful and deliver valuable information about the upper layers of the sites, such as in Uivar, Roumania[15], Okolište[16], Tall Chuēra[17] and Tall ar-Rauḍa (Tall al-Rawda)[18].

3.5.3.4. Results

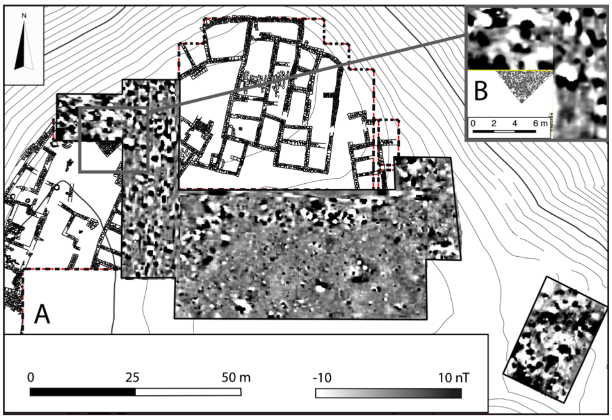

Fig. 3.55 Northern area of Tall Zirā'a. Magnetic prospection with detail of the tower base (Source: K. Rassmann/S. Reiter).

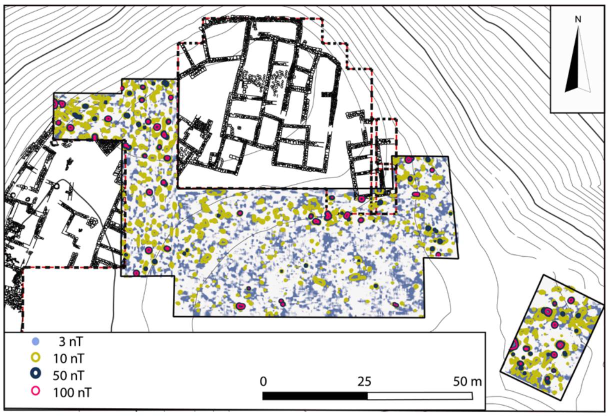

Fig. 3.56 Northern area of Tall Zirā'a. Contour map of the magnetic prospection (Source: K. Rassmann/S. Reiter).

Aside from the grey-scale maps (*Figs. 3.54, 3.55* and *3.57*) another key element for analysing the data are the contour maps, especially with a resolution of -10 to +10 nT. As was mentioned above, the coarser resolution of 10 nT can be used to reveal iron objects or larger basalt stone. The large excavation area is helpful insofar as it allows us to detect more general linear patterns (like the orientations of walls) in the magnetic data. Magnetic data immediately adjacent to the excavation are especially valuble in order to determine whether or not all walls are truly visible in the magnetic data. As mentioned, the low contrast of limestone was a serious limitation to our prospection. This is most clearly apparent in the coarse visibility of the base of the tower in the northern area (*Fig.*

15 Schier – Drașovean 2004, 151.

16 Hofmann et al. 2007, 55 f.

17 Meyer 2010, 199 ff.

18 Gondet – Castel 2004.

Fig. 3.57 Southern area of Tall Zirā'a. Magnetic prospection (Source: K. Rassmann/S. Reiter).

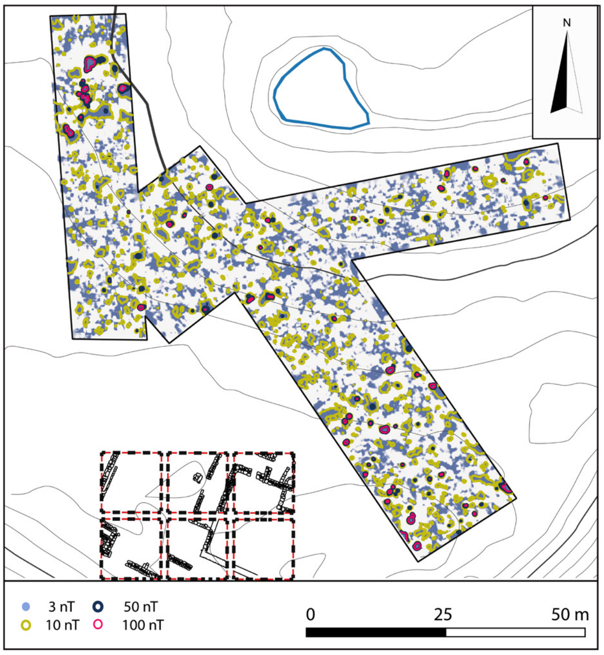

Fig. 3.58 Southern area of Tall Zirā'a. Contour map of the magnetic prospection (Source: K. Rassmann/S. Reiter).

3.55). The excavation data opens a window from which one might reconstruct the course of the tower base in the magnetic data. However, without these data, the magnetic signature is not clearly interpretable.

Another source for the analysis of the magnetic data are the architectural remains which are visible on the surface of the ground. In some spots, building materials were only partly covered by topsoil. The majority were limestone with some (much rarer) basalt stones. As expected, the limestone demonstrated low magnetic contrast which was not clearly visible in the magnetic data while the basalt elicited a clear response.

In the case of the magnetic data from Tall Zirā'a, four valuable classes has been found within the contour map (3 nT, 10 nT, 50 nT and 100 nT—*Figs. 3.56* and *3.58*) The 3 nT line represents mainly limestone while the 10 nT and 50 nT presumably represent basalt. Behind the 100 nT line, one might assume the presence of iron objects and/or larger basalt stones.

A more general trend which is remarkable would be the concentration of basalt stones close to the excavation areas (*Figs. 3.54, 3.55* and *3.57*). On the top of the tall close to excavation Area II is an area with a lower density of magnetic anomalies which exhibit readings of >10 nT. There are different explanations for this occurance. While it might be possible that the surrounding area simply exhibits fewer architectural remains, other feasible alternatives would be that either the building remains which are present were covered by a massive layer of toposoil or that the walls were principlly made of limestone.

Interestingly, the 100 nT and 50 nT contours generally deliver only point structures without noticeable structures. However, the 10 nT and especially the 3 nT contours indicate linear features (presumably wall; see *Figs. 3.56* and *3.58*). The general patterns of these linear features corresponds in part with the excavation.

In order for the architectural remains to be revealed, the 3 nT lines were selected in order to find indications of the courses of wall remains. The anomalies were mainly linear, within a general pattern of lines often with a right angle.

In the northern Area A, the general pattern revealed by the geomagnetics corresponded less with excavation Area II. Interestingly, the orientation was more similar to excavation Area I. Presumably the buildings from Stratum 3 in excavation Area II did not continue in the prospection area.

The linear structure in prospection Area C close to the southern excavation corresponded (at least in part) in terms of its direction. It is obvious that the intensity of dipols is high in the prospection area between excavation Areas I and II. The linear structures are marked by the 3 nT and 10 nT lines as well as by 50 nT.

The geomagnetic prospection revealed some coarse indications of architectural remains. The evidential value for single features is low, but the more general pattern of linear anomalies is more reliable. The evaluation of the geomagnetic data can be done by small test trenches or via the use of other geophysical methods, such as Ground Penetrating Radar (GPR). When one considers the low magnetic contrast of the limestone, GPR has more potential at Tall Zirā'a.

Fig. 3.59 Tall Zirā'a. Contour map (2 nT) with possible indications of walls (Source: K. Rassmann/S. Reiter).

3.6. Landscape Archaeology

by Patrick Leiverkus/Katja Soennecken/Linda Olsvig-Whittaker

Fig. 3.60 Tall Zirā‘a and its enviroment. Photograph taken in 2007 (Source: BAI/GPIA).

Archaeological sites are located within a landscape, the surrounding physical, cultural and biological environment which provides the context, driving factors and the system in which an ancient settlement functioned. The study of the archaeology of such environments, called landscape archaeology, came late to the Near East, in the 1970's but was well developed in Europe for much of the twentieth century[19].

Landscape archaeology attempts to describe and understand spatial and functional relationships of features such as settlements, roads, installations, fields, etc. with their physical, ecological and cultural environment. Important questions of this research discipline are, for example:

- What is the importance of water in determining site locations?
- How does political change drive the location of roads?
- What are the patterns of land use by settlements?

Sometimes there is a wealth of data already available to address such questions, which has not yet been examined in the context of landscape. This is particularly true for archaeological surface field surveys in which information about location, distribution and organisation of past human cultures across a large area are collected.

Surface survey results can be studied spatially against physical and ecological features using GIS methodology; and can also be assessed with knowledge of ancient trade routes, political boundaries, etc. For this work, GIS systems are invaluable and have become freely available for the individual user via tools such as Google Earth and QGIS, greatly enhancing such work.

In the years 2009 to 2012 a survey in Wādī al-‘Arab and Wādī az-Zaḥar was carried out by the Biblical Archaeological Institute Wuppertal (BAI) and the German Protestant Institute of Archaeology (GPIA), in order to get more information on the settlement patterns in the environment around Tall Zirā‘a and in different periods (*Chap. 3.6.1.*)[20]. The aim was to get a thorough understanding of the landscape in which the Tall Zirā‘a is the most prominent archaeological site. At the very heart of such an exploration are the questions of settlement pattern, distribution, relations and relative importance through time. Furthermore, the Wādī al-‘Arab is one of the few easily passable ascents from the Jordan Valley to the Irbid-Ramtha basin and so has always been part of trade routes from the Mediterranean coast to Dimašq (Damascus), Baġdād or ‘Ammān (*Figs. 1.21–1.23*). Questions of the actual trade routes through this area and their shifting importance arise. The survey kept a special focus on evidence that could help answer these questions.

Furthermore, the location of archaeological sites and features have been mapped and preliminary results have been analysed using Correspondence Analysis (DCA) and Canonical Correspondence Analysis (CCA).

This investigations will be described in the following sections. Further and extensively presented results of the surface survey will be published in Volume 8.

19 Wilkinson 2003, 10 f.

20 Leiverkus – Soennecken 2016, 509–518.

3.6.1. The Wādī al-ʿArab Survey

by Patrick Leiverkus/Katja Soennecken

Fig. 3.61 Area of investigation: Zone A (Tall Zirāʿa hinterland) and Zone B (Wādī al-ʿArab region) (Source: BAI/GPIA).

The Wādī al-ʿArab has been surveyed several times before. The most notable surveys are the ones by N. Glueck in 1942[21], by S. Mittmann in 1963–1966[22] and by J. W. Hanbury-Tenison in 1983[23]. While all of them are valuable and gave rich sources of information, they cannot give the completeness and level of detail needed for the purpose of the 'Gadara Region Project'. The former two surveys had a much broader area in view and therefore could only cover the major sites of the area of interest. J. W. Hanbury-Tenison's survey in its level of detail is much closer to the 'Gadara Region Projects' aims, but is restricted to two areas and does not cover the full Wādī al-ʿArab (*Fig. 1.27*). Furthermore, almost 30 years later, a fresh look on all the given data seems appropriate considering the now much more elaborate stratigraphy and typology of the region is available due to the continuing efforts of the 'Gadara Region Project'.

With the knowlegde of the previous surveys and the target of a hinterland survey in mind, the approach chosen was two-fold: On the one hand revisiting the known sites enriching the information about them, on the other hand filling gaps by surveying the areas that had not been surveyed before. During the three seasons (2009 to 2012) the hinterland of Tall Zirāʿa was examined. The area of investigation was divided into Zone A (Tall Zirāʿa hinterland; c. 20 % of the survey area) and Zone B (Wādī al-ʿArab region; c. 80 % of the survey area), together covering about 400 km^2 from Tall Zirāʿa to Irbid in the east, and north to the Yarmūk River watershed (*Fig. 3.61*). An effort was made to cover Zone A completely, whereas in Zone B the survey concentrated on the known larger sites.

The exact location of all sites was measured by a GPS, pottery and small finds were collected for comparison and all descriptions of the current state were refreshed. Detail and overview pictures taken. All gathered information was entered into a database.

21 Glueck 1951a.

22 Mittmann 1970.

23 Hanbury-Tenison et al. 1984, 385–424; Hanbury-Tenison 1984, 230 f.

Fig. 3.62 Site 215/226-8. Ottoman penstock mill at the south side of the Wādī al-ʻArab (Source: BAI/GPIA).

Fig. 3.63 Location of Sites 211/225-7 and 211/225-8 in relation to Tall Zirāʻa and Gadara (Source: BAI/GPIA).

Fig. 3.64 Site 211/225-8. Architectural remains dated to the Middle Bronze Age (Source: BAI/GPIA).

Fig. 3.65 Site 219/227-1. Overview on Tall Kinīse (Source: BAI/GPIA).

In the 2009 campaign 78 sites were recorded; 30 of them have not been known before. Over 80 % of the sites relate to the Classical era. The other sites were inhabited in the Bronze Age, Iron Age or different Islamic periods. Lithic sites could not be discovered. The large Tall Qāq (Ḫirbet Bond) and Tall Kinīse (Ra'ān; Site 219/227-1; *Fig. 3.65*) were revisited. The area around the Wādī al-ʻArab Dam was covered as well, which was partly surveyed by T. M. Kerestes in 1978 and J. W. Hanbury-Tenison in 1983 (*Chap. 1.4.3.2.*). Furthermore, the slopes of the Wādī al-ʻArab from Tall Zirāʻa upwards to the region of Ṣēdūr and Dōqara were surveyed. Most parts of this area had not been surveyed in detail before. While Ṣēdūr and Dōqara are mentioned by S. Mittmann, the surroundings revealed many sites which shed new light on the settlements' agricultural subsistence.

The northern slopes of the wādī directly upwards from Tall Zirāʻa are characterised by a dense occurrence of water sources. Many of the sites found there relate to them. This can shed further light on water management in the region (*Fig. 3.62*). One smaller site directly across the wādī from Tall Zirāʻa deserves special attention. This site was published first by T. M. Kerestes in 1978 (Site 2 in the Wādī al-ʻArab; i.e. Site 211/225-8; *Fig. 3.64*) and identified to be of Middle Bronze Age date[24]. Its position relates this site directly to Tall Zirāʻa. Together they control a narrow passage in the wādī and of course a direct line of sight is given between them (*Fig. 3.63*). Just 50 m up the slope another previously unknown site could be recorded with architectural remains of the Roman period (Site 211/225-7; *Figs. 3.63* and *3.65*). This site does not only overlook the lower wādī, as the nearby older one, it has also a direct line of sight to Gadara which is missing in the lower position. This gives a hint on the shifting of central settlement from Tall Zirāʻa to Gadara during the Classical era.

In the Wādī al-ʻArab above the Tall Zirāʻa five penstock mills were recorded together with two dams (see e.g. *Figs. 1.37* and *3.62*). J. W. Hanbury-Tenison only mentioned three mills. All of them can be dated to the Ottoman period.

24 Kerestes et al. 1977/1978, 119.

Fig. 3.66 Site 214/227-3 on the edge high above the Wādī al-ʻArab (Source: BAI/GPIA).

Fig. 3.67 Site 233/229-1. Ottoman mosque in Ḫarǧā with a Roman or Byzantine sarcophagus (Source: BAI/GPIA).

Fig. 3.68 Site 224/217-3. Dolmen north-west of Kafr Yūbā (Source: BAI/GPIA).

Fig. 3.69 Site 228/213-5. Roman – Byzantine sarcophagus fragments and grave niches near ʻAydūn (Source: BAI/GPIA).

During the season of 2010, 57 sites were recorded. While during the first season of 2009 the lower part of the Wādī al-ʻArab from North Šūna up to Dōqara was surveyed, this season the survey covered the area from Dōqara up to the vicinity of Irbid. The nature of the landscape changes while approaching the upper part of Wādī al-ʻArab. The wādī is deeper incised and one can find the settlements mostly at the edges high above the wādī (*Fig. 3.66*). The majority of the ancient settlements were known before by the work of N. Glueck and S. Mittmann.

In Season 2011 the close inspection of the hinterland of the Tall Zirāʻa (Zone A) was enhanced with a broad view on the Wādī al-ʻArab region by revisiting the major sites in the whole area (Zone B). The exact location of all sites was measured by GPS, pottery was collected for comparison and descriptions of the current state were refreshed. Thus several caves, graves, dolmens, cisterns, water basins, and a water mill could be documented (*Figs. 3.67–3.69*).

Altogether 206 sites were identified, georeferenced and described, of which 30 were previously undescribed. It was possible to discover a representative amount of pottery from all sites, a concise overview of the occupational history of the Wādī al-ʻArab can be derived.

One important result of revisiting the previously published sites during the survey in the Wādī al-ʻArab is the observation of heavy destruction on many sites in the last decades. The rapid increase of deterioration is alarming. Only recently a large tall with Roman, Byzantine and Islamic occupation (no. 026 in the J. W. Hanbury-Tenison Survey[25]; Site 211/224-2; *Figs. 3.70* and *3.71*) south of Tall Zirāʻa has been completely destroyed by bulldozing. Ancient remains could be seen covering an area of approx. 130 m x 90 m—some of the stones still *in situ*, but most of them shoved away. The section produced by a bulldozer showed at least two layers of Roman – Byzantine settlement, divided by layers of ash (*Fig. 3.71*).

Almost all of the modern villages date back at least to the Roman – Byzantine period, some of them to the

25 Hanbury-Tenison et al. 1984, 390.

Fig. 3.70 Site 211/224-2. Settlement on a tall (Source: BAI/GPIA).

Fig. 3.71 Site 211/224-2. Two layers of Roman – Byzantine settlement divided by layers of ash (Source: BAI/GPIA).

Fig. 3.72 Site 228/221-1. Ḫirbet Srīs. Robbery trench with a wall, around it burnt vegetation (Source: BAI/GPIA).

Fig. 3.73 Site 220/224-1. Grave entrance with robbery trench (Source: BAI/GPIA).

Iron or Bronze Age. Only very few of the ancient settlements are not covered and destroyed by modern settlements. That includes most of the Islamic history of the Wādī al-ʻArab. It is especially sad to note that none of the old mosques in the area of the wādī, some oft them dating back to the Medieval period, are in existence today. The oldest mosque in the area, to our knowledge, can be found in the village Ḫarǧā (Site 233/229-1; *Fig. 3.67*). Even this one is in a very bad condition.

Despite the continuing demolition of the old sites, a huge amount of pottery from all sites could be recovered. They give us a precise insight of the wādīs' history.

Several smaller sites are destroyed by agricultural activities (especially olive tree cultivation) which leaves sites in an unrecognizable state. These observations lead the members of the 'Gadara Region Project' to the firm commitment to execute this survey not only as a necessary complement to an excavation but also as a preservation of knowledge on the history of the Wādī al-ʻArab, most of which will be lost in the near future.

Apart from the heavy destructions another problem emerged clearly: most of the unknown or at least unpublished sites showed traces of recent unauthorised excavation/digging, mainly concentrating on tombs (metal detectors) and removing most of the finds. In the following two examples will be presented.

Site 228/221-1 is first described by S. Mittmann (M 059)[26] and called Ḫirbet Srīs and comprises 1.5 ha. By visiting it, the vegetation was burnt down (*Fig. 3.72*). Pottery, *tesserae*, a cistern and a robber trench (three layers of ashlar masonry visible) could be found. The pottery could be dated to Roman, Byzantine, and Islamic (Umayyad) periods.

Site 220/224-1 was not published before and is located north of Fūʻarā, south-west of Wādī al-ʻArab. An area of approx. 2 ha (250 m x 80 m) was covered with pottery, *tesserae* and some pieces of glass. Additionally cisterns, a quarry, some natural caves and graves were found (*Fig. 3.73*). Most of the graves were only visible because of recent robber trenches and nearly all of them were shaft tombs. In one robber trench ashlar blocks could be seen. The pottery dates to Roman, Byzantine, and Islamic periods and suggest at least two phases of occupation.

26 Mittmann 1970, 28 no. 59.

3.6.2. Landscape Archaeology and its Methods Used in the 'Gadara Region Project'

by Linda Olsvig-Whittaker

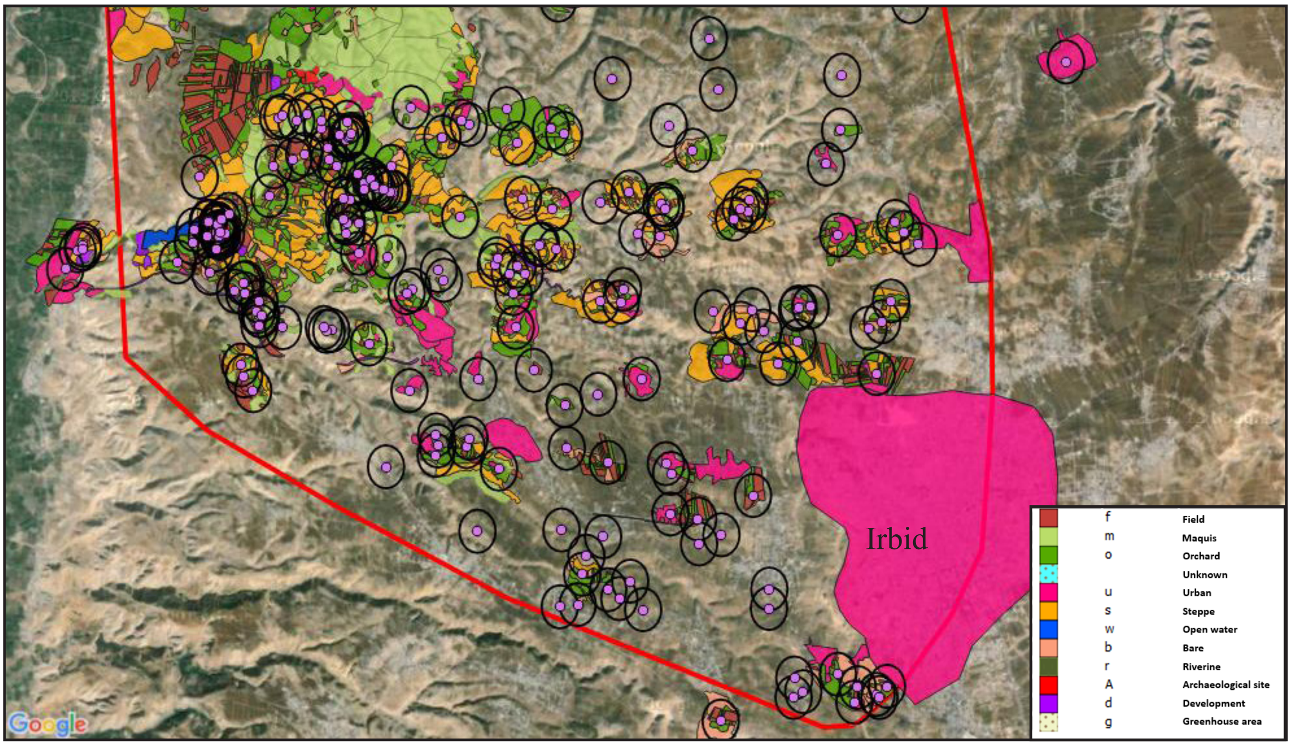

Fig. 3.74 Habitat mapping of Zone A and Zone B. Large scale (Source: L. Olsvig-Whittaker).

Within the 'Gadara Region Project' several methods of Landscape Archaeology have been used. But this work in 2016 is still in its very early stages and methods are likely to change substantially as the research continues. For this reason only preliminary results are given in this chapter. A full report of results will be presented in Volume 8. So far, habitat mapping according to methods developed in BioHab[27] and EBONE[28] as well as the multivariate analysis methods of Canonical Correspondence Analysis (CCA)[29] and Detrended Correspondence Analysis (DCA)[30] have been used as methods. They will be described in the following sections.

3.6.2.1. Habitat Mapping

Habitat mapping as developed in BioHab and EBONE uses physiognomic categories—growth form and height categories—rather than species composition as the basis for classification of habitat. The system is now widely used for European habitat monitoring since the reliance on remote sensing and orthophotos enables coverage of large areas in a standardised fashion. The mapping begins from aerial photographs or remote sensing images. In the present study, the images used were from Google Earth Satellite Imagery[31] maps at different resolutions, using the Open Layers Plugin option in QGIS 2.12[32].

The boundaries of the survey area and the sites were superimposed on a Google Earth image, and sites were mapped from their centroid coordinates on QGIS (*Fig. 3.74*). Half kilometre buffers around each site were done in QGIS.

Originally the entire area was to be mapped to habitat, but this proved very time consuming. Instead each site is currently being mapped by eye and classified based on the Google Earth images (see *Fig. 3.74* with Site 219/221-1 as an example). Polygons were drawn by eye at the 1 : 10,000 level (at time reduced to 1 : 5,000 when clarity was needed). The landscape observed by satellite was relatively simple, and was intuitively classified into crude categories as orchard, maquis, steppe (which later proved to be mostly open shrubland), urban, riverine, field, bare,

27 Bunce et al. 2011.

28 Olsvig-Whittaker et al. 2011.

29 Jongman et al. 1995, 137–144.

30 Jongman et al. 1995, 105–109.

31 https://en.wikipedia.org/wiki/Google_Earth (12.7.2016).

32 https://en.wikipedia.org/wiki/QGIS (12.7.2016).

water, archaeological site, and development (not urban, can include military bases, water installations, etc.). The ground verification started in summer 2016.

For the multivariate analysis, categorical data were used. The habitat mapping provided the environmental matrix data as the percentage of the area around each site in each habitat category. The response 'species' variables were of two types: epoch classification and size categories. These variables were provided as follows.

Habitat Categories Used in this Mapping (from QGIS Properties of the Layer)

Habitat categories used in this mapping are (see the legend in *Figs. 3.74* and *3.76*):

- Field (brown colour)
- Maquis (light green colour)
- Orchard (dark green colour)
- Unknown (turquoise colour with red point
- Urban (pink colour)
- Steppe (yellow colour)
- Open water (blue colour)
- Bare (light pink colour)
- Riverine (olive green colour)
- Archaeological site (red colour)
- Development (purple colour)
- Greenhouse area (white colour with brown point)

Visually on Google Earth satellite images, steppe, fields and bare areas are difficult to distinguish, but fields are generally rectangular, while steppe has some vegetation (obviously grading into bare areas). Maquis is more open vegetation. Orchards (presumably nearly all olive groves) are regular in form. Urban areas are quite clear with their roads. Riverine vegetation is relatively dark, dense and linear. Archaeological sites are a little difficult but can be checked as known locations. Development is a catch-all term for military camps, water systems, and other non-urban constructions. Greenhouse areas look like fields but are white from the plastic coverings.

Ground verifications started in summer 2016 for the habitats mapped from satellite images. Hence the categories used are preliminary. The site types are categorised as follows:

- Building
- Cave
- Cistern
- Installation
- Quarry
- Scatter
- Settlement
- Tall
- Tomb

Natural vegetation appeared to include a range from steppe to shrubland to riverine forest; anthropogenic landscape (which dominate) included fields, urban areas, large installations and large archaeological sites. Open water, though rare, was important.

These are only preliminary findings. The immediate next steps will be to develop automated mapping on GIS of the habitats for the entire area, based on algorithms derived from the habitat polygons drawn by eye. This will make possible the analysis of all sites much more rapidly and with different scales of relation to environment.

Epoch Classification

Epochs were used as provided from the survey database, but broader groupings were made as follows in order to provide enough sites in each class for data analysis:

- Neolithic and Chalcolithic
- Bronze Age
- Iron Age
- Hellenistic
- Roman
- Byzantine
- Islamic
- 'Undetermined' and 'modern' not into a group

Fig. 3.75 Site 220/225-1. Agricultural installation (Source: BAI/GPIA).

Size Categories

Site size is a continuous variable. However to be used as an environmental variable in the analysis, this had to be changed to a categorical variable.Three very coarse size categories are used in the analysis:

- A few metres in area
- A dunum (0.1 ha) in area or less
- Several dunums in area

An Exapmple for Habitat Mapping: Site 220/225-1

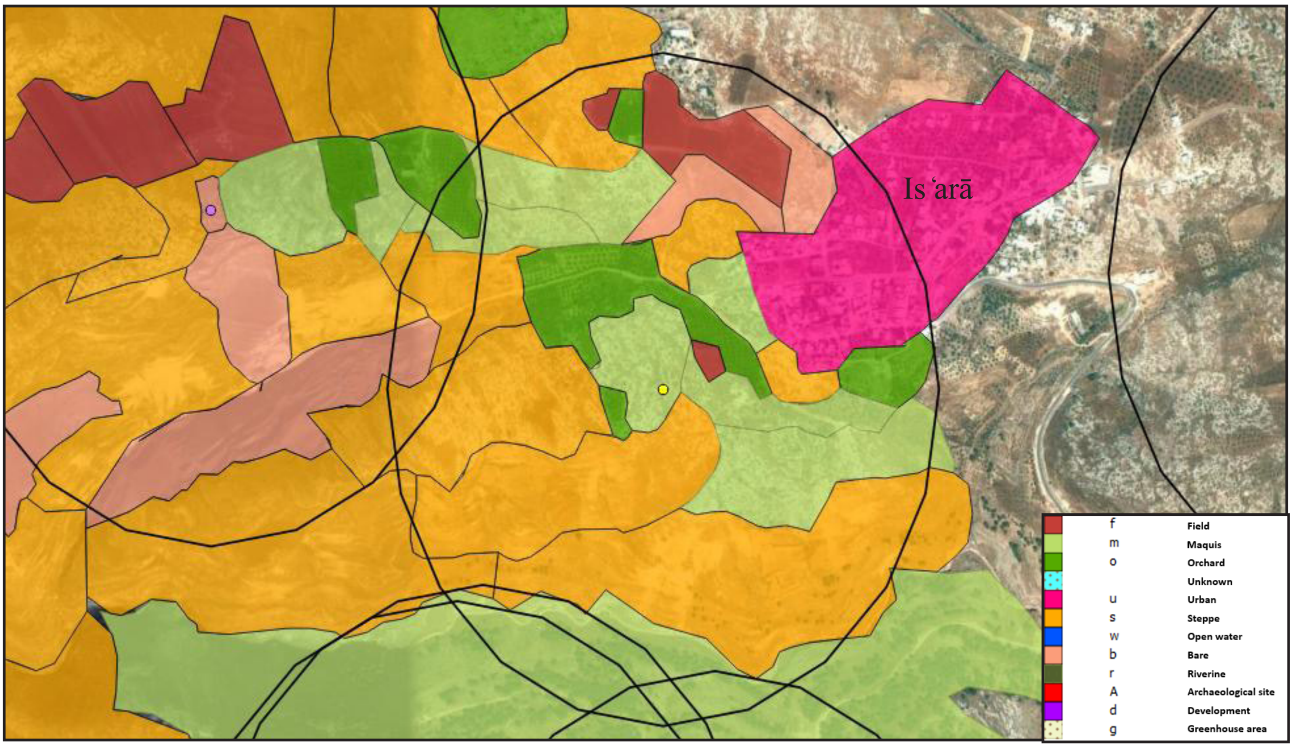

Fig. 3.76 Habitat mapping. Small scale. Site 220/225-1 in the middle (yellow) and Site 219/226-1 on the left (pink) (Source: L. Olsvig-Whittaker).

Site 220/225-1 is located south-west of the modern village of Isʿarā at the western slope of Wādī al-ʿArab (*Fig. 3.76*). A part of the site is still used for agriculture. Olive trees are planted in the northern part of the site. Pottery collected dates it to late Roman to Umayyad periods. Former surveyers described Iron Age and Hellenistic occupations, but this could not be verified[33]. At least six cisterns with various sizes have been found and documented as well as some agricultural installations (*Fig. 3.68*). In a 0.5 km radius, the habitat is dominated by steppe, but the direct surrounding is characterised by maquis. Towards the modern settlement, anthropogenic landscape with orchards and fields increases.

3.6.2.2. Multivariate Analysis of Assemblage Patterns

Multivariate analysis is a form of exploratory data analysis which uses multivariate statistics to observe the behavior of multiple response variables, usually in a regression based approach. In this particular case the response variables are multiple habitat types and multiple size categories for sites. The driving ‘environmental’ factors are site attributes of epoch and size. Multivariate analysis has been used successfully[34] in a manner similar to its more common usage in community and landscape ecology[35].

In these studies, multivariate analyses are used for the statistical correlation of archaeological sites and habitat. Multivariate analysis—indirect ordination and direct ordination—using CANOCO 5[36] was selected as

33 Mittmann 1970, 31 f. no. 67.

34 Olsvig-Whittaker et al. 2015.

35 Jongman et al. 1995.

36 Šmilauer – Lepš 2014.

the tool for assessing patterns and correlations in site attribute and habitat attribute data. While ordination has long been in use in community ecology, its application to archaeological data is somewhat more recent[37]. There is a vast literature on the subject of ordination and many algorithms to do it[38].

In general, ordination methods help to find structure in complex matrix data sets, i.e. site by attribute or habitat by attribute tables. In the case of direct ordination, this is basically a regression of the site data versus the habitat data, conceptually similar to multiple regressions. Direct ordination can be used either heuristically or as a statistical test of correlation with measured driving factors, using Monte Carlo simulations.

When a heuristic search for pattern is desired, indirect ordination is the proper tool. Most algorithms for indirect ordination calculate similarity/dissimilarity between habitats or sites and their attributes, from a single table. Results are projected onto two dimensions in such a way that similar habitats or sites and most closely correlated attributes are plotted close together, and dissimilar habitats or sites and their attributes are placed far apart[39].

Most importantly, in both direct and indirect ordinations, the scatter plots for habitat and site values can be superimposed. In this way the habitats factors driving the pattern in sites can be seen, and *vice versa*.

3.6.2.3. Detrended Correspondence Analysis (DCA)

Detrended Correspondence Analysis (DCA) was used on the habitat matrix, with site data carried passively, to determine major trends in variation of habitat distribution and the response of site factors to them. DCA is an indirect ordination method using only one matrix. It is an analytical approach in its own right, and is also a necessary first step in every CANOCO analysis, regardless of algorithm. The first information obtained in DCA is the habitat turnover along the first gradient (Axis 1, horizontal), which is either short (less than four standard deviation units in habitat composition), in which case a linear model such as PCA or RDA can be used in subsequent steps. If the gradient is longer than four standard deviation units, a unimodal model such as DCA, or Canonical Correspondence Analysis (CCA) is used in subsequent steps.

3.6.2.4. Canonical Correspondence Analysis (CCA)

Canonical Correspondence Analysis (CCA) is a direct ordination method which correlates two matrices using eigenvector methods. In this study habitat has been used as the ‘species’ matrix and the two factors of sites size and age as the environmental matrix factors. Monte Carlo tests can be run to determine the significance of the correlation of habitat with site factors.

3.6.2.5. Preliminary Results

A preliminary analysis using DCA and CCA was done of Roman sites, both those on previously occupied locations and those with no previous occupation. By type, the ‘New Roman’ sites were predominantly installation and scatter (no building). This would fit with a predominantly agricultural expansion.

DCA (*Graph 3.10*) showed a close relationship of larger archaeological sites and open water. The analysis used DCA with supplementary variables. Total variation was 0.84771, supplementary variables accounted for 2.6 % (adjusted explained variation is 0.4 %).

CCA (*Graph 3.9*) was run on habitat with site size and age as environmental variables. Total variation was 0.84771, explanatory variables accounted for 2.6 % (adjusted explained variation is 0.4 %). Permutation tests on all axes provided a probability of correlation of $p = 0.304$, hence the Monte Carlo testing of the correlations of site and habitat factors was not significant.

The ordinations, despite the lack of statistical significance of correlations, suggest that natural open water, riverine habitats, and large archaeological sites all seemed connected. In addition, CCA indicated a correlation of older (more successful or established?) sites with open water. Water was of course critical for human settlement, and it was reasonable that larger archaeological sites would be close to water sources. What was interesting in the CCA analysis was that new Roman sites were less related to water. We knew that Roman engineering both of cistern systems and aqueducts opened new areas (such as plateaus) for settlement and exploitation. Hence the weaker correlation of ‘New Roman’ sites with water also made sense.

37 However, see Olsvig-Whittaker et al. 2015 for a review and case study.

38 See Jongman et al. 1995 for a review.

39 Peet 1980.

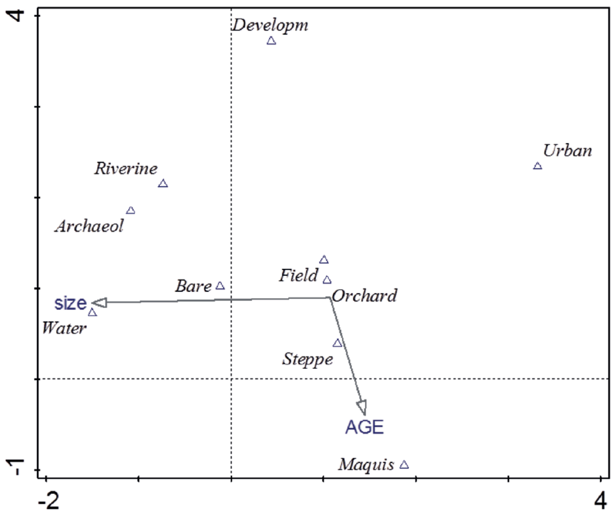

Graph 3.9 Canonical Correspondence Analysis (Source: L. Olsvig-Whittaker).

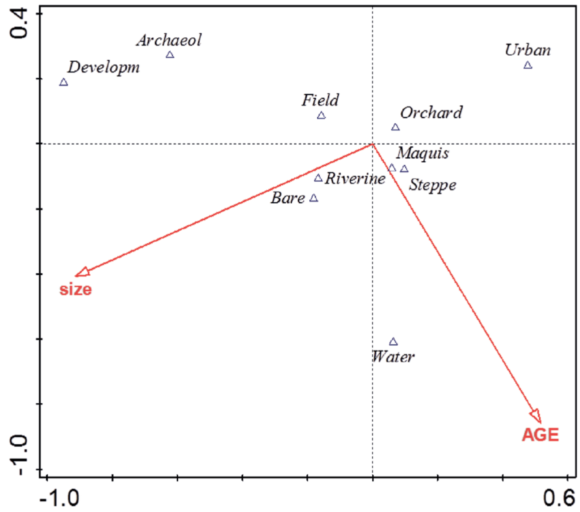

Graph 3.10 Detrended Correspondence Analysis (Source: L. Olsvig-Whittaker).

3.7. Archaeobotany

by Linda Olsvig-Whittaker

Fig. 3.77 Landscape with olive groves around Tall Zirā'a. Photograph taken in spring 2012 (Source: BAI/GPIA).

Archaeobotany, the study of plant remains from archaeological sites is a relatively new but important and necessary branch of archaeology and an integral part of archaeological projects[40]. While in some cases, plant remains may persist due to the extreme dryness of conditions, in most cases what can be obtained in sites such as Tall Zirā'a will be carbonised plant remains from destruction layers, hearths or middens where hearth remains were deposited.

Most of the findings will be carbonised seeds. These may come either from agricultural and weed species or from natural vegetation, especially where dung was used as fuel[41]. These can be extracted and identified under a microscope. From such carbonised macrofossils it can be learned which plants were raised or traded. Where dung was burned there are clues about natural vegetation.

Until now, very little was known about the botanical remains in Tall Zirā'a. The main plant remains are olive

40 Grieg 1989.

41 See Olsvig-Whittaker et al. 2015.

kernels from 22 contexts dating between the Late Bronze Age and the Umayyad period. It was originally thought that few plant macrofossils were available on Tall Zirā'a, but experience suggests this was more a matter of not sampling specifically for plant remains, and there should be plant materials if one looks for them properly[42].

Sampling for archaeobotanical macrofossils involves specialised sampling and extraction; much small material is lost in dry sifting using classical archaeological methods. In this chapter a preliminary study will be presented. Its aim was to see if more material could be obtained using methods designed for archaeobotanical sampling. While this is strictly a pilot study, the potential for future work is also discussed.

3.7.1. Ecological Background

3.7.1.1. Ecological Background of Northern Jordan

Northern Jordan has a fairly steep gradient from Mediterranean climate in the west (475 mm/year at Irbid) to arid in the east (150 mm/year in Mafraq)[43]. In response to this, according to the excellent review by S. A. Ghazanfar et al. the area around Tall Zirā'a would comprise two major vegetation zones: Mediterranean degraded non-forest vegetation to the west merging into Irano-Turanian steppe to the east, with some minor riverine vegetation in the wādīs[44]. Remote sensing images reveal a mosaic of open shrubland, steppe, farmland, orchards and riverine vegetation, with a predominance of open shrubland to the north-west and a predominance of steppe to the east. The area is generally regarded as transformed and degraded. As for the two major 'natural' vegetation types described by S. A. Ghazanfar et al.:

> "Mediterranean Non-Forest vegetation. Land classification: Northern and southern mountains and foothills. Approx. area: undetermined, Altitude range: > 1000 m; Annual rainfall: 400–600 mm. Localities: Mediterranean region not covered by forests, often treated as degraded forest. Vegetation: Dominant shrubs: *Rhamnus palaestinus, Calicotome villosa, Echinops spp, Dactylis glomerata, Teucriumpolium, Ononis natrix, Ballota undulata, Eryngium glomeratum, Noaea mucronata*".

> "Steppe. Land classification: This vegetation forms a strip surrounding the Mediterranean non-forest region, except in the north; excluding wooded areas and cultivations. Altitude range: 1000 m; Annual rainfall: 400–600 mm. Vegetation: Dominated by large shrubs; occasional tree species; composition varies in the north and south. Shrubs: *Pistacia atlantica, Retama raetam, Ziziphus lotus, Z. nummularia, Ferula communis (north), Anabasis syriaca, Artemisia sieberi, Sarcopoterium spinosum* (NE and S Mediterranean), *Tamarix* spp., *Noaea mucronata, Gypsophila arabica, Astragalus spinosus*; geophytes: *Crocus moabiticus. Aspodelus aestivus*, *Drimia maritima; Moraea sisyrinchium*. Biogeography: Irano Turanian; Mediterranean or Saharo-Arabian in parts"[45].

3.7.1.2. Ecological Background of Tall Zirā'a

Tall Zirā'a is situated in a region of rapid transition from Mediterranean to steppe to desert environment[46]. This area has experienced vegetation changes over time due to both climatic fluctuations and human activity, as amply demonstrated by D. Langgut et al. in their analysis of pollen records from several stations along the Jordan, Sea of Galilee and Dead Sea[47]. As already known, this region has experienced periods of extended drought as well as wetter periods, and the pattern of climate change is now available[48]. While pollen analysis gives information on the climate and vegetation of the region, plant macrofossils within a given site can give the human response to changing climate, including crops and in some cases pasture. If it is possible to obtain a good continuous record

Fig. 3.78 Flora at Tall Zirā'a (Source: BAI/GPIA).

42 Helbaek 1969.
43 http://www.jordan.climatemps.com (14.10.2015).
44 Ghazanfar et al. 2013.
45 Ghazanfar et al. 2013, 28 f.
46 Ghazanfar et al. 2013, 28 f.
47 Langgut et al. 2015.
48 Langgut et al. 2015.

of plant remains at Tall Zirāʻa, one can connect this agricultural information to the climate information available from regional pollen studies that is now available.

Tall Zirāʻa is a major tall which not only sits on a major caravan route and ancient highway of the Near East (see *Chaps. 1.2* and *1.3.2.)*; it is also located in a marginal, ecologically shifting environment, a finger of Irano-Turanian steppe extending into the Mediterranean[49]. If plant remains can be extracted, they should represent local agriculture, long distance trade and, possibly, shifting vegetation composition through time in response to climate change.

3.7.2 Archaeobotanical Background

While little archaeobotanical work has been done on Tall Zirāʻa until now, there has been extensive work on sites around the Dead Sea-Jordan River-Sea of Galilee-area which together give a general idea of what has happened over time. Changes should be anticipated related to climatic fluctuations and to cultural changes such as the introduction of vastly improved water management and introduction of better industrial agriculture in Roman times[50].

Changing climatic regimes and anthropogenic influences should be reflected in changing vegetation of the site through time. While northern Jordan experienced the same Late Bronze Age collapse around 1200 BC that was happened around the Eastern Mediterranean, this is mostly attributed to the Sea People[51]. However, climate records around the Dead Sea suggest that a major desiccation of the environment may have also been involved. It should be possible to distinguish that by getting adequate archaeobotanical samples[52].

The work by D. Langgut indicates that drought was a major factor leading to the Bronze Age collapse[53]. Their review of recent studies show a decrease in trees requiring a great deal of water and an increase in the cultivation of dry-climate trees, such as olive trees, during the period between 1250 and 1100 BC. This is most likely a human response to changing climate.

3.7.3. Methods

In May 2014 a preliminary manual flotation sampling of 43 soil samples was conducted by the author of this chapter[54]. The soil samples had been collected at Tall Zirāʻa during the past ten years and covered achaeological periods ranging from Early Bronze Age to Mameluk period (see *Tab. 3.1*)[55]. The samples had not been originally collected for flotation sampling, but were contributed for this purpose from the archived soil and soil-like samples stored at the dig house.

Most of the samples contributed for this study were contents of pots, floor fillings, mortar, etc. A detailed listing is given in *Tab. 3.1*. The most productive samples came from hearths, pits, and collapse debris, as might be expected.

The sampling was inspired by work which has been done by the Tel es-Safi/Gath team based at Bar Ilan University (BIU)[56]. The methods which were used by the author of this chapter were recommended by the archaeobotany lab under E. Weiss at BIU as suitable for pilot studies[57]. They are also described by J. Grieg as ʻmanual flotation' or ʻwashing over'[58].This is also called bucket flotation and is widely used for pilot studies[59].

Despite the primitive nature of this method it was used successfully in earlier decades and vastly increased knowledge of plant macrofossils. Since its beginnings in the 1960's different methods were developed and it is a standard procedure in excavations worldwide[60].

The bucket and wash over methods were modified by the author of this chapter somewhat to fit the equipment at hand, using local buckets and washtubs, as well as fine-meshed commercial flour sieves. Soil samples varied from a few grams to a kilogram, but no more than a half kilo could be processed at one time (for the process see *Figs. 3.79–3.84*).

The residues were inspected by using an Olympus binocular microscope. The organic residue was put in a plastic Petri plate, and any interesting objects in it (bones, shells, metal, possible and obvious seeds) were

49 Zohary 1962; Ghazanfar et al. 2013.
50 Petit et al. 2006, 179–188.
51 Cline 2014; see http://www.kinghussein.gov.jo/his_citystates.html (9.9.2015).
52 See Olsvig-Whittaker et al. 2015 for analytical methodology.
53 Langgut et al. 2015.
54 Grieg 1989, 32–39.
55 I would like to thank the staff and students of the archaeobotany laboratory at Bar Ilan University, in particular Ehud Weiss and Suembikya Frumin, for their invaluable advice and practical help on methodology and taxonomic identification. Without their help this project would have been impossible. I also wish to thank the staff of the BAI/GPIA for providing the field facilities and samples from which the seeds were extracted.
56 Cf. Frumin et al. 2015.
57 E. Weiss and S. Frumin, personal communication.
58 Grieg et al. 1989, 32–39.
59 See illustration in https://sites.google.com/site/archaeobotany/buckets and https://sites.google.com/site/archaeobotany/buckets2 (4.3.2016).
60 Neef et al. 2012

transferred to a tripartite Petri plate. Those samples which had possible or probable seeds were taken to the Bar Ilan archaeobotanical laboratory, where S. Frumin verified the identification of seeds using the accumulated fossil collection there.

Fig. 3.79. Sieving out large stones and gravel (Source: L. Olsvig-Whittaker).

Fig. 3.80. Pouring soil sample into basin of water (Source: L. Olsvig-Whittaker).

Fig. 3.81 Wash over of water and floating organic material through a sieve (Source: L. Olsvig-Whittaker).

Fig. 3.82 Moving the organic material to a filter paper for drying (Source: L. Olsvig-Whittaker).

Fig. 3.83 Sample poor in organic material (Source: L. Olsvig-Whittaker).

Fig. 3.84 Sample rich in organic material (Source: L. Olsvig-Whittaker).

3.7.4. Preliminary Results of the Archaeobotanical Researches on Tall Zirā'a

The samples were often rich in mollusk shells and some had vertebrate bones, which have been saved. There were also modern seeds (sometimes rich collections of them) which were saved but not of interest for present concerns. According to L. Kolska, archaeozoologist on the 'Tel es-Safi Project', land mollusks often gather to aestivate in soil samples, and ants frequently collect modern seeds in the same samples. This may explain the large cache of modern seeds in one sample. Only carbonised seeds can be regarded as true archaeological specimens.

It should be noted that most of the carbonised seeds were in poor condition, but nearly all were cultivars or weeds[61]:

- *Olea europaea* (domestic olive)
- *Vitis vinifera* (domestic grape)
- *Ficus carica* (domestic fig)
- *Triticum aestivum* (common wheat)
- *Hordeum vulgare* (domestic barley)
- *Vicia ervilia* (domestic bitter vetch)
- *Gynandyris sp* (a wild iris-like geophyte)
- Unknown *Asteraceae* species (daisy, sunflower family)

The bitter vetch is an interesting find; originating in Anatolia and northern Iraq but not native to Jordan[62]. It was widely cultivated in the past both for animal feed and (after repeated washing to remove toxins) for human consumption as well. Most of the remaining species are typical Middle Eastern crops; *Gynandyris* may have been a weed in cereal fields. At this point in time, the data are far too sparse to say anything about vegetation, agriculture, trade or living conditions apart from the fact that the crop species found are typical for this region. Hence there are indeed archaeobotanical macrofossils at Tall Zirā'a that are typical for Middle Eastern agriculture.

3.7.5. Potential Future Archaeobotanical Researches on Tall Zirā'a

Fig. 3.85 At the south-western foot of Tall Zirā'a. View to the water reservoir. Photograph taken in 2009 (Soure: BAI/GPIA).

The feasibility study demonstrated that seeds can be obtained by flotation sampling in Tall Zirā'a. The poor condition of the seeds obtained for research may be due to preservation conditions in the site. The climatic conditions on Tall Zirā'a are disadvantageous for the preservation of the samples.

Future surveys and excavations will include systematic archaeobotanical sampling. Archaeobotanical macrofossils should be found comparable to those found elsewhere in the region when flotation extraction has been used, most likely thousands of seeds, as F. Hole et al. described in their experience[63].

In addition, this site is in an ecologically marginal zone which experienced times of drought. One should be able to document changing environmental conditions, if we have adequate sampling spread over the long time frame represented on Tall Zirā'a.

If wood rather than animal dung was the main cooking fuel on Tall Zira'a, the rich collections of wild plant species found in hearth sites where dung was burned cannot be expected here. However, the presence of a weed species in this small collection is encouraging. Probably nearly all the plant species which have been found will be related to cultivation or trade.

61 Found, according to the BIU archaeobotany laboratory staff.

62 Zohary – Hopf 2000, 116.

63 Hole et al. 1969.

Period	Identification of sample	TZ-No.	Context-No. and Description	
Early Bronze Age III	/	019311-001	6327	Content of pot TZ 021630-001 // filling/pit
Late Bronze Age I–II	/	018818-001	6125	Filling
Late Bronze Age II	/	012193-001	3574	Clay // filling/fireplace?
Late Bronze Age II	/	016362-001	5129	Content of pot TZ 020405-001 // pit
Late Bronze Age II	/	018821-001	6057	Chalk // fireplace
Iron Age I	/	018819-001	5942	Seeds? // filling
Iron Age I	/	011752-001	3365	Content of pot // pit
Iron Age I	***Echium judaeum*** // modern seeds prob. from an ant. storage	**011753-001**	**3449**	**Earth/seeds // filling/fireplace?**
Iron Age I	/	016360-001	5209	Content of pot TZ 020378-013 // mudbrick-wall
Iron Age I	/	018815-001	6146	Content of pot TZ 021558-001 // filling
Iron Age I	/	018817-001	6124	filling
Iron Age IIA/B	possible ***Ficus sp***	**012191-001**	**3494**	**Pit/fireplace?**
Iron Age IIA/B	/	018816-001	5513	Content of cooking pot TZ 021560-001 // filling
Iron Age IIA/B	/	019001-001	5738	Content of pot TZ 021031-001 // chalk // filling
Iron Age IIA/B	/	012192-001	3458	Content of pot TZ 005205-001 // earth/ash
Hellenistic	/	112232-001	11186	Mortar // wall
Hellenistic	/	111855-001	11106	Earth around pot TZ 101236-001 // hearth
Hellenistic	**Wheat (*Triticum aestivium*)** // with glume attached	**111856-001**	**11106**	**Content of pot TZ 101236-001 // hearth**
Hellenistic	/	112233-001	11296	Mortar // pit
Hellenistic – Early Byzantine	**Barley (*Horduem vulgare*)** // wheat?	**110822-001**	**10611**	**Content of pot // filling**
Early Roman	/	016357-001	5095	Part of floor // filling
Early Roman	/	016358-001	5116	Part of floor // filling/fireplace?
Early Roman	/	016359-001	5189	Mortar // filling
Early Roman	/	018820-001	5522	Mortar // pit
Early Roman	possible ***Ficus***	**016361-001**	**4940**	**Content of pot TZ 020062-041 //**
Byzantine	/	112231-001	11346	Mortar // filling
Byzantine	***Gynandiris sp*** // possibly a weed in a cereal field	**012261-001**	**3539**	**Content of kernos TZ 005383-001**
Byzantine	/	310468-001	30121	Filling between two floor levels // filling
Byzantine	**Unidentifiable seed**	**310693-001**	**30416**	**Clay // floor**
Byzantine	/	310696-001	30420	Mortar // part of mosaic floor
Byzantine	/	310697-001	30420	Mortar // part of mosaic floor
Byzantine – Umayyad	***Olive fragment (Olea europaea)***	**310695-001**	**30421**	**Clay with organic material // floor**
Umayyad	/	009646-001	2502	Pottery and mortar // filling
Umayyad	/	310692-001	30398	Destroyed mosaic floor
Umayyad	/	310698-001	30398	Mortar ? // part of mosaic floor
Umayyad	**Grape (*Vitis vinifera*)**	**110931-001**	**10578**	**Content of amphora // filling/collapse debris**
Umayyad	possibly ***Asteraceae //*** shells	**110788-001**	**10571**	**Content of amphora // filling/collapse debris**
Umayyad	/	110757-001	10571	Content of pot // filling
Abbasid–Mamluk	/	310418-001	30150	Content of pot TZ 300132-001 // filling
Abbasid–Mamluk	/	111002-001	10655	filling
Abbasid–Mamluk	**Wheat (*Triticum aestivium*) and bitter vetch (*Vicia ervila*)**	**310694-001**	**30386**	**Clay // floor**
Modern	**Barley (*Horduem vulgare*)**	**310419-001**	**30023**	**Content of pot TZ 300173-001 // *colluvium***

Tab. 3.1 Samples processed in 2015 (Source: BAI/GPIA).

3.8. Archaeometry

edited by Dieter Vieweger/Jutta Häser[64]

with a contribution by David Adan-Bajewitz

Archaeometry evaluates scientific data yielded by the excavated artefacts. This allows conclusions on an object's manufacture, the technologies used, the place of manufacture, and the trade route it has followed. Basically, the aim was finding out how the Tall Zirā'a's inhabitants managed in the course of thousands of years to adapt their survival strategies to the natural conditions of the wādī, and in what manner they reacted to changing resources. In the field of skilled crafts and trades, this can be inferred from the raw materials they were able to work, from the goods that were manufactured, and from the extent of improvement of the finished products' serviceability. Over the centuries, all this necessitated technical knowledge, mechanical skills, and novel ideas, combined with target-oriented experiments, as well as innovation.

The archaeometrical project conducted by the Biblical Archaeological Institute Wuppertal (BAI) was started in 2003. The cooperation partners are:

- German Mining Museum Bochum (A. Hauptmann, M. Prange, and D. Kirchner; especially with regard to studies of ceramics in the years 2003 and followings)
- Leibniz University of Hannover, Institute of Inorganic Chemistry, Work Group Archaeometry (C. Vogt, R. Lehmann, and M. Schulze; pottery studies and metal examinations since 2009)
- Martin (Szusz) Department, Land of Israel Studies and Archaeology, Bar Ilan University (D. Adan Bayewitz, and M. Osborn; studies on Hellenistic and Roman ceramics since 2010)[65]
- The Austrian Academy of Sciences, OREA – Department of Europe, and University Bonn (R. Jung, H. Mommsen; analyses of the origin of Mycenaean ceramics)[66]
- University of Massachusetts Amherst, Department of Anthropology (graduate student Mary Larkum; analyses of the contents of Iron Age cooking pots)[67]
- The Hashemite University, Department of Conservation Science, Queen Rania Institute of Tourism and Heritage (Ph.D. student A. Mayyas; analyses of the contents of Early Bronze Age ceramic vessels)

Thanks to the kind support of the 'Department of Antiquities (Jordan)' (DoA), important finds could be exported to Germany (Wuppertal). Here, they were cleaned—and, if necessary, also restored—, photographed, sampled for further scientific examination and/or given to experts such as numismatists, osteologists, botanists, etc. for inspection. Finally the finds were returned to Jordan.

The abundance of finds on the Tall Zirā'a allowed the comprehensive examination of various artefacts as well as raw materials, such as different types of ore, rocks, and minerals. A representative selection was taken from the multitude of finds on the Tall Zirā'a, made of ceramic, glass, faience, metal, or minerals, and analyzed both chemically and mineralogically. Among these, particular focus was placed on the archaeometrical examinations of pottery and glass finds.

First results from the archaeometrical testings—regarding glass beads and ceramics—have already been published in the following articles:

- Auge – Vieweger 2006, 54–56
- Lehmann – Schulze 2015, 28–30
- Schulze et al. 2013, 294–296
- Schulze et al. 2014, 13
- Schulze et al. 2015, 219–221
- Vieweger et al. 2009, 245–258
- Vieweger 2013, 231–242
- Vieweger et al. 2014, 57–77

Since the archaeometrical examinations of the various materials can supply important insights into the skilled crafts and trades on Tall Zirā'a, a separate volume of the final report of the excavations on Tall Zirā'a, Volume 9, written by W. Auge, who was in charge of the Biblical Archaeologival Institute's (BAI) investigations and advanced them vigorously, will be solely dedicated to this topic. The objectives of these examinations will therefore only be introduced and broadly outlined below.

64 This article is edited by D. Vieweger and J. Häser and is based on the research results of W. Auge. They are published on http://www.tallziraa.de/Gadara-Region-Project/Archaeometrie/0_415.html and http://www.bai-wuppertal.de/arch%C3%A4ometrie; written by W. Auge and M. Schulze (BAI Wuppertal) as well as R. Lehmann and C. Vogt (both Leibniz University Hannover, Institute of Inorganic Chemistry, WG Archaeometry).

65 The detailed results of these examinations will be published in the Volume 6 of this publication series.

66 The detailed results will be published in Volume 3 of this publication series.

67 The detailed results will be published in Volume 4 of this publication series.

3.8.1. Pottery

edited by Dieter Vieweger/Jutta Häser[68]

Fig. 3.86 Pottery from Tall Zirā'a (Source: BAI/GPIA).

The Biblical Archaeological Institute's (BAI) most comprehensive archaeometrical project deals with the examination of pottery since ceramics dating from all periods represented on Tall Zirā'a are remarkably abundant and can be allocated to almost every 'sphere of life': domestic home (application and decoration), crafts, and cult. The project was started in 2003. By 2012, eighteen excavation campaigns had yielded 350,000 ceramic sherds and objects, 80,000 of them diagnostics, that were divided into 90 ware groups (groups with specific unique characteristics) by D. Vieweger, A. Schwermer, and F. Kenkel. Of this bulk, so far approx. 300 that were deemed representative, and some further, particular sherds could be analyzed chemically and mineralogically by means of the ICP, RFA, and XRD methods. Likewise, 60 samples of clay bricks, tabuns, kilns as well as soils, minerals, and clays that had been collected in the course of geological explorations in the tall's surroundings were subjected to similar testings. The material analyses were performed at the German Mining Museum Bochum, Research Field Archaeometallurgy/Laboratory of Materials Science (A. Hauptmann, M. Prange, D. Kirchner) and, from 2009, at the Leibniz University of Hannover (C. Vogt, R. Lehmann, M. Schulze).

3.8.1.1. Provenance Study

In order to determine an object's provenance, not only ceramics from the tall were analysed but also more than a hundred pieces of pottery that had been found during various surveys conducted in its immediate and distant surroundings (survey by P. Leiverkus and K. Soennecken [BAI Wuppertal]), or that, thanks to the kind support of the German Archaeological Institute (DAI) (C. Bührig [DAI] und B. Liesen [Römermuseum Xanten]), were made available to the researchers from the nearby Decapolis city of Gadara. A comparison of the ceramics' chemical/mineralogical compositions and of further, deduced geochemical 'fingerprints' allowed assigning them to different groups, each with common characteristics (*Graph 3.11*).

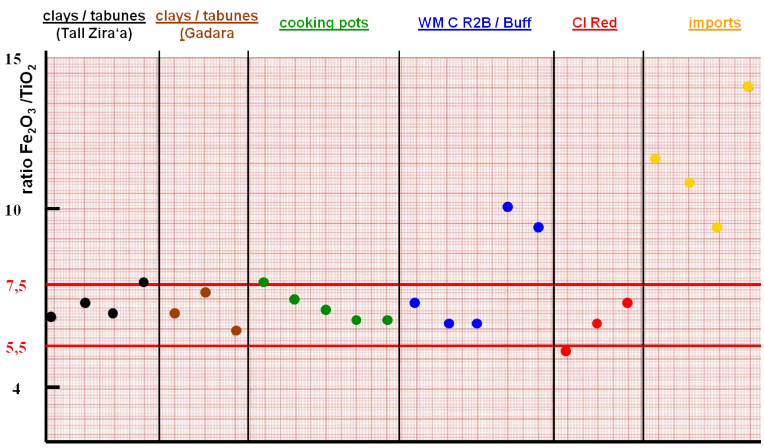

Graph 3.11 Geochemical fingerprint of some ware groups (BAI/GPIA).

68 This article has been translated from the German language. It is based on http://www.bai-wuppertal.de/keramikprojekt and http://www.tallziraa.de/Gadara-Region-Project/Archaeometrie/Keramikprojekt/0_416.html, written by W. Auge, BAI Wuppertal (5.6.2016).

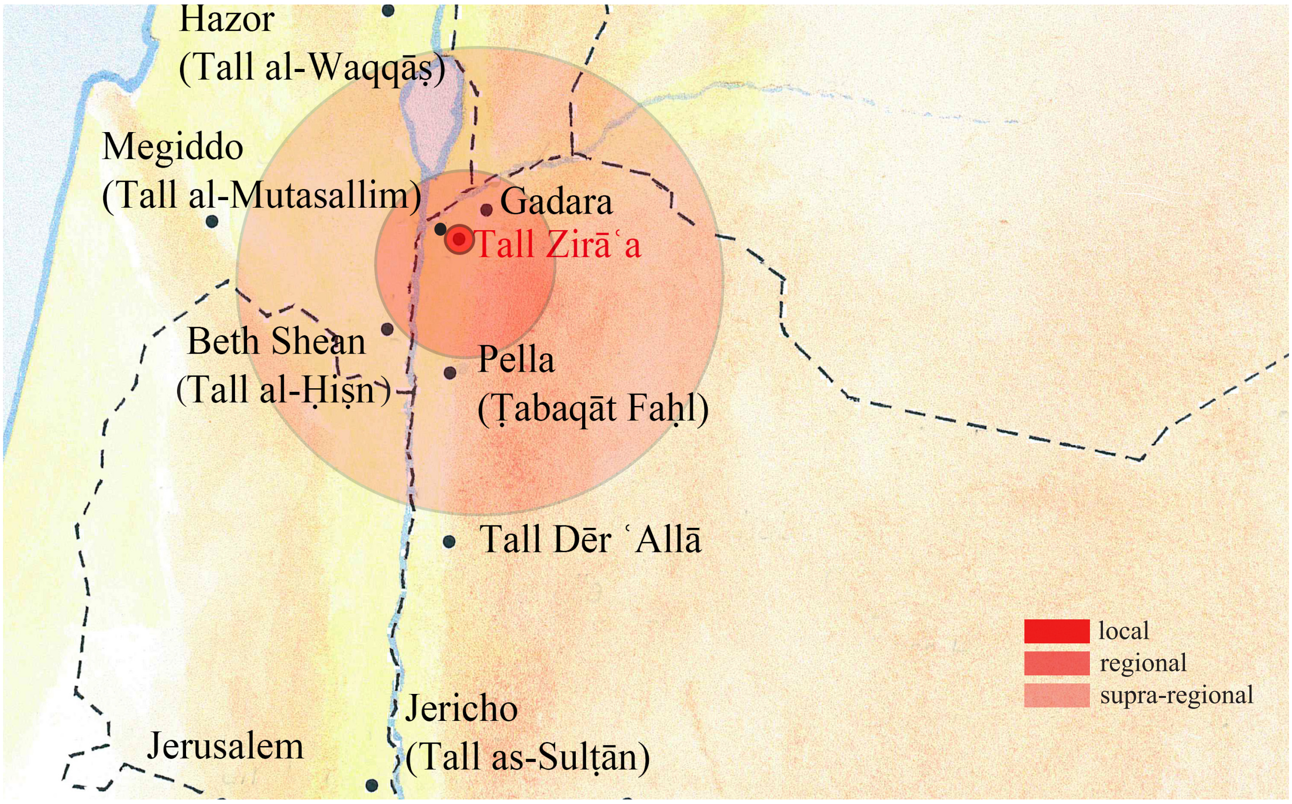

Fig. 3.87 Provenance of the pottery found on Tall Zirāʿa (Source: BAI/GPIA).

Moreover, these data often also enabled the researchers to determine whether a piece of pottery was of local, regional, or supraregional origin or whether it had been 'imported' from even farther away.

The determination of a piece of pottery's origin is based on the postulate of provenance:

> "If ceramics and clays match in terms of their chemical and mineralogical compositions then the place of storage is regarded as the likely place of manufacture"[69].

Following this rule, the analytical data of soils or clays, non-ceramic clay products, and ceramics that had been found 'regionally', i.e. within a 20 km radius, 'supra-regionally', i.e. within a radius of 20 to 100 km, or that had even been imported from beyond Palestine, were compared with those of the ceramics that had been excavated on the tall (*Figs. 3.87–3.91*).

Unfortunately, due to the large variability of the clays' chemical and mineralogical composition, resulting from their often very complex formation, statements regarding the origin of ceramics are only rarely scientifically valid. Even the application of different analytical methods or of mathematical programmes such as the multivariate cluster analysis, cannot resolve this shortcoming.

Figs. 3.88–3.91 Pottery from Tall Zirāʿa. Left: Iron Age pyxis, TZ 002926-001 (local). Dimensions: W 10.5, H 8.0; centre-left: Pyxis, TZ 002863-001 (Mycenaean, imported). Dimensions: H 9.0; centre-right: Late Bronze Age jar, TZ 005556-001 (regional). Dimensions: H: c. 25, D (opening) 12.5, D (foot) 3.5; right: Iron Age II jar, TZ 001212-001 (local). Dimensions: H 45, W 35 (Source: BAI/GPIA).

69 McGovern 1997, 69–108.

3.8.1.2. Typology

Extensive sequences of development, reaching from the Early Bronze Age to Islamic periods, and comprising more than 100 types and subtypes, can be established for cooking pots as a category of pottery that has been specifically manufactured and that meets particular requirements[70].

Since the ceramics' 'plastic' and the 'non-plastic' components (pl/npl) that were deduced from analytical data with respect to their types and percentages can be correlated fairly well to the time-dependent parameters such as ware groups (type and colour of the clay), shape variability (typology), wall thickness, opening diameter, and vessel size, as well as firing temperatures, they can serve as instruments in reconstructing the technical history of the cooking pots found on the Tall Zirāʻa and in its surrounding environs.

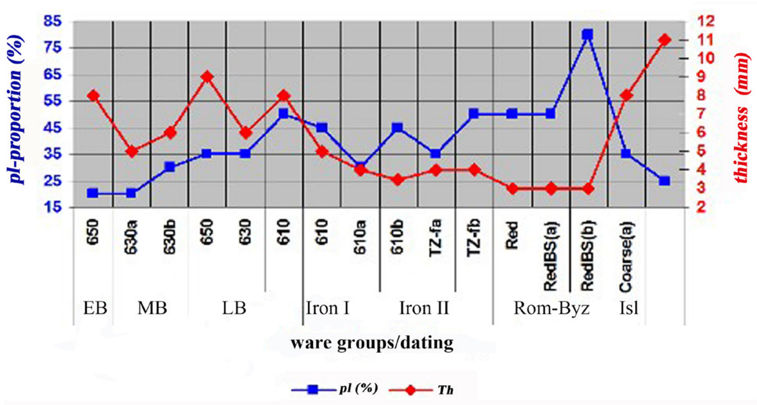

Graph 3.12 Relation between plastic components and wall thickness of cooking pots from Tall Zirāʻa (Source: BAI/GPIA).

The firing temperatures were ascertained by means of multiple tests designed to reenact the firing processes of former times, and by further firing experiments.

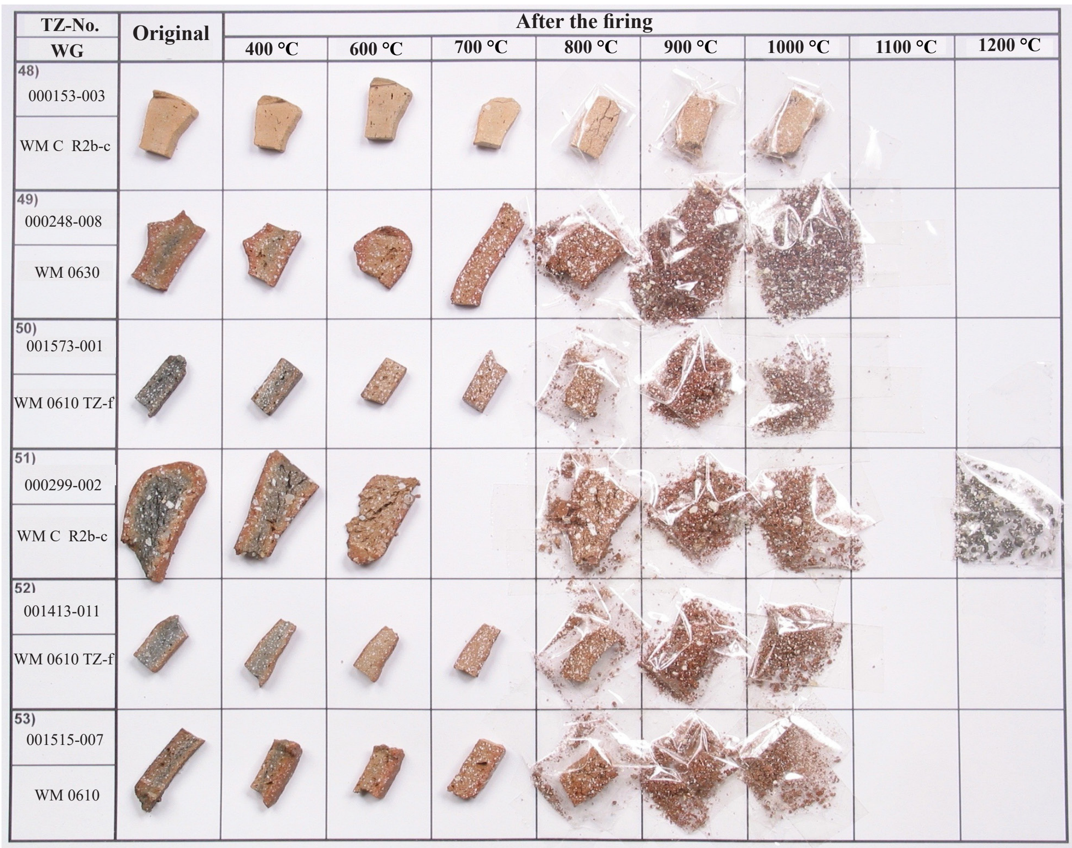

Fig. 3.92 Refiring of ceramics (Source: BAI/GPIA).

70 Schwermer 2014.

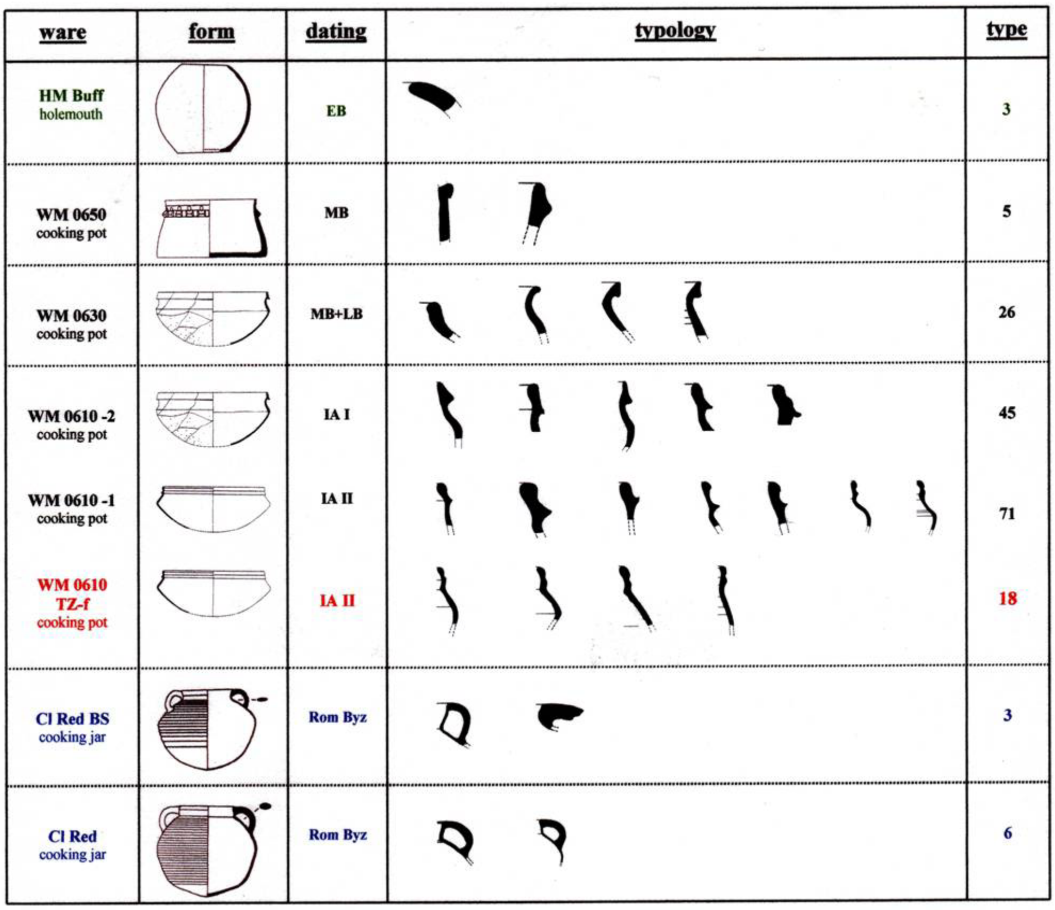

Fig. 3.93 Typology of cooking pots (Source: BAI/GPIA).

3.8.1.3. Compositional and Provenance Study of Roman Period Pottery

by David Adan-Bajewitz

Under the auspices of the Biblical Archaeology Institute Wuppertal (BAI), the German Protestant Institute of Archaeology Amman/Jerusalem (GPIA) and Bar-Ilan University, Ramat-Gan, an extensive compositional and provenance study of the common, utilitarian pottery found in Roman-period levels at Tall Zirāʻa was begun in 2012. The Principal Investigator are Prof Dr D. Adan-Bayewitz, Dr S. Krauthammer (Professor of Archaeology at Bar-Ilan University), and, from 1999–2013, Senior Guest Scientist at the Lawrence Berkeley National Laboratory, with Dr M. Osband as Co-Investigator, in close collaboration with Prof Dr Dr Dr D. Vieweger and Dr J. Häser (Directors of the Tall Zirāʻa excavations), and Dr F. Kenkel. The goals of the project include determining the sources of the Roman-period pottery used at Tall Zirāʻa from the early through the late Roman periods (the first through fourth centuries AD) and documenting diachronic change in the trade contacts of the settlement. This work will contribute to clarifying the production and distribution networks of everyday pottery in the Southern Levant during the Roman period.

The analytical methods employed include Instrumental Neutron Activation Analysis (INAA) of the sampled Tall Zirāʻa pottery at the Missouri University Research Reactor, under the direction of Dr M. D. Glascock, multivariate statistical analysis of the chemical element data, and micromorphological analysis. The chemical element data will be compared with a large data base from measurements, by Dr F. Asaro and Prof Dr D. Adan-Bayewitz at the Lawrence Berkeley National Laboratory, of pottery from many other sites in the Southern Levant. The work is still in progress.

3.8.2. Glass, Glass Frit, and Faience

edited by Dieter Vieweger/Jutta Häser[71]

3.8.2.1. Glass

Figs. 3.94–3.96 Left: female figurine, TZ 015318-001. Dimensions: H 4.9, W 2.2; centre: zoomorphic pendant, TZ 015314-001. Dimensions: L 2.1, W 1.3; right: spacer with floral motiv, TZ 010337-001. Dimensions: L 3.1, H 1.8, Th 0.9 (Source: BAI/GPIA).

Glass was an object of trade, especially for jewellery making, as early as the Late Bronze Age. It was a very precious material that was being produced only in a few places in Egypt, Mesopotamia, Syria, and Anatolia. In those times, its value was similar to that of the noble metals silver and gold.

The Late Bronze and Iron Age glass finds on Tall Zirāʻa included numerous beads, a female figurine (TZ 015318-001; *Fig. 3.94*), a zoomorphic pendant (TZ 015314-001; *Fig. 3.95*), five spacers (e.g. TZ 014558-001), objects with floral motivs (e.g. TZ 010337-001; *Fig. 3.96*), and several rod-shaped beads (e.g. TZ 013881-001; *Fig. 3.46*). A considerably larger number of glass finds, dating from the Classical periods, are mainly vessel sherds.

Moreover, raw glass (e.g. TZ 015494-001; *Fig. 3.105*), spherical glass granules (TZ 016622-001; *Fig. 3.106*), a spherical bead without piercing (TZ 007546-001; *Fig. 3.40*), and a wound bead the clay core of which had notbeen removed (TZ 016663-001; *Fig. 3.39*), were found.

About 10 % of the 350 glass objects found in the Middle Bronze Age to the Iron Age II strata were analyzed with the aid of the ICP, OES, and RFA methods (status quo: 2011).

Based on the examinations carried out so far, the glass finds can be grouped into four categories (*Tab. 3.2*):

- Soda-lime glass (‘normal’): spherical beads and faulty bead cast
- Cupriferous (Cu): raw glass, spherical beads, figurine, bangle, and faulty bead cast
- Antimonial (Sb): raw glass, spherical beads, disc-shaped beads, and pendants
- Plumbiferous (Pb): spherical bead and bangle

Material	**Quartz**	**Fluxing agent**					**Colour**			
	Si	Al	Na	K	Ca	Mg	Fe	Cu	Sb	Pb
normal	64–94	2–5	1–14	1–4	1–7	0–8		< 1	-	-
Cu-bearing	48–74	1–7	nn	1–2	1–33	2–6	1–4	2–17	-	-
Sb-bearing	58–82	2–4	nn	1–2	2–6	0–8	1–3	2–10	4–19	-
Pb-bearing	68–73	2–7	nn	1	2–9	0–11	2–3	1–2	0–4	6–9

Tab. 3.2 Chemical composition of glass types on Tall Zirāʻa (all data are expressed in grams) (Source: BAI/GPIA).

71 This article of W. Auge has been translated from the German language. It is based on http://www.bai-wuppertal.de/glasprojekt; and http://www.tallziraa.de/Gadara-Region-Project/Archaeometrie/Glas/0_429.html (5.6.2016), written by W. Auge, BAI Wuppertal.

3.8.2.2. Glass Frit and Faience

All cylinder seals (38) and scarabs (10)[72] that have been found on the tall to date, along with a selection of faiences, were analyzed with respect to their mineralogical and, in some instances, also chemical compositions.

Cylinder Seals

The cylinder seals are typical of the 'Common Style' of the Mitanni glyptics that was common in Mesopotamia, Syria, and Palestine between the fifteenth and twelfth century BC[73] (see *Figs. 3.97* and *1.55*).

Of the 38 cylinder seals, 35 are made of glass frit (85 %; predominantly SiO_2), and many of them have a green or blue (faience) coating in varying degrees of perceptibility. One of the cylinder seals is made of calcite, and two consist of black stone (chlorids?) (*Tab. 3.3*).

Fig. 3.97 Cylinder seal, TZ 008558-001. Dimensions: H 2.4, D (max.) 1 (BAI/GPIA).

Scarabs

Among the scarabs, eight consist of glass frits of whichmost of the cylinder seals are made of. Two are composed of the mineral enstatite ($MgSiO_3$). The material analyses show that several of these scarabs could definitely be of regional or local provenance.

The analyses of some faience artefacts, such as the scarab TZ 015313-001 (*Fig. 3.99*), showed that the cores of these objects was mostly made of glass frit or of stone (*Tab. 3.3*).

Figs. 3.98–3.99 Left: Scarab, TZ 010112-001. Dimensions: L 3.7, W 2.4, H 1.4; scarab, TZ 015313-001. Dimensions: L 2.3, W 1.6, H 1 (BAI/GPIA).

Find No.	Object	Material	SiO_2	Al_2O_3	MgO	CaO	K_2O	Fe_2O_3
TZ 010334-001	Cylinder Seal	Frits	97.1	0.5	< 0.1	0.6	0.1	0.1
TZ 012357-001	Cylinder Seal	Calcite	51.8	11.4	-	20.0	0.2	0.1
TZ 012203-001	Scarab	Frits	96.1	1.8	-	0.6	0.1	<0.1
TZ 015313-001	Scarab	Steatite	69.0	5.6	19.4	1.5	0.3	3.0
TZ 011778-001	Billet	Frits	94.8	2.3	-	0.6	0.2	0.3

Tab. 3.3 Chemical composition of cylinder seals, scarabs, and billet (all data are expressed in grams) (Source: BAI/GPIA).

72 See for example: Häser et al. 2016, 497–507; Häser – Vieweger 2007a, 13 Fig. 9; Häser – Vieweger 2007b, 68 Fig. 9; Häser – Vieweger 2007c, 26 Fig. 6; Häser – Vieweger 2009, 488 f. Fig. 4 (drawing of the seal TZ 008972-001 and impression). Fig. 5; Vieweger – Häser 2007, 12 Fig. 2; Vieweger – Häser 2008a, 1842 f.; Vieweger – Häser, 2008b, 64; Vieweger – Häser 2008c, 151–162; Vieweger – Häser 2008d, 382 f. Fig. 8; Vieweger – Häser 2009a, 15–17, Fig. 11 (photograph of the scarab). Fig. 14 (photograph of several cylinder seals). Fig. 15 (photograph of a silver amulet). Abb. 28 (drwaing of the cylinder seal TZ 008558-001 with impression); Vieweger – Häser 2009b, 670 Fig. 9 (drawing of the cylinder seal TZ 008558-001 with impression). 672 Fig. 12; Vieweger – Häser 2010, 9–11, Pl. 6 B. Vieweger 2010, 758 Fig. 7d.

73 For the cylinder seals, see Häser et al. 2016, 497–507.

Glass Beads[74]

Glass beads have always played an important role in the cultural life of a multitude of peoples and tribes. They were worn as jewellery, used as an instrument of payment, applied for ritual purposes, and they were indicators of their wearer's social status and wealth. For this reason, glass beads are precious archaeological finds that can allow a detailed insight into a nation's, a tribe's, or a family's traditions, economic standing, and trade connections, as well as those of the region where they were excavated.

In the spring campaign of 2009, two Ottoman bead complexes consisting of 51 and 920 beads, respectively, were found on Tall Zirāʿa (*Fig. 3.100*). The beads, displaying a large spectrum of colours, sizes, and forms, had been manufactured from amber, semiprecious stones, shells, corals, ivory, and bones. It was particularly the glass beads, though, that were examined by means of state-of-the-art analytical methods (p-RFA, µ-RFA, LA-ICP-MS, ICP-OES, PIXE) in the context of a bachelor thesis written at the Leibniz University of Hannover's Institute of Inorganic Chemistry[75].

Fig. 3.100 Beads found on Tall Zirāʿa in spring 2009 (Source: HTW Berlin/BAI/GPIA).

Fig. 3.101 Late Bronze Age glass beads, TZ 010757-001. Dimensions: D (max.) c. 1.5 (Source: BAI/GPIA).

Apart from examinations regarding manufacturing techniques (*Fig. 3.102*) and the identification of the chromophoric components, the main focus was placed on trying to find out the place of manufacture and on an approximate age determination. These questions are important for reconstructing the development of trade connections and the transfer of technology in the Tall Zirāʿa's immediate and distant surroundings.

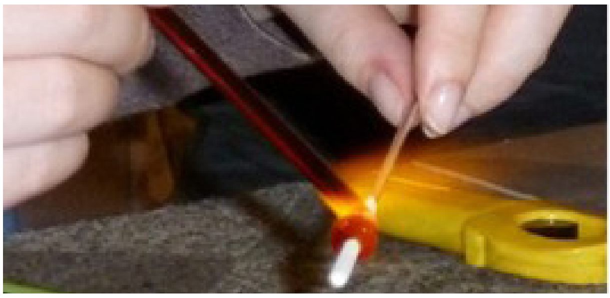

Fig. 3.102 Production of beads by winding technique (Source: M. Schulze/BAI/GPIA).

With the aid of elemental mapping images that were generated by means of µ-XRF (Micro X-ray Fluorescence), the chromophoric elements could be impressively detected (*Fig. 3.103*).

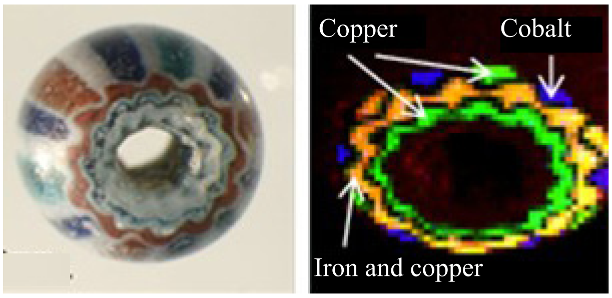

Fig. 3.103 Elemental mapping. 'Chevron bead' (Source: M. Schulze/BAI/GPIA).

Among the glass beads, there are two 'chevron beads'. This type of beads is particularly precious and was manufactured in Venice in the fifteenth century; from the seventeenth century on it was also produced in Amsterdam. In order to verify the assumption that the chevron beads found on Tall Zirāʿa originated from either of these places of manufacture, glass beads of known Amsterdam, Venetian, or Near Eastern provenance were examined in the Allard Pierson Museum in Amsterdam (*Fig. 3.104*).

In addition, several beads were subjected to measurements of isotope ratios in order to determine the origin of plumbiferous components in the raw material. These

74 This article has been translated from the German Language. It is based on http://www.tallziraa.de/Gadara-Region-Project/Archaeometrie/Glas/Osmanische-Glasperlen/0_465.html; written by M. Schulze, R. Lehmann, C. Vogt. See Schulze 2012; Schulze et al. 2013, 294–296.

75 Schulze 2012.

revealed that the beads found on the Tall Zirāʿa had obviously been collected from different places of manufacture and that the 'chevron beads' in all likelihood do indeed originate from an Amsterdam manufacturing site. Characteristic differences in the glass quality almost certainly rule out a Venetian provenance since the glassblowers of Venice used higher-quality raw materials with a higher lead content for bead manufacturing, thus enhancing light refraction and adding a particular lustre to the glass (*Graph 3.13*). Consequently, the bead complexes as they were found cannot have been compiled earlier than the seventeenth century.

Fig. 3.104 Beads in the Allard Pierson Museum Amsterdam (Source: BAI/GPIA/M. Schulze).

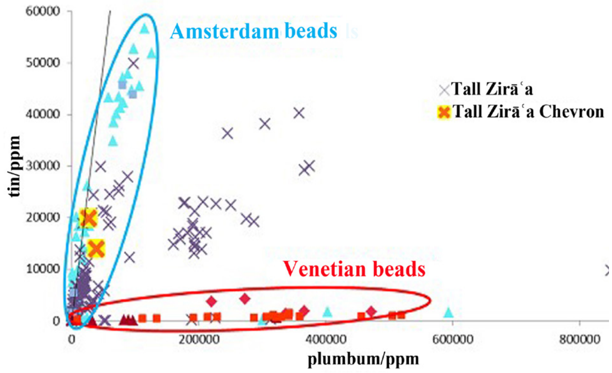

Graph 3.13 Beads in the Allard Pierson Museum Amsterdam (Source: BAI/GPIA/M. Schulze).

3.8.3. Production of Glass and Faience

edited by Dieter Vieweger/Jutta Häser[76]

3.8.3.1. Glass

Figs. 3.105–3.106 Left: Raw glass, TZ 015494-001. Dimensions: L 1.5, W 1.2, H 0.7; right: glass granule, TZ 016622-001. Dimensions: D 0.3 in average (Source: BAI/GPIA).

Figs. 3.107–3.108 Left: Hammer stone, TZ 015313-001. Dimensions: L 7.7, W 6.3, H 4.4; right: faience knob, TZ 015317-001. Dimensions: H 5.6, D (max.) 7.4 (Source: BAI/GPIA).

Evidence in favour of a local glass processing facility are the finds of raw glass (e.g. TZ 015494-001; *Figs. 3.105* and *Fig. 3.37*), amorphous and spherical glass granules (TZ 016622-001; *Fig. 3.106*), a spherical bead without piercing (TZ 007546-001; *Fig. 3.40*), and a wound bead, the clay core of which was not removed (TZ 001666-001; *Fig. 3.39*).

A room with very special finds like a well-insulated kiln (Stratum 13, Area I, Square AP 120, Context 4850), a working stone (TZ 015991-001) surrounded by thick layers of ashes was excaveted in the reused and altered entrance area of the Late Bronze Age temple in the north of Area I. On the floor of this room, a two-chambered basket-shaped vessel (TZ 006835-001; *Fig. 3.43*) was detected. Its specific function is unknown. Moreover, further working stones (TZ 015343-001), and a faience knob (TZ 015317-001; *Fig. 3.108*) were uncovered.

This ensemble of findings and the finds of glass and faience in its vicinity lead to the assumption that the place might have been used as glass processing work-

76 This article has been translated from the German language. It is based on http://www.tallziraa.de/Gadara-Region-Project/Archaeometrie/Glas/-Glasherstellung/0_432.html; written by W. Auge, BAI Wuppertal.

shop. However, a definit prove of this suggestion cannot be given. The experiments comcerning glass production or processing on Tall Zirāʻa have shown that both was possible with local means, in respect to technology (kiln) and raw materials (flint and quartz) (see *Chap. 3.4.3.4.*).

3.8.3.2. Glass Frit and Faience

The multitude of finds like vessel sherds, cylinder seals and (raw) glass, all composed from similar base materials, of characteristic equipment such as cylindrical ‘industrial vessels’, working stones, grinding balls, and mortars, and, finally, the existence of copper minerals are indicative of corresponding local processing facilities. The presence of faulty and flawed faience beads (e.g. TZ 011143-001; *Fig. 3.109*) may point to a local faience manufacture.

Figs. 3.109–3.110 Left: Faience bead, TZ 011143-001. Dimensions: H 1.3, D (max.) 2.2; right: vessel sherd, TZ 004295-003. Dimensions: H 7, W. 5.5 (Source: BAI/GPIA).

3.8.4. Metals

edited by Dieter Vieweger/Jutta Häser[77]

3.8.4.1. Copper (Ores/Slags) and Bronze

Along with a number of copper and bronze finds there were also smaller chunks of copper ores as well as several pieces of copper slags. The chemical analyses of three chunks of ore (TZ 009459-001, TZ 007572-001, and TZ 007756-001; *Fig. 3.111*) revealed that some of them contain a high percentage of copper; the mineralogical analysis showed that the predominant mineral enclosed in the ores TZ 009459-001 is malachite. The specific use the ore was assigned to could not yet be established with certainty. Possibly, it generally served as a source of copper or it was used as a colouring component (blue) for the manufacture of glass or faience.

Figs. 3.111–3.112 Left: Copper ore, TZ 009459-001. Dimensions: L c. 2; right: copper slag, TZ 012480-001. Dimensions: L 6.5, W 4.5 (Source: BAI/GPIA).

3.8.4.2. Metal Artefacts

The most important Bronze and Iron Age copper and bronze objects that have been discovered on the tall are a sitting idol TZ 007367-001 (of the El-type figurines known in the Levant and Syria; *Figs. 3.121* and *3.122*), a skilfully crafted wine sieve TZ 010281-001 (*Fig. 3.115)* comparable with a Late Bronze Age find from Tall as-Saʻīdīya, and an amulet representing a female idol with Hathor hairstyle (TZ 012618-001; *Figs. 3.113* and *3.114*)

Most of the approx. 500 metal objects found so far can be assigned to one of the realms of household, craft, hunt/war, cult, and numismatics.

The chemical analyses of several objects revealed that quite a number—including daggers, needles, and knives—are made of copper and that the bronze objects

Figs. 3.113–3.114 Amulet with a female idol, TZ 012618-001. Dimensions: W (max.) 3.2, H 6.1 (Source: BAI/GPIA).

77 This article has been translated from the German language. It is based on http://www.tallziraa.de/Gadara-Region-Project/Archaeometrie/Metalle/0_430.html and http://www.bai-wuppertal.de/kupferbronze (16.5.2016); written by W. Auge, BAI Wuppertal.

usually have a tin content of 2 to 10 weight per cent. The composition of the wine sieve TZ 010281-001 (*Fig. 3.115*) and of the axe TZ 007992-001 (*Fig. 3.116*) is particularly interesting: they are made of bronzes with unusually high contents of SiO_2 (8 to 10 weight per cent). The SiO_2 may have reduced the material's flexibility[78] and thus made it possible to pierce the bronze sheet in the case of the wine sieve.

The little head of a bear TZ 010004-001 (*Fig. 3.117*) may have been a drawer knob or balance weight; the arm TZ 010019-001 (*Fig. 3.120*) could have formed part of an idol or warrior figure made of organic matter, and held a spear in its hand.

Figs. 3.115–3.116 Left: Wine sieve, TZ 010281-001. Dimensions: H 4.3, D (max.) 9.8; right: axe, TZ 007992-001. Dimensions: L 8, W 5.3, H 0.2 (Source: BAI/GPIA).

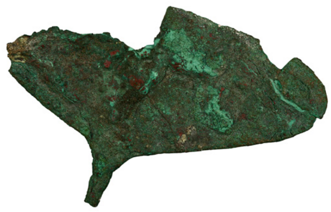

Figs. 3.117–3.120 Left: Head of a bear (balance weight?), TZ 010004-001. Dimensions: L 2.2, W 2, H 1.5; centre left: restored Iron Age I bowl, TZ 007082-001. Dimensions: D (max.) c. 14; centre right: Late Bronze Age mirror, TZ 001612-001. Dimensions: D (max.) c. 9; right: arm of a Late Bronze Age figurine, TZ 010019-001. Dimensions: L 5, W 5.9 (Source: BAI/GPIA).

Find No.	Object	Period	Cu	Sn	SiO_2	CaO	Al_2O_3
TZ 009459-001	Copper ore	Iron Age IIA/B	14–20	< 0.01	67–72	0.3–1.5	1.9–4.7
TZ 007756-001	Copper ore	Iron Age IIA/B	14–20	< 0.01	67–72	0.3–1.5	1.9–4.7
TZ 007572-001 MN 005	Copper ore	Iron Age I	49–50	< 0.01	9–17	0.1–3.8	0.2–0.4
TZ 001611-001	Needle	Late Bronze Age	97–98	0.03–0.8	ND	ND	ND
TZ 008878-001	Needle	Iron Age IIA/B	93	5.6	ND	ND	ND
TZ 001508-001	Knife	Late Bronze Age	97–98	0.03–0.8	ND	ND	ND
TZ 010117-001	Knife	Late Bronze Age	97–98	0.03–0.8	ND	ND	ND
TZ 001004-001	Bears's head (Balance weight?)	Iron Age IIA/B Late Bronze Age	91.6	7.8	ND	ND	ND
TZ 001612-001	Mirror	Late Bronze Age	94–97	2.0–3.8	ND	ND	ND
TZ 007366-001	Dagger	Late Bronze Age	94–97	2.0–3.8	ND	ND	ND
TZ 007992-001	Axe	Iron Age A IA/B Late Bronze Age	77–80	9.3	8.0–9.9	0.8–1.0	0.03–0.09
TZ 010281-001	Wine sieve	Iron Age IA/B Late Bronze Age	77–80	9.3	8.0–9.9	0.8–1.0	0.03–0.09
TZ 015262-001	Content of melting vessel	Middle Bronze Age	8.6	6.5	33.6	20.3	3.1

Tab. 3.4 Chemical composition of copper and bronze (weight per cent; elements As, S, Pb, and Fe < 1 weight per cent) (all data are expressed in grams) (Source: BAI/GPIA).

78 Bienkowski 1991.

3.8.4.3. Silver and Gold Objects

The upper part of the bronze figurine TZ 007367-001 (*Fig. 3.121* and *3.122*) is plated with gold, and the lower part with silver. Both are executed as an alloy: Au 39.1, Ag 38.4, Cu 22.5, and Ag 71.5, Au 3.9, Cu 24.7 (weight per cent). The unusually high copper content in both alloys probably results from the underlying bronze as some small flat plates that were also discovered (e.g. TZ 010447-001: 52–65 weight per cent Au und 38–44 weight per cent Ag) had a significantly lower copper content of 2 to 5 weight per cent.

Moreover, an earring (TZ 012889-001; *Fig. 3.123*), a pendant (TZ 012871-001), and two bead bezels (TZ 006992-001; *Fig. 3.125*) made of gold were excavated. The silver amulet TZ 010114-001 (*Fig. 3.124*) and the bottom of a little silver bowl (TZ 012479-001; *Fig. 3.126*) have corroded almost completely, so that more or less only silver sulphides and silver oxides were detectable.

Figs. 3.121–3.122 Iron Age IIA/B bronze figurine, TZ 007367-001. Dimensions: H 7.5, W 1.5 (Source: BAI/GPIA).

Figs. 3.123–3.126 Left: Earring, TZ 012889-001. Dimensions: D (max.) 1.8; centre left: silver amulet, TZ 010114-001. Dimensions: W 3.4, H 5.8; centre right: bead bezel and stone bead, TZ 006992-001. Dimensions: D (max.) 1; right: silver bowl, TZ 012479-001. Dimensions: L 4.3, W 3.6, H 1 (Source: BAI/GPIA).

3.8.4.4. Metal Processing on Tall Zirā‘a

The presence of smaller chunks of copper ores (TZ 009459-001; *Fig. 3.111*) and of several pieces of copper slag (TZ 012480-001; *Fig. 3.112*) seems to indicate the existence of workshops where copper ore was either fused in order to extract copper, or exploited otherwise. The fact that copper ores were processed in small quantities is also evidenced by a crucible (bowl of coarse pottery, TZ 020229-019; *Fig. 3.127*) that was discovered in the spring of 2010. On its inside, on top of a thick black layer, a thin molten layer containing particles of copper (ore) was discernable. On its outside, the bowl shows no black fire traces. Quite obviously, the material was heated directly by mingling the minerals with the fuel (= reduction agent).

It is known that up to the third millennium BC, copper ores were smelted inside the settlements and that from the Middle/Late Bronze Age at the latest, the smelting took place in the close vicinity of ore deposits[79].

Fig. 3.127 Crucible, TZ 020229-019. Dimensions: H 12, D (opening) 20, D (foot) 8.5. Stratum 17, Area I, Square AN 118, Context 4726/7 (Source: BAI/GPIA).

79 Hauptmann 2007, 115–137; Hauptmann 2008, 125–140.

3.8.5. Stone and Minerals

edited by Dieter Vieweger/Jutta Häser[80]

A further project comprised examination of the minerals found on Tall Zirāʿa—especially those not naturally occurring at this location—with respect to their origin, their immediate applicability, or regarding the question whether they could be processed to become any of the artefacts that were also discovered.

The number of different minerals is relatively high: alabaster ($CaSO_4$), various types of basalt, pumice stone, bitumen, iron minerals (haematite, magnetite, red haematite, pyrite, and slags) and copper minerals (ores, but also slags), calcite/chalk, quartzes (carnelian, obsidian, flint), and others.

These examinations were extended to some of the 40 balance weights made of stone that had been found to date.

3.8.5.1. Minerals

Bitumen

Bitumen is a mixture of high-molecular hydrocarbons. It has been utilised in almost every era, from the Bronze Age until today. It probably originates from the Dead Sea and was traded as a coveted sealing compound for vessels, houses, ships, etc.

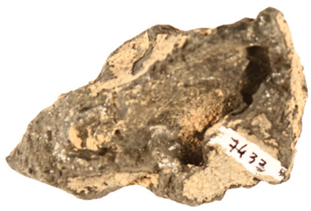

Fig. 3.128 Bitumen, Iron Age, TZ 007433-001. Dimensions: L c. 7, W c. 5 (Source: BAI/GPIA).

Fig. 3.129 Bitumen, TZ 012660-001. Dimensions: L 3.5, W 2 (Source: BAI/GPIA).

Calcite/Chalk/Limestone

To date, approx. 1,200 artefacts made of calcite/chalk/limestone have been found. Since vessels from this material are heavier than pottery and neither heat-resistant nor acidoresistant, they were almost certainly produced for ornamental, cultic, or religious purposes rather than for everyday use.

A number of miniature vessels are noteworthy, e.g. TZ 002900-001 and TZ 011565-001 (*Fig. 3.130*; libation vessels?), as well as two fragments of a bowl (TZ 009802-001; *Fig. 3.131*) that display two birds (cranes?), two figurines (TZ 007282-001 and TZ 015417-001; *Fig. 3.132*), and a cylinder seal (TZ 012357-001; *Fig. 3.134*).

Of particular importance are vessels made of chalk that were predominantly used by Jewish communities (*Fig. 3.133*)[81]. Around the beginning of the Common Era, they were used in the daily lives of Jewish persons because they conformed to the Jewish purity requirements.

The chemical analysis of some calcite/chalk artefacts shows that they are made of a $CaCO_3$ that is essentially impurified with larger or smaller amounts of SiO_2. Moreover, there are particularly strong disparities regarding the objects' magnesium levels. As hardly any magnesian sediments can be found in the tall's surroundings it can be assumed that the artefacts containing magnesium were not manufactured locally. However, in order to resolve the question pertaining to these artefacts' provenance, further examinations are necessary.

Fig. 3.130 Late Bronze Age miniature vessels. Left: TZ 002900-001. Dimensions: H 1.5, D (max.) 4; right: TZ 011565-001. Dimensions: H 2.3, D (opening) 3 (Source: BAI/GPIA).

80 This article has been translated from the German language. It is based on http://www.bai-wuppertal.de/mineralien and http://www.tallziraa.de/Gadara-Region-Project/Archaeometrie/Stein-und-Mineralien/0_431.html (16.5.2016); written by W. Auge, BAI Wuppertal.

81 Vieweger – Häser 2014; Häser – Vieweger 2015, 20–23.

Figs. 3.131–3.134 Left: Fragment of an Iron Age bowl, TZ 009802-001. Dimensions: D (max.) 10, H 7.2; centre left: Conical figurine, TZ 007282-001. Dimensions: H 7.2; centre right: Fragment of Early Roman mug, TZ 111726-001. Dimensions: H 10.5, D (foot) 8; right: cylinder seal, TZ 012357-001. Dimensions: H 3.2, D (max.) 1.6 (Source: BAI/GPIA).

Find No.	Object	Period	CaO	SiO_2	Al_2O_3	MgO
TZ 007282-001	Figurine	Finding context Ottoman	42.3	18.9	0.6	08
TZ 012357-001	Cylinder seal	Late Bronze Age (Finding context Early Roman)	23.2	39.5	9.8	-
TZ 111443-001	Mug	Early Roman	21.8	46.8	9.0	-
TZ 015378-001	Mug	Early Roman	18.6	45.2	11.0	7.6
TZ 011565-001	Miniature vessel	Finding context Iron Age IIC	18.9	46.4	12.7	6.5

Tab. 3.5 Chemical composition of calcite/chalk objects (all data are expressed in grams) (Source: BAI/GPIA).

Alabaster

On various occasions, alabaster (chemically: Ca_2SO_4; mineralogically: gypsum, anhydrite) was found as a mineral. The analysis of such a sample showed that chemically it was almost pure Ca_2SO_4 (impurified with 0.8 % SiO_2), and mineralogically a mixture of gypsum, anhydrite, and stelite.

A small, unfinished jug (TZ 015416-001; *Fig. 3.135*) suggests that indeed several objects were manufactured from the locally occurring material. Other alabaster objects are not only made of a finer substance but also more intricately wrought, such as a stand (TZ 001511-001 or the possible decorative knob of a chariot's axle (TZ 009176-001; *Fig. 3.136*)[82].

Figs. 3.135–3.136 Left: Alabaster jug, TZ 015416-001. Dimensions: H 6.2, D (max.) 4.2; alabaster knob, TZ 009176-001. Dimensions: H 3.2, D (max.) 5.3 (Source: BAI/GPIA).

Pumice Stone

Pumice could be found in large quantities and dating from all eras. The way that some of the excavated pieces are shaped suggests that it was applied both for washing laundry and for personal hygiene. Many of these pieces lie comfortably in one's hand and are pierced—presumably for suspending them. Since pumice is a porous, glassy volcanic rock, this material can very well originate from the Gadara plateau and its surroundings.

82 Koenen 2010.

Silex

Silex was used for the fabrication of weapons and tools for a very long time, even into the Roman Age; accordingly, large numbers of artefacts made of this material could be found (*Figs. 3.37* and *3.38*). As a result of a compaction process in chalk formations, silex often occurs in the shape of nodules (similar to iron nodules) or in layers, hence the excavations also yielded a multitude of crude pieces. Silex is a cryptocrystalline quartz (chalcedony) and may have been used as a base material for the production of glass frits which has been shown by experiments (cf. *Chap. 3.4.3.1.*). Flint can be found on the tall in large quantities but of minor quality.

Figs. 3.137–3.138 Left: Silex, Late Bronze Age scraper, TZ 012482-001; right: Silex, Iron Age II arrowhead, TZ 009202-001 (Source: BAI/GPIA).

Carnelian

Carnelian is a quartz that is coloured by iron oxide (a variety of chalcedony). It plays an important role in mysticism, and since it does not naturally occur in Palestine, it is very precious. The XRD analysis of one of the pieces of carnelian (TZ 009648-001) shows it to be pure quartz. As carnelian does not occur naturally on Tall Zirāʻa or in its surroundings these pieces must have arrived there by trade for further processing (maybe for manufacturing beads).

Larger pieces of this mineral (e.g. TZ 001613-001; *Fig. 3.139*) and 20 beads in different shapes suggest that, among other minerals, carnelian was also processed on the tall. They were found in strata dating from the Middle Bronze Age to the Ottoman period.

Figs. 3.139–3.140 Left: Iron Age I red coloured carnelian as mineral, TZ 001613-001. Dimensions: H c. 2, W c. 3.5; right: Iron Age beads, TZ 011780-001, TZ 011781-001 and TZ 011782-001. Dimensions: D 0.9 (Source: BAI/GPIA).

Iron (Sulfide) Nodules

The iron (sulfide) nodules that are abundant on Tall Zirāʻa can be found as pyrite concretions in the surrounding chalk formations. In several instances, light or dark red iron oxide from completely corroded (oxidised) nodules (TZ 012504-001; *Fig. 3.142*) was discovered. Since red iron oxide could also be traced on a basalt pestle (TZ 015449-001; *Fig. 3.144*) and on various grinding bowls or stones, this material was obviously used as a mineral colour for cosmetics, wall paintings, or ceramics. Accordingly, an SEM analysis carried out by the German Mining Museum Bochum revealed that the red paint on the coloured ceramic jug TZ 002989-001 (*Fig. 3.141*) contains 36 % of Fe_2O_3 (the black paint 9 % and 7 % of MnO and Fe_2O_3, respectively, and the white paint 45 % of CaO).

Figs. 3.141–3.144 Left: Ceramic jug, TZ 002989-001. Dimensions: H 40, D (max.) 32; centre left: corroded (oxidised) Late Bronze Age nodules, TZ 012504-001. Dimensions: L 2.5, B 2, H 0.5; centre right: Iron sulfid nodules; right: Late Bronze Age basalt pestle, TZ 015449-001. Dimensions: L 7.8, W 4.7, H 3.8 (Source: BAI/GPIA).

Red Haematite

Some light, intensely red, soft pieces of mineral were discovered that had clearly been used for painting. One of them is distinctively ashlar-shaped and pierced at one end so that it could be either suspended or hung around one's neck. With these crayons, it was very easy to apply an intense hue of red. The chemical analysis showed that it is red haematite, a clay mineral (sheet silicate) with a relatively high content of Fe_2O_3. A different red, ferruginous mineral, such as TZ 015333-001 and TZ 0185334-001 (*Fig. 3.145*), is much harder and thus not suitable for reddening objects.

Fig. 3.145 Late Bronze Age red haematite. Left: TZ 015333-001. Dimensions: L 6.0, W 4.2, H 4.1; right: TZ 015334-001. Dimensions: L 3.0, W 3.4, H 2.5 (Source: BAI/GPIA).

Find No.	Object	Period	Fe_2O_3	SiO_2	Al_2O_3	CaO	K_2O
TZ 015334-001	Red haematite	Late Bronze Age	28.1	44.3	18.5	2.9	1.6
TZ 015333-001	Rock	Late Bronze Age	3.3	64.0	24.4	5.6	2.1

Tab. 3.6 Chemical composition of red haematit (Source: BAI/GPIA).

3.8.5.2 Balance Weights

Almost all of the c. 40 weights discovered so far are made of stone, usually a hard, slightly abrasive/corrosive matter, in various but characteristic shapes such as cubes, discs, balls, cones, and double cones with flattened ends.

Apart from a number of basalt and calcite weights that may be of local/regional manufacture those made of haematite, goethite, and jadeite count among the more valuable objects as these minerals do not occur naturally in the region, moreover some of the objects had to be wrought laboriously.

The weights weigh between 2.3 g (TZ 007373-001; *Fig. 3.147*) and 433 g (TZ 001388-001; *Fig. 3.146*). Four of them are of biconical shape (TZ 007373-001, made of goethite; TZ 007374-001, TZ 012317-001, TZ 012322-001, made of haematite, *Figs. 3.148* and *3.149*) circulating in the Mediterranean and in the Levant, found for example in Ugarit in Syria, on the island of Cyprus and on the shipwreck of Uluburun on the Turkish shore, in Late Bronze Age contexts[83]. On Tall Zirāʻa all of them were found in the Late Bronze Age stratum.

Figs. 3.146–3.149 Balance weights: Left: TZ 001388-001. Dimensions: H 4.8, D (max.) 5.7; centre left: TZ 007373-001. Dimensions: L 1.2, D 0.8; centre right: TZ 007374-001. Dimensions: L 2.7, D (max.) 1.4, H 1.1; right: TZ 012317-001. Dimensions: L 2.5, D (max.) 1.1, H 0.9 (Source: BAI/GPIA).

83 Pulak 2005, 87 f. 616–619; Petrusco 1984, 296. 302 f.

3.9. Bibliography

Archimetrix 2005

Eine virtuelle Zeitreise zum Tell Zera‘a – Eisenzeitliches Vierraum-Haus (1200–520 v. Chr.) Palästina, <http://www.bai-wuppertal.de/node/237> (1.5.2016)

Auge – Vieweger 2006

W. Auge – D. Vieweger, Ein Keramikprojekt zu den Funden vom Tall Zirā‘a, Gemeindebrief der Evangelischen Gemeinde Deutscher Sprache zu Jerusalem 3, 2006, 54–56

Benson 1972

J. B. Benson, Bamboula at Kourion. The Necropolis and the Finds Excavated by J. F. Daniel (Philadelphia 1972)

Bienkowski 1991

P. Bienkowski (ed.), Treasures from an Ancient Land. The Art of Jordan (Stroude 1991)

Bongartz 2011

G. Bongartz, Entwicklung und Erprobung eines Stereophotogrammetriesystems (MA Thesis Bergische Universität Wuppertal 2011) (unpubl.)

Bongartz 2016

G. Bongartz, 3D Technology for Archaeological Documentation, in: M. Jamhawi (ed.), SHAJ 12 (Amman 2016) 489–495

Bülow – Große Frericks 2009

G. Bülow – J. Große Frericks, Die Entwicklung eines CIELAB-basierten Farbklassifizierungsprogramms für archäologische Funde (Project Work Bergische Universität Wuppertal 2009) (unpubl.)

Bunce et al. 2011

R. G. H. Bunce – M. M. B. Bogers – P. Roche – M. Walczak – I. R. Geijzendorffer – R. H. G. Jongman, Manual for Habitat and Vegetation Surveillance and Monitoring. Temperate, Mediterranean and Desert Biomes, Alterra Report 2154 (Wageningen 2011)

Chambon 1984

A. Chambon, Tell el-Far‘ah I. L‘Âge du Fer. Éditions Recherche sur les Civilisations (Paris 1984).

Cline 2014

E. H Cline, 1177 BC: The Year Civilization Collapsed (Princeton 2014)

Eiland 1998/1999

M. L. Eiland, Ceramic Replications at Tell Brak, Syria Special Issue. Ceramic Ethnoarchaeology. From Sardina to Iraq, NewsletterPoTech 16/17, 1998/1999, 69–83

Farbmessung 2010

Centroplast Engineering Plastics GmbH, Farbmessung 2010, <http://www.centroplast.de/de/030Anwendungen/020Qualitaetsmanagement/farbmessung.php> (13.3.2010)

Frumin et al. 2015

S. Frumin – A. M. Maeir – L. Kolska Horwitz – E. Weiss, Studying Ancient Anthropogenic Impacts on Current Floral Biodiversity in the Southern Levant as Reflected by the Philistine Migration, Scientific Reports 5, 2015, 1–20

Ghazanfar et al. 2013

S. A. Ghazanfar – H.Taifour – A. Aloqlah – R. Borosova – J. Osborne, A Quantitative Analysis of the Flora of Jordan and its Conservation Status. Royal Botanic Garden (Jordan 2013)

Glueck 1951

N. Glueck, Explorations in the Eastern Palestine IV. Part I, AASOR 25–28 (New Haven 1951)

Gondet – Castel 2004

S. Gondet – C. Castel, Prospection géophysique à al-Rawda et urbanisme en Syrie au Bronze ancien, Paléorient 30, 2, 2004, 93–109.

Grieg 1989

J. Grieg, Handbooks for Archaeologists 4. Archaeobotany, European Science Foundation (Birmingham 1989)

Hanbury-Tenison 1984

J. W. Hanbury-Tenison, Explorations du Wadi el-‘Arab. Chronique archéologique, RB 91, 1984, 230–231

Hanbury-Tenison et al. 1984

J. W. Hanbury-Tenison with contributions by St. Hart – P. M. Watson – R. K. Falkner, Wadi Arab Survey 1983, AAJ 28, 1984, 385–424 (text). 494–496 (plates)

Häser et al. 2016

J. Häser – K. Soennecken – D. Vieweger, Cylinder Seals from Tall Zar‘a as Indicators of Transparent Borders, in: M. Jamhawi (ed.), SHAJ 12 (Amman 2016) 497–507

Häser – Vieweger 2005a

J. Häser – D. Vieweger, Preliminary Report on the Archaeological Investigations of the Wādī al-‘Arab and the Tall Zar‘a 2003 and 2004, AAJ 49, 2005, 135–146

Häser – Vieweger 2005b

J. Häser – D. Vieweger, Der Tell Zera'a im Wadi al-'Arab. Das 'Gadara Region-Project' in den Jahren 2001 bis 2004, ZDPV 121, 1, 2005, 1–30

Häser – Vieweger 2007a

J. Häser – D. Vieweger, Das 'Gadara-Region Project'. Der Tell Zerā'a in den Jahren 2005 und 2006, ZDPV 123, 1, 2007, 1–27

Häser – Vieweger 2007b

J. Häser – D. Vieweger, "... sechzig große Städte, ummauert und mit eisernen Riegeln". Archäologische Untersuchungen in der Gadara-Region geben einen Einblick in fünf Jahrtausende Geschichte Palästinas, AW 1, 2007, 63–69

Häser – Vieweger 2007c

J. Häser – D. Vieweger, The 'Gadara Region Project' in Northern Jordan. The Spring Campaign 2006 on Tall Zar'a, AAJ 51, 2007, 21–34

Häser – Vieweger 2009

J. Häser – D. Vieweger, Five Years (2003–2007) of Excavation on Tall Zar'a, in: F. Khraysheh (ed.), SHAJ 10 (Amman 2009) 483–492

Häser – Vieweger 2015

J. Häser – D. Vieweger, Tall Zira'a, Jordanien: Die Kalksteingefäße aus der frührömischen Zeit – Religiöse und sozio-ökonomische Implikationen, e-Forschungsberichte des DAI 2015 Faszikel 2, 20–23 <urn:nbn:de:0048-DAI-EDAI-F.2015-2-06-7.DAI_e-Forschungsberichte_Faszikel_2-2015> (1.6.2016)

Hauptmann 2007

A. Hauptmann, Alten Berg- und Hüttenleuten auf die Finger geschaut. Zur Entschlüsselung berg- und hüttenmännischer Techniken, in: G. A. Wagner (ed.), Einführung in die Archäometrie (Berlin 2007) 115–137

Hauptmann 2008

A. Hauptmann, Vom Erz zum Metall. Naturwissenschaftliche Untersuchungen innerhalb der Metallurgiekette, in: A. Hauptmann – V. Pingel (eds.), Archäometrie. Methoden und Anwendungsbeispiele naturwissenschaftlicher Verfahren in der Archäologie (Stuttgart 2008) 125–140

Helbaek 1969

H. Helbaek, Plant Collecting, Dry-Farming, and Irrigation Agriculture in Prehistoric Deh Luran, in: F. Hole – K. F. Lannery – J. Neely (eds.), Prehistory and Human Ecology of the Deh Luran Plain, Memoirs of the Museum of Anthropology (Michigan 1969) 383–426

Hofmann et al. 2007

R. Hofmann – Z. Kujundzic-Vejzagić – J. Müller – N. Müller-Scheeßel – R. K., R. Hofmann – Z. Kujundzic-Vejzagic – J. Müller – N. Müller-Scheeßel – K. Rassmann, Prospektionen und Ausgrabungen in Okoliste (Bosnien-Herzegowina). Siedlungsarchäologische Studien zum zentralbosnischen Spätneolithikum. Ber. RGK 87, 2007, 43–212.

Hole et al. 1969

F. Hole – K. V. Flannery – J. A. Neely, Prehistory and Human Ecology of the Deh Luran Plain. An Early Village Sequence from Khuzistan, Iran, Memoirs of the Museum of Anthropology University of Michigan 1 (Ann Arbor 1969)

Jongman et al. 1995

R. H. G. Jongman – C. J. F. ter Braak – O. F. R. van Tongeren, Data Analysis in Community and Landscape Ecology (Cambridge 1995)

Kerestes et al. 1977/1978

T. M. Kerestes – J. M. Lundquist – B. G. Wood – K. Yassine, An Archaeological Survey of Three Reservoir Areas in Northern Jordan, AAJ 22, 1977/1978, 108–135

Kerner – Maxwell 1990

S. Kerner – L. A. Maxwell, Keramik, in: P. C. Bol – A. Hoffmann – Th. Weber (eds.), Gadara in der Dekapolis. Deutsche Ausgrabungen bei Umm Qais in Nordjordanien 1986–1988. Vorbericht, AA 1990, 193–266

Koenen 2010

K. Koenen, Bet-Schean, <http://www.bibelwissenschaft.de/wibilex/das-bibellexikon/details/quelle/WIBI/zeichen/b/referenz/15152///cache/a13805a3fcbc16368835c617b84a2d90/> (23.6.2010)

Kraushaar et al. 2008

A. Kraushaar – F. Geßner – C. Bickeböller, Fogra-Forschungsbericht Nr. 60.054. Untersuchung moderner Farbabstandsformeln (München 2008)

Langgut et al. 2015

D. Langgut – I. Finkelstein – T. Litt – F. H. Neumann – M. Stein, Vegetation and Climate Changes During the Bronze and Iron Ages (~ 3600–600 BCE) in the Southern Levant Based on Palynological Records, Radiocarbon 57, 2, 2015, 217–235

Lehmann – Schulze 2015

R. Lehmann – M. Schulze, Tall Zira'a, Jordanien: Archäometrische Forschungen zur Herkunftsbestimmung der Metallfunde im Rahmen des Gadara Region Projects. e-Forschungsberichte des DAI 2015 Faszikel 2, 28–30 urn:nbn:de:0048-DAI-EDAI-F.2015-2-08-1 (25.5.2016)

Leiverkus – Soennecken 2016

P. Leiverkus – K. Soennecken, Survey in the Wādī al-'Arab 2009–2011, in: Jamhawi (ed.), SHAJ 12 (Amman 2016) 509–518

London 1990

G. London, Töpferei auf Zypern. Damals – heute (Mainz 1990)

Majidzadeh 1975–1976

Y. Majidzadeh, The Developement of the Pottery Kiln in Iran from Prehistoric Times to Historical Periods, Paléorient 3, 1975–1976, 207–221

Mazar 1999

A. Mazar, The Conservation and Management of Mudbrick Buildings at Tell Qasile, Israel, Conservation and Management of Archaeological Sites 3, 1999, 103–108

Mazar 2008

A. Mazar, The Iron Age Dwellings at Tell Qasile, in: D. Schloen (ed.), Exploring the Longue Dure. Essays in Honor of Lawrence E. Stager (Winonalake 2008) 319–335

McGovern 1997

P. E. McGovern, Wine of Egypt's Golden Age. An Archaeochemical Perspective, JEA 83, 1997, 69–108

Meyer 2010

J.-W. Meyer, Überlegungen zur Siedlungsstruktur. Eine erste Analyse des Ergebnisse des geomagnetischen Prospektion, in: J.-W. Meyer – W. Orthmann (eds.), Ausgrabungen in Tell Chuēra in Nordost-Syrien: Vorbericht zu den Grabungskampagnen 1998 bis 2005.Vorderasiatische Forschungen der Max-Freiherr-von-Oppenheim-Stiftung (Saarbrücken 2010) 199–222

Mittmann 1970

S. Mittmann, Beiträge zur Siedlungs- und Territorialgeschichte des nördlichen Ostjordanlandes, Abhandlungen des Deutschen Palästina-Vereins (Wiesbaden 1970)

Näser 2005

C. Näser, Ethnoarchäologie, Analogiebildung und Nomadismusforschung. Eine Einführung mit einer Fallstudie aus Nordafrika, in: J. Gertel (ed.), Methoden als Aspekte der Wissenkonstruktion. Fallstudien zur Nomadismusforschung (Halle 2005) 17–42, <http://www.nomadsed.de/fileadmin/user_upload/redakteure/Dateien_Publikationen/Mitteilungen_des_SFB/owh8naeser.pdf> (1.3.2016)

Neef et al. 2012

R. Neef – R. T. J. Cappers - R. M. Bekker, Digital Atlas of Economic Plants in Archaeology (Groningen 2012), <http://www.plantatlas.eu (13.6.2016)

Nicholson 1995

P. T. Nicholson, Construction and Firing of an Experimental Updraught Kiln, in: B. J. Kemp (ed.), Amarna Reports VI (London 1995) 239–278

Ohnefalsch-Richter 1913

M. H. Ohnefalsch-Richter, Griechische Sitten und Gebräuche auf Zypern. Mit Berücksichtigung von Naturkunde und Volkswirtschaft sowie der Fortschritte unter englischer Herrschaft dargestellt (Berlin 1913)

Olsvig-Whittaker et al. 2011

L. Olsvig-Whittaker – E. Frankenberg – Y. Magal – Y. Shkedy – S. Amir – M. Walczak – M. Luck-Vogel – D. Jobse – A. de Gelder – L. Blank – Y. Carmel – N. Levin – R. Harari-Kremer – D. Blankman – B. Boeken, EBONE in Mediterranean and Desert Sites in Israel, with Notes on South Africa. Report on Field Tests in LTER Sites and Habitat Monitoring, Alterra Report 2260 (Wageningen 2011), <http.//edepot.wur.nl/192666> (26.4.2016)

Olsvig-Whittaker et al. 2015

L. Olsvig-Whittaker – A. M. Maeir – E. Weiss – S. Frumin – O. Ackermann – L. Kolska Horowitz, Ecology of the Past. Late Bronze and Iron Age Landscapes, People and Climate Change in Philistia (the Southern Coastal Plan and Shephelah), Israel, Journal of Mediterranean Ecology 13, 2015, 57–75

Peet 1980

R. K. Peet, Ordination as a Tool for Analyzing Complex Data Sets, in: E. van der Maarel (ed.), Classification and Ordination. Symposium on Advances in Vegetation Ccience, Nijmegen May 1979 (Springer Netherlands 1980), 171–174

Petit et al. 2006

L. P. Petit – E. Kaptijn – F. M. Hourani – O. al-Ghul – E. B. Grootveld – G. van der Kooij, Dayr 'Alla Regional Project: Settling the Steppe Second Campaign 2005, AAJ 50, 2006, 179–188

Petrusco 1984

K. M. Petrusco, Prolegomena to Late Cypriot Weight Metrology, AJA 88, 293–304

Pulak 1995

C. Pulak, Das Schiffswrack von Uluburun und seine Ladung, in: B. Andreae – Th. Weber (eds.), Poseidons

Reich. Archäologie unter Wasser, Zaberns Bildbände zur Archäologie 23 (Mainz 1995) 43–58

Schier – Draşovean 2004

W. Schier – F. Draşovean, Vorbericht über die rumänisch-deutschen Prospektionen und Ausgrabungen in der befestigten Teilsiedlung von Uivar, jud. Timiş, Rumänien (1998–2002). Praehistorische Zeitschrift 79, 2, 2004, 145–230

Schläpfer 2002

K. Schläpfer, Farbmetrik in der grafischen Industrie, UGRA Verein zur Förderung Wiss. Untersuchungen in der Graf. Industrie (St. Gallen 2002)

Schulze et al. 2013

M. Schulze – R. Lehmann – C. Vogt – D. Vieweger, Charakterisierung mittelalterlicher Glasperlen aus dem Heiligen Land. Characterisation of Medieval Glass Beads from the Holy Land, Tagungsband Archäometrie und Denkmalpflege Weimar, METALLA Sonderheft 6 (Bochum 2013) 294–296.

Schulze et al. 2014

M. Schulze – R. Lehmann – C. Vogt, Tall Zira'a. Archaeometry, in: F. Kenkel – D. Vieweger (eds.), With Trowel and Hightech. German Archaeological Projects in Jordan (Berlin 2014) 13

Schulze et al. 2015

M. Schulze – R. Lehmann – D. Vieweger – C. E. Loeben – I. Horn – C. Vogt, Provenienzanalytik an archäologischen Objekten aus dem Nahen Osten mittels Bleiisotopenverhältnismessungen (fs-LA-ICP-MC-MS), in: Archäometrie und Denkmalpflege Tagungsband Mainz 2015, METALLA Sonderheft 7 (Bochum 2015) 219–221

Schwermer 2014

A. Schwermer Die Kochtopfkeramik des Tall Zira'a: eine typologische und funktionale Analyse der Funde von der Frühen Bronze- bis in die späte Eisenzeit (Diss. Bergische Universität Wuppertal 2014), <http://elpub.bib.uni-wuppertal.de/edoes/dokumente/fba/geschichte/diss2014/schwermer> (19.5.2015)

Šmilauer – Lepš 2014

P. Šmilauer – J. Lepš. Multivariate Analysis of Ecological Data Using CANOCO 5 (Cambridge 2014)

Vieweger 2010

D. Vieweger Archaeological Research on Tall Zira'a. The Gadara Region Project. 5000 Years of Culture, Technology, and Trade in Northern Jordan, in: P. Matthiae – F. Pinnock – L. Nigro – N. Marchetti (eds.), Proceedings of the 6th International Congress on the Archaeology of the Ancient Near East Roma 5th–10th May 2008 II. Excavations, Surveys and Restorations. Reports on Recent Field Archaeology in the Near East (Wiesbaden 2010) 755–768

Vieweger 2013

D. Vieweger, The Transition from Bronze to Iron Ages in Northern Palestine: Archaeological and Archaeometric Investigations at Tall Zar'a, in: F. al-Hmoud (ed.), SHAJ 11 (Amman 2013) 231–242

Vieweger – Häser 2007

D. Vieweger – J. Häser, Tall Zar'a, Munjazāt 8, 2007, 2008, 12–13

Vieweger – Häser 2008a

The New Encyclopedia of Archaeological Excavations in the Holy Land 5, Suppl. (2008) 1841–1843 s.v. Zira'a, Tell (D. Vieweger – J. Häser)

Vieweger – Häser 2008b

D. Vieweger – J. Häser, Ein außergewöhnlicher Fundkomplex, Welt und Umwelt der Bibel 2, 2008, 64

Vieweger – Häser 2008c

D. Vieweger – J. Häser, Tall Zira'a. Five Thousand Years of Palestinian History on a Single Settlement Mound, NEA 70, 3, 2008, 151–162

Vieweger – Häser 2008d

D. Vieweger – J. Häser, The Tall Zar'a and the Gadara Region Project in the Years 2007 and 2008, ADAJ 52, 2008, 382–383

Vieweger – Häser 2009a

D. Vieweger – J. Häser, Das 'Gadara Region Project' und der Tall Zirā'a. Fünf Jahrtausende Geschichte Palästinas – eine Zwischenbilanz nach fünf Grabungskampagnen, Das Altertum 54, 1, 2009, 1–36

Vieweger – Häser 2009b

D. Vieweger – J. Häser, Tall Zar'a – Excavations on a Multi-Period Site in Northern Jordan, Abhath Al-Yarmouk 25, 3, 2009, 655–680

Vieweger – Häser 2010

D. Vieweger – J. Häser, Das Gadara-Region-Projekt. Der Tall Zerā'a in den Jahren 2007 bis 2009, ZDPV 126, 1, 2010, 1–28

Vieweger – Häser 2014

J. Häser – D. Vieweger, Die Kalksteingefäße aus der frührömischen Zeit vom Tall Zirā'a. Religiöse und sozio-ökonomische Implikationen, in: J. Elschenbroich

– J. de Vries (eds.), Worte der Weissagung. Studien zu Septuaginta und Johannesoffenbarung. Festschrift Martin Karrer, Arbeiten zur Bibel und ihrer Geschichte 47 (Leipzig 2014) 137–156

Vieweger et al. 2003

D. Vieweger with contributions by J. Eichner – P. Leiverkus, Der Tell Zera'a im Wadi el-'Arab. Die Region südlich von Gadara. Ein Beitrag zur Methodik des Tell-Surveys, Das Altertum 48, 2003, 191–216

Vieweger et al. 2009

D. Vieweger – W. Auge – A. Hauptmann, Archaeometry in Archaeological Research 5000 Years of History on Tall Zar'a: Pottery. Everyday Life, Trade and Technology in Northern Jordan, in: F. al-Khraysheh (ed.), SHAJ 10, 2009, 245–258

Vieweger et al. 2014

D. Vieweger – K. Soennecken – J. Häser, Verlieren hat seine Zeit, wegwerfen hat seine Zeit. Wandel und Kontinuität im Ostjordanland am Übergang von der Bronze- zur Eisenzeit, in: J. J. Kotjatko-Reeb – S. Schorch – J. Thon – B. Ziemer (eds.), Nichts Neues unter der Sonne – Zeitvorstellungen im Alten Testament. Festschrift Ernst-Joachim Waschke, Beihefte zur Zeitschrift für die alttestamentliche Wissenschaft 450 (Berlin 2014) 57–77

Watson 1999

P. J. Watson, Ethnographic Analogy and Ethnoarchaeology, in: T. Kapitan (ed.), Archaeology, History and Culture in Palestine and the Near East. Essays in Memory of Albert E. Glock (Atlanta 1999) 47–65

Wilkinson 2003

T. J. Wilkinson, Archaeological Landscapes of the Near East (Tuscon 2003)

Zohary – Hopf 2000

D. Zohary – M. Hopf, Domestication of Plants in the Old World 3(Oxford 2000)